Quasiparticle Description of Quantum Chromodynamics at Finite Temperature in the Presence of Magnetic Fields

Thesis submitted to the University of Calicut
in partial fulfillment of the requirements
for the award of the degree of

Doctor of Philosophy

in

Physics

Sebastian Koothottil

Department of Physics

University of Calicut

P. O. Calicut University, PIN-673 635

Malappuram Dt., Kerala.

December 2020

UNIVERSITY OF CALICUT
Department of Physics

Calicut University P.O.,
Kerala, 673635, INDIA
0494 2400727, 2407373, 2407374
Email: shahin@uoc.ac.in
www.universityofcalicut.info

Dr. Mohamed Shahin Thayyil
Assistant Professor

Phone: +91-4952731190
Mob: +91-9961824725

CERTIFICATE

Certified that the corrections / suggestions from the adjudicators of the PhD thesis entitled **'Quasiparticle Description of Quantum Chromodynamics at Finite Temperature in the Presence of Magnetic Fields'** submitted by **Mr. Sebastian Koothottil**, research scholar of Department of Physics under my supervision and guidance (Co-Guide), have been incorporated in this copy of the thesis. The thesis has been checked for plagiarism, using URKUND software at CHMK library, University of Calicut. The contents in the hard copy and the soft copy are the same.

Calicut University

Date: 09/08/2021

Dr. Mohamed Shahin Thayyil

DECLARATION

I hereby declare that the work presented in this thesis entitled 'Quasiparticle Description of Quantum Chromodynamics at Finite Temperature in the Presence of Magnetic fields' is based on the original work done by me under the guidance of Dr. Vishnu Mayya Bannur (Guide), and Dr. Mohamed Shahin Thayyil (Co-Guide). Department of Physics, University of Calicut, and has not been included in any other thesis submitted previously for the award of any degree.

University of Calicut

Date: **Sebastian Koothottil**

Publications and Presentations

International Journals/Proceedings

1. **Sebastian Koothottil** and Vishnu M. Bannur, Thermodynamic behavior of magnetized quark-gluon plasma within the self-consistent quasiparticle model, *Physical Review C* 99 (2019) 3, 035210.

2. **Sebastian Koothottil** and Vishnu M. Bannur, Thermomagnetic properties and Debye Screening for magnetized quark-gluon Plasma using the extended self-consistent quasiparticle model , *Physical Review C* 102 (2020) 1, 015206.

3. J.P. Prasanth, **Sebastian Koothottil** and Vishnu M. Bannur, Revisiting Cornell potential model of the quark-gluon plasma, *Physica* A 558 (2020) 124921.

4. **Sebastian Koothottil**, J.P. Prasanth and Vishnu M. Bannur, Equation of state of a strongly coupled quark gluon plasma using cornell potential , *DAE Symposium on Nuclear Physics* 61 (2016) 814-815.

5. **Sebastian Koothottil**, J.P. Prasanth and Vishnu M. Bannur, Cornell potential model for strongly coupled quark gluon Plasma , *DAE Symposium on Nuclear Physics* 62 (2017) 912-913.

Papers Presented in International/National conferences:

1. *Thermo-magnetic properties of $2-$flavor quark-gluon plasma using the extended self-consistent quasiparticle model*, International Conference on Theoretical and Experimental Physics (ICTEP - 2020), Feb. 5-6, 2020, Farook College, Kozhikode.

2. *Thermodynamics of magnetized 2-flavor quark-gluon plasma Using the Self-Consistent Quasiparticle Model*, DAE-BRNS symposium on Contemporary

and Emerging Topics in High Energy Nuclear Physics, Nov. 25-27, 2019, VECC Kolkata.

3. *Thermodynamics of magnetized QGP within the self-consistent quasiparticle model, XXIII* DAE-BRNS High Energy Physics Symposium, Dec. 10-14, 2018, IIT Madras, Chennai.

4. *Cornell potential model for strongly coupled quark gluon plasma,* Dec. 20-24, 2017, 62nd DAE-BRNS symposium on nuclear physics, Thapar Institute of Engineering and Technology, Patiala.

5. *Equation of state of a strongly coupled quark gluon plasma using cornell potential,* Dec. 5-9, 2016, 61st DAE-BRNS Symposium on Nuclear Physics, Saha Institute, Kolkata.

Acknowledgements

Contents

List of Figures

Preface

The study of the behavior of the quark-gluon plasma in an external magnetic field has recently attracted much interest. Equations describing the quark-gluon plasma need modifications in the presence of the magnetic field. Some phenomenological models have been quite successful in describing the quark-gluon plasma. It is interesting to explore how these models can be modified to incorporate the external magnetic field's effects. We work within the quasiparticle description and extend the so-called self-consistent quasiparticle model to describe magnetized quark-gluon plasma. The thesis is organized as follows.

The purpose of Chapter 1 is to give a brief introduction to quark-gluon plasma. We start with a historical introduction to quantum chromodynamics, the theory of quarks and gluons, and give a brief description of the final theory. We then see how a deconfined state of matter, the quark-gluon plasma, is predicted by quantum chromodynamics.

Throughout this thesis, we work within the quasiparticle approach. The system is considered an ideal gas of quasi-quark and quasi-gluons with mass depending on temperature and possibly other variables relevant to the situation. We are particularly interested in one of the successful quasiparticle models, the self-consistent quasiparticle model. In chapter 2, we concern ourselves with this model's study with the details necessary for our work.

We notice that the self-consistent quasiparticle model is suitable and allows an extension to incorporate the magnetic field's effects. The extension involves

considering magnetized quark-gluon plasma as an ideal gas of quasiparticles with thermomagnetic masses. The formulation and technical details of the extension can be found in chapter 3.

In chapter 4, we apply our model to study the behavior of the magnetized quark-gluon plasma. Using the extended model, we examine the energy density, pressure, entropy density, and speed of sound of magnetized quark-gluon plasma, shedding light on some of its exciting features.

The anisotropy due to the external magnetic field and the screening properties of the magnetized quark-gluon plasma are the subject of study in chapter 5.

Chapter 6 deals with the further generalization of this model to include the effects of chemical potential too. We apply the further-generalized model to study the number density, number susceptibility, pressure difference, and the screening properties of magnetized quark-gluon plasma at finite temperature and density.

Chapter 7 summarizes the conclusions and provides our outlook on the potential avenues of research in the direction of this work.

Chapter 1

Quark-Gluon plasma

1.1 Introduction: The Standard model of particle physics

The standard model of particle physics describes the fundamental particles, quarks, and leptons, using quantum field theory. These are spin $\frac{1}{2}$ particles that interact through the four fundamental forces; gravity, weak, electromagnetic, and strong interaction. However, the gravitational interaction among fundamental particles is not included within the standard model.

The leptons interact via the electromagnetic and weak interaction but do not participate in the strong interaction. Quarks are the elementary particles that make up the hadrons. They participate in electromagnetic, weak, and strong interactions.

The elementary particles come in three generations. The first generation consists of the electron, electron neutrino, the up quark, the down quark, and the corresponding antiparticles. The second generation has the muon, muon neutrino, strange quark, charmed quark, and the corresponding antiparticles. The third-generation includes the tau, the tau neutrino, the top quark, and the

bottom quarks along with the respective antiparticles.

The gauge principle and the principle of spontaneous symmetry breaking are cornerstones of the standard model of particle physics. According to the gauge principle, all the standard model interactions are described by the exchange of gauge bosons. Bosons are particles with integer spins, and the gauge bosons of the standard model all have spin 1.

Spontaneous symmetry breaking combined with the gauge principle led to the unification of the electromagnetic and the weak interactions into one interaction called the electroweak interaction. The principle of spontaneous symmetry breaking also led to the theoretical discovery of a new field called the Higgs field, which is believed to fill all space throughout the universe. According to the standard model, the fundamental particle acquires mass by interacting with the Higgs field. If the coupling between the Higgs field and the particle is strong, so is the particle's mass. Quantum of the Higgs field, the Higgs boson has been recently found, completing the standard model.

The strength of an interaction is given by its coupling constant. This quantity turns out not to be a constant but depends on the distance of the interacting particles. At high energies ($10^{15}GeV$), the coupling constants of weak, strong, and electromagnetic interactions are expected to merge, opening up the possibility of unifying all the fundamental forces. Electromagnetism and the weak force have already been unified into a single theoretical framework called the electroweak theory. Attempts to unify all three standard model forces known as Grand Unified Theories (GUT).

1.2 Quantum chromodynamics

1.2.1 Historical survey

In our work, we focus on the properties of strongly interacting matter. The corresponding gauge field theory is Quantum Chromodynamics [1].

In the late sixties, Gell-Mann and Zweig proposed the quark model to describe the physics of hadrons [2, 3]. According to this model, all hadrons could be understood as bound states of three fictitious constituents with fractional electric charges. This model could provide a classification of hadrons, explain the hadron mass spectra, and the hadronic interactions. The dynamics obeyed by the quark system was yet to be developed.

Deep Inelastic Scattering (DIS) experiments provided the initial experimental information of the structure of hadrons. In DIS, the hadrons are probed by applying a beam of particles with no structure. A higher resolution could be attained at higher energies and momentum transfers. SLAC (Stanford Linear Accelerator Center), in the 1960s, initiated such experiments where electrons were used to probe the interior of protons.

Bjorken in 1969 reported that the hadron structure functions exhibited a scaling property where the momentum transferred square q^2 and energy transfer ν of electrons are very large with a fixed ratio q^2/ν [4]. This scaling property was called Bjorken Scaling. It was claimed that the structure functions depended only on the ratio q^2/ν rather than on q^2 and ν separately. Experiments confirmed the existence of Bjorken scaling [5].

The parton hypothesis explained the scaling behavior by assuming that the hadrons consisted of pointlike particles, which are almost free [6, 7]. The large momentum transfer squared q^2 in the DIS provided high spatial resolution for observing the target nucleon. The Bjorken scaling thus implied that the

constituents of the nucleon are almost free and structureless particles called Partons. These Partons were identified with quarks as experiments showed that the Partons had the same charge and spin as quarks.

The success of the Parton model led to searches for a theory describing the dynamics of quarks. The quarks of Gell-Mann and Zweig were supposed to be firmly bound in mesons and Baryons so that they could not be isolated free particles. At the time, it was not clear how a quantum field theory could describe the interaction which gets weaker at short distances. All the known quantum field theories at the time were shown not to enjoy the property of weaker interaction at short distances [8].

Non-Abelian gauge theories were not initially considered as candidates for describing the dynamics of the quarks. These are gauge theories with a non-Abelian gauge symmetry, and the generators of the symmetry group are noncommutative. Such theories are called Yang-Mills theories, named after Yang and Mills, who originally introduced them [9].

Examination of such theories by 't Hooft [10], Gross and Wilczek [11] and Politzer [12] using the renormalization group method revealed that they satisfied the desired property. This property of weak interaction at short distances and high energies has come to be known as asymptotic freedom. It was soon shown that only the non-Abelian gauge theories exhibited the property of asymptotic freedom in four-Dimensional space-time [13]. The proof of asymptotic freedom was achieved [14], and the quantization of non-Abelian gauge theories had already been achieved.

Thus it became clear that the right candidate for describing the quark dynamics was a non-Abelian gauge theory, necessitating the identification of an extra symmetry among the quarks.

It had already been suggested that the quarks must have a new quantum

number so as to overcome some of the theoretical difficulties [15–18]. This new quantum number was called Color by Gell-Mann. It was Fritzsch and Gell-Mann who identified the additional symmetry needed for the theory with color symmetry [19]. With this, all the difficulties were resolved, and the quantum field theory describing the dynamics of quarks was established. The theory was named quantum chromodynamics (QCD), the word "chromo" referring to the quantum number color. QCD enjoys asymptotic freedom at short distances (high energy) and possibly quark confinement at long distances or low energy.

The property of asymptotic freedom allows the use of perturbation theory for sufficiently short distance reactions. This approach is referred to as perturbative QCD. Application of QCD to deep inelastic scattering at the lowest-order was found to reproduce Bjorken scaling behavior, thus reducing to the Parton model. Moreover, it showed that Bjorken scaling holds only approximately and provided higher-order corrections [20–22]. These corrections were confirmed in deep inelastic muon-nucleon scatterings [23, 24].

Hagedorn [25] predicted the existence of a critical temperature even before the formulation of QCD. The correct interpretation of this critical behavior was given based on the property of asymptotic freedom of QCD by Cabibbo and Parisi [26]. They proposed the existence of a phase transition from hadrons to the underlying quark-gluon matter at sufficiently high temperatures. Shuryak coined the term quark-gluon plasma (QGP) to describe this new state of matter [27]. The experiments at the large hadron collider (LHC) provided evidence for the formation of the QGP. Initial expectations that the QGP would behave like a free gas of deconfined quarks and gluons were shown to be wrong when experiments carried out at the LHC and the relativistic heavy ion collider (RHIC) indicated that the QGP formed remained strongly coupled, near-perfect liquid even at significantly high energies [28–30].

1.2.2 QCD at zero temperature

The interactions of colored quarks are described by QCD, which is a non-abelian gauge theory. The quarks belong to the fundamental representation of the gauge group $SU(3)_C$, meaning that each quark has three components in color space [31],

$$
\psi = \begin{pmatrix} \psi_r \\ \psi_g \\ \psi_b \end{pmatrix}.
\tag{1.1}
$$

The local gauge invariance with respect to the $SU(3)$ rotations in color space introduces 8 gauge bosons, the number of generators for group $SU(3)$. Quarks are spin $\frac{1}{2}$ particles that belong to the fundamental representation of $SU(3)$. The gluons are spin 1 particles defined in the adjoint representation of $SU(3)$.

The QCD lagrangian is given as,

$$
\mathscr{L} = \underbrace{-\frac{1}{4}(F_{\mu\nu}^a)^2}_{\mathscr{L}_G} + \underbrace{\bar{\psi}\left(i\slashed{D} - m\right)\psi}_{\mathscr{L}_q},
\tag{1.2}
$$

with,

$$
\slashed{D}\psi = \gamma^\mu D_\mu \psi,
$$
$$
D_\mu \psi = \partial_\mu \psi - ig A_\mu^a F^a \psi,
$$
$$
F_{\mu\nu}^a = \partial_\mu A_\nu^a - \partial_\nu A_\mu^a + g f_{abc} A_\mu^b A_\nu^c.
\tag{1.3}
$$

$A^{\mu a}$ are the eight gauge fields, the quanta of which are called gluons. F^a are the generators of $SU(3)$ satisfying the commutation relations $\left[F^a, F^b\right] = i f^{abc} F^c$. f_{abc} are the group structure constants forming the adjoint representation of $SU(3)$, represented by 8×8 matrices under which the gluon field transforms. $F^{\mu\nu}$ transforms in this adjoint representation. The term $i\bar{\psi}\slashed{D}\psi = i\bar{\psi}\slashed{\partial}\psi + j^{\mu a} A_\mu^a$

8

describes the interactions of the gluons A^a_μ with the color current of the quarks $j^{\mu a}$. $j^{\mu a} = g\bar{\psi}\gamma^\mu F^a \psi$ is the Noether Current corresponding to color symmetry transformations. It is to be noted that the Lagrangian includes terms corresponding to vertices with three gluons and four gluons due to the non-abelian character of the theory.

Symmetries of $\mathscr{L}_{QCD}$

The classical QCD Lagrangian has a number of symmetries in the chiral limit, $m_q \to 0$.

The symmetry group for classical QCD Lagrangian apart from the Poincaré invariance is [32]

$$S[\mathscr{L}_{QCD}]_{cl} = SU(3)_c \otimes SU(N_f)_L \otimes SU(N_f)_R \otimes U(1)_V \otimes U(1)_A \otimes \mathcal{C}. \quad (1.4)$$

The $SU(3)_c$ local color symmetry determines the dynamics of the quark and gluon fields. The global symmetry $U(1)_V$ leads to Baryon number conservation. The axial $U(1)_A$ symmetry is broken at the quantum level due to what is known as the chiral anomaly.

$\mathcal{C}$ are global scale transformations in the Minkowski space. The corresponding conserved quantity is dilaton current. This is also a broken symmetry due to the introduction of a scale of Λ_{QCD} by Renormalization.

In the limit of vanishing quark masses, the classical QCD Lagrangian is invariant under global vector and axial-vector transformations in the flavor space of $SU(3)$. We can decompose the quark fields into right-handed and left-handed components $\psi_{R,L} = \frac{1}{2}(1 \pm \gamma_5)\psi$ giving a global $SU(3)_L \otimes SU(3)_R$ chiral symmetry in the flavor space. A consequence of this symmetry is that the associated parameter, the *condensate* $\langle\bar{q}q\rangle$ should be zero.

However, the *condensate* is not zero [33]. With $m_u = 5 MeV$ and $m_d =$

$7 MeV$, the quark condensate has value $\langle \bar{u}u \rangle = \langle \bar{d}d \rangle \approx -(250 MeV)^3$. Thus $SU(3)_L \otimes SU(3)_R$ is spontaneously broken. QCD explains the existence of Goldstone bosons (pions, kaons, and eta mesons) and their interaction cross-sections by predicting the spontaneous breaking of chiral symmetry. At high energies, the symmetry should be restored.

Quantization of QCD

The quantization can be carried out starting from the Faddeev-Popov Lagrangian [34],

$$\mathscr{L}_{FP} = -\frac{1}{4}(F_{\mu\nu}^a)^2 - \frac{1}{2\xi}(\partial^\mu A_\mu^a)^2 + \bar{\psi}(i\slashed{D} - m)\psi + \bar{c}^a(-\partial^\mu D_\mu^{ac})c^c, \qquad (1.5)$$

where, the anticommuting Lorentz scalars c and $\bar{c}$ are called the Faddeev-Popov ghosts and Faddeev-Popov antighosts respectively. The Feynman rules can be obtained from this Lagrangian [35].

The gauge-fixed Lagrangian is no more gauge invariant. However, it has a new symmetry called the BRST invariance [36, 37]. BRST invariance is essential in proving the renormalizability of non-abelian gauge theories.

1.2.3 Asymptotic freedom

At high energies the running coupling constant in Yang-Mills theories approaches zero. This property is known as asymptotic freedom. The expression for running coupling constant at the one-loop order in QCD is [38],

$$\alpha_s(\mid q \mid^2) = \frac{\alpha(\mu^2)}{1 + (\alpha_s(\mu^2)/12\pi)(11N_c - 2N_f)\ln(\mid q^2/\mid \mu^2)} \quad (\mid q^2 \mid \gg \mu^2),$$

$$(1.6)$$

where, N_c is the number of colors and N_f the number of flavors which are 3 and 6 respectively, in the standard model. μ is a parameter that is sufficiently large so that $\alpha_s(\mu^2) < 1$. It can be seen that the coupling constant decreases with increasing $\mid q^2 \mid$ (or small distances). This property is known as asymptotic freedom and leads to Bjorken scaling. This is how the successful parton model could be reconciled with the very strong binding forces between quarks.

The behavior of QCD at low energies or large distances is still not clear. This property is called 'infrared slavery' [39] and is not understood as rigorously as the property of asymptotic freedom. In these circumstances, the collective behavior may be easier to understand than the dynamics of the individual particles.

1.2.4 Lattice QCD

The property of asymptotic freedom allows perturbative QCD calculations for high energy processes. However, QCD should explain many other phenomena where perturbative calculations cannot be carried out. There are fundamental questions about the QCD vacuum structure, hadron masses, hadron structure, and nuclear properties, which ultimately should be explained by the underlying theory, QCD. The difficulty in applying perturbative calculations in the relevant energy domains calls for non-perturbative techniques. Many effective models have been developed to investigate the domain of hadronic and nuclear physics theoretically.

The lattice method for non-Abelian gauge theories is the most successful non-perturbative technique used to solve QCD equations. Lattice simulations are carried out by replacing space-time with a Euclidean lattice, which allows for theoretical understanding and computational analysis. It has become a standard tool used in particle physics. Lattice QCD calculations are carried out using the following steps [40].

1. The continuous space-time is replaced by a 4D Euclidean lattice with a lattice constant a. The Lattice constant has the physical dimension of length, and it serves as the ultraviolet regulator necessary to make expressions finite.

2. The spinors for quarks and antiquarks are defined at the lattice points only.

3. The gauge fields are introduced through link variables in order to make the fermionic action invariant under the local $SU(3)_c$ transformations. The link variables live on the link which connects the lattice sites.

4. The discrete action has all the relevant symmetries. It also satisfies the condition that it should reduce to the continuum action when the lattice spacing is taken to be zero (continuum limit).

5. All the measurable quantities associated with the strong force can be extracted from this action. The path integrals can be evaluated using Monte Carlo Methods.

1.2.5   QCD at finite temperature

QCD is formalized at zero temperature. However, the verification of consistency between theory and experiment may require studying field theories at finite temperature. A useful theoretical framework for that is known as thermal field theory [41].

All thermodynamic information of a system is incorporated in the the partition function, connectd to the statistical density matrix by,

$$\mathcal{Z}(T,V) = Tr[\rho] = Tr[e^{-\beta H}] = \sum_n \langle n \mid e^{-\beta E_n} \mid n \rangle, \tag{1.7}$$

where, $\beta = 1/T$ and H is the Hamiltonian operator. The trace is calculated by

choosing a complete set of physical eigenstates as basis. The statistical average of an operator is then,

$$\langle \mathcal{O} \rangle_\beta = \frac{1}{\mathcal{Z}} Tr[\rho \mathcal{O}]. \tag{1.8}$$

The statistical density operator $\rho = exp(-\beta H)$ is similar to the time evolution operator in imaginary time in the interval $[0, \beta]$. This identification allows expressing the partition function for the field in terms of a Euclidean path integral. In the case of the scalar field ϕ with lagrangian $\mathscr{L}[\phi]$, the partition function can be represented as,

$$\mathcal{Z}(T, V) = \int_{periodic} \mathcal{D}\phi \, exp\left(-\int_0^\beta d\tau \int_V d^3x \mathscr{L}_E[\phi(\tau, \vec{x})]\right), \tag{1.9}$$

where ϕ satisfies the periodic condition $\phi(0, \vec{x}) = \phi(\beta, \vec{x})$. Spinors for fermionic fields obey anti-periodic boundary conditions. L_E is the Euclidean version of $L[\phi]$. Field theory at finite temperature thus becomes a Euclidean field theory in four dimensinal space-time where the time component is compactified on a ring with circumference $\beta = 1/T$. The expection value of an operator can be found from

$$\langle \mathcal{O} \rangle_\beta = \frac{1}{\mathcal{Z}} \int_{periodic} \mathcal{D}\phi \, \mathcal{O}[\phi] \, exp\left(-\int_0^\beta d\tau \int_V d^3x \mathscr{L}_E[\phi(\tau, \vec{x})]\right). \tag{1.10}$$

The formal similarity of this expression to the generating functional allows both perturbative and lattice techniques to evaluate the expectation values.

For QCD, the partition function may be expressed as,

$$\mathcal{Z}(T, V, m_0, \mu) = \oint \mathcal{D}A_\mu \mathcal{D}\bar{\psi}\mathcal{D}\psi \, exp\left[- \int_0^\beta d\tau \int_V d^3x \Big(\mathscr{L}_E^G \right.$$

$$\left. + \mathscr{L}_E^q(m_q) - \mu\psi^\dagger\psi \Big) \right], \qquad (1.11)$$

where μ, the chemical potential, and m_q the bare quark mass are introduced as additional parameters.

1.3   The transition to QGP

In the nuclear matter at low energies, quarks and gluons are confined inside the nucleons. The energy density in these conditions is $\epsilon = 0.15 GeV/fm^3$ [42]. If the energy density increases beyond $1 GeV/fm^3$, the interaction between quarks and gluons becomes weaker due to the property of asymptotic freedom. Eventually, the quarks and gluons are deconfined, and the state of matter is called the QGP.

Such high energy densities are attained at increased temperature or density. QGP is believed to have existed at the early stages of the universe, up to a few microseconds after the Big Bang. The QGP state can occur in dense astrophysical objects such as neutron stars. Extreme conditions of density and temperature can be reproduced in high energy collisions happening in accelerators.

The paradigm of confinement has not yet been understood completely. Understanding of confinement requires dealing with non-perturbative physics, and the best available tool for that is Lattice QCD.

1.3.1   QCD phase diagram

There has been a lot of progress over the last 30 years in describing the QCD phase diagram. The complete description has yet to be developed. In Figure. 1.1
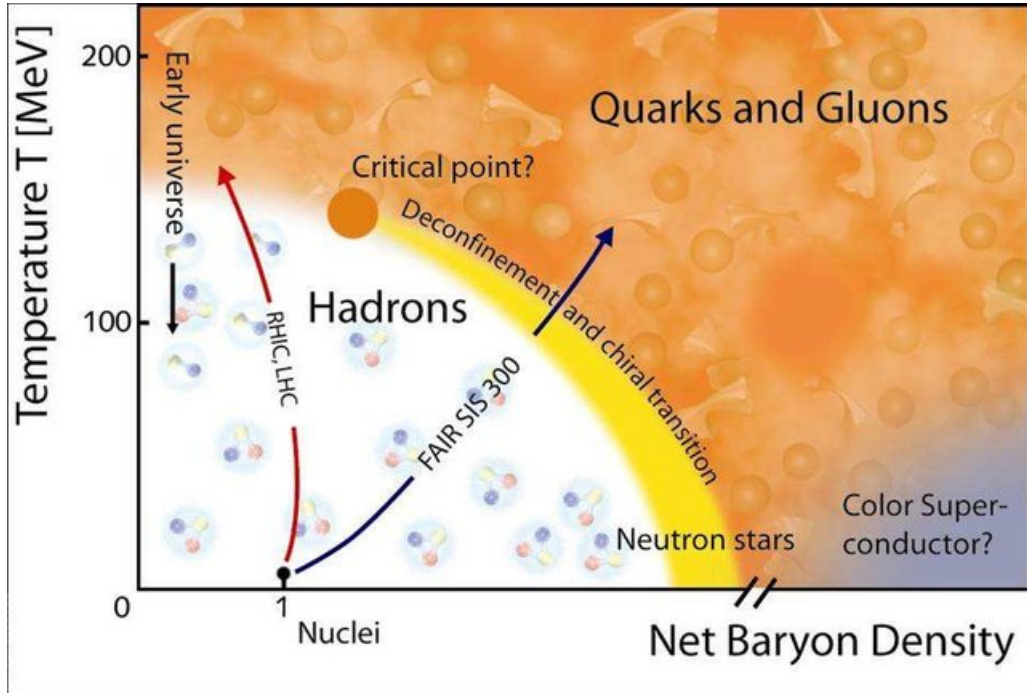
Figure 1.1: Sketch of the QCD phase diagram in the plane of temperature and baryon density.

we show a sketch of the contemporary version of the QCD phase diagram in the (μ_B, T) plane[1]. At low temperatures and low values of the Baryon-chemical potential, the system is in the hadronic phase. QCD matter enters in the phase described by color superconductivity as μ_B is increased at low temperatures [44]. The quarks and gluons are in a deconfined plasma phase at high temperatures, but low values of μ_B and the chiral symmetry is restored [45].

1.4 Phenomenological models for the QGP

The QGP, in principle, can be seen as a gas of quarks and gluons. However, a perturbative calculation with these degrees of freedom does not work well at all temperatures, due to the bad convergence properties of the perturbative series caused by infra-red sensitive contributions. The QCD lattice calculation is the

[1]Figure taken from Ref. [43].

only systematic and fully non-perturbative method available. Hence, various QCD-motivated models are used for describing the thermodynamics of deconfined hadronic matter and its equation of state (EoS). Phenomenological models of the QGP are theoretical models inspired by the behavior of the fundamental theory of strong interactions.

The MIT Bag model incorporates confinement and asymptotic freedom into a simple phenomenological model. The hadrons are considered as bags embedded into a non-perturbative QCD vacuum. The quarks are confined to the bags but can move about freely in the interior [46, 47].

The Cornell potential model [48–50] considers the QGP as consisting of quarks and gluons which interact via the Cornell potential.

The strongly coupled QGP model (SCQGP) [51, 52] is based on the Strongly Coupled Plasma (SCP) in QED. SCQGP model is a generalization of SCP with modifications to include color degrees of freedom and running coupling constant and provides a reasonably good fit to lattice results.

Quasiparticle models consider the QGP as a collection of ideal quasiparticles with effective mass [53]. Quasiparticle models include Nambu-Jona-Lasinio and PNJL based quasiparticle models [54–58] or those that include effective mass with the Polyakov loop [59–61]. There are also quasiparticle models based on Gribov-Zwanziger quantization [62]. Yet another class of quasiparticle models incorporates the medium-effects by considering quasiparticles with effective fugacities. Such models have been quite successful in describing the lattice QCD results [63, 64].

1.5   Magnetized QGP

High energy collisions have succeeded in recreating the state of matter called the QGP, which is believed to have existed shortly after the big bang. It has been observed that the QGP produced in high energy collisions behave very much like

a nearly perfect fluid [65–68].

These collisions mostly occur with a finite impact parameter. During off central collisions, the charged ions thus can produce a very large magnetic field reaching up to $eB \approx (1-15)m_\pi^2$ [66, 69]. The magnetic field may exist only for a short time, but depending on the transport coefficients, they may reach their maximum value and be stationary during this time [70–73]. The magnetic field can cause different phenomena, such as magnetic catalysis [74–77], chiral magnetic effect [78–80], etc., in the QGP. The equation of state is important for studying the particle spectra created in heavy-ion collisions. Strong magnetic fields are estimated to have existed right after the big bang [81]. Effects of an external magnetic field is relevant in the context of strongly magnetised neutron stars too [82–86]. Therefore, it is important to investigate the behavior of the QGP under the magnetic field, particularly the effect on the QCD thermodynamics [87, 88]. The theoretical tools used to study the QGP need modifications to incorporate effects of the external magnetic field, and there has been a flurry of research activity in this area [76, 77, 89–108]. Measurements at the LHC [109] are capable of providing new insights that can constrain the theoretical modeling. The equation of state has a significant impact on the evolution of the QGP [110].

1.6   Summary

According to the standard model of particle physics, quarks and leptons are the fundamental building blocks of the visible universe. Bosons carry the interaction between the primary constituents of matter. The theory of quarks and gluons is QCD. QCD predicts the existence of a deconfined state of matter, the QGP.

QCD is not easy to solve. Lattice QCD is one of the successful non-perturbative methods for studying QCD. Phenomenological models are useful in understanding the underlying physics of the QGP better. There are different phenomenological

models with varying success.

The QGP is produced during high energy collisions and relevant to the study of cosmology and dense stars. It has been noticed that strong magnetic fields can exist in these contexts. The efforts to modify the existing theory to include the effects of the external magnetic field have attracted huge interest. There has been a lot of research activity in the area.

Chapter 2

Quasiparticle description of QCD at finite temperature

2.1 Introduction

Quasiparticles models are phenomenological models, widely used to describe the QGP. In quasiparticle descriptions, the system is considered as a collection of effective degrees of freedom called quasiparticles. The thermal properties of interacting particles are modeled by noninteracting quasiparticles. The early development of the quasiprticle description to the QCD plasma can be traced back to the works of Biró [111], and Golovizin and Satz [112]. Subsequently, Peshier et al. [113] proposed a quasiparticle model to explain the equation of state of the QGP as obtained in Lattice Gauge Theory simulations of QCD.

It was Gorenstein and Yang [114] who pointed out that the naive quasiparticle model which considers QGP as an ideal gas of quasiparticles, with effective-masses, is thermodynamically inconsistent. They showed that the inconsistency could be remedied by introducing a temperature-dependent term called the vacuum energy. This method has been used in many quasiparticle models to ensure thermodynamic consistency [114–118].

Bannur, in a series of papers [119–124], showed how a thermodynamically consistent quasiparticle model could be constructed, without introducing ad-hoc terms like the vacuum energy. These works demonstrated that all thermodynamic quantities could be derived consistently, starting with the expressions for energy density and number density, and following standard statistical mechanics. The premise of this class of models is that total thermal energy is used to excite the quasiparticles. Such models have been able to obtain good results in good agreement with the lattice data.

Gardim and Steffens [125, 126] found a generalized formalism for quasiparticle description. They showed that there are many ways to render the thermodynamics of the system consistent and that the formulation due to Gorenstein and Bannur are special cases of this general formalism.

The quasiparticle models have generally been quite successful in describing the lattice data.

2.2   The self-consistent quasiparticle model

In quasiparticle models, the thermal properties of interacting real particles are modeled by non-interacting quasiparticles. The quasiparticles have an effective mass, determined by the collective properties of the medium [112, 113].

In the self-consistent quasiparticle model, QGP consists of non-interacting quasiparticles. The quasiparticles have effective masses that depend on thermodynamic quantities and encodes all medium interactions [119, 123]. The thermodynamic quantities depend on the thermal mass and the thermal mass depends on the thermodynamic quantitites. So, the whole problem is solved self-consistently. See appendix A for detailed calculations.

In the self-consistent model, following standard thermodynamics, all thermodynamic quantities are derived from the expressions for energy density and

number density. The expression for energy density is,

$$\varepsilon = \frac{g_f}{2\pi^2} \int_0^\infty dk \; k^2 \frac{\omega_k}{z_{q/g}^{-1} e^{\frac{\omega_k}{T}} \mp 1}, \tag{2.1}$$

where g_f is the degeneracy and $\mp$ refers to bosons and fermions. z is the fugacity. The expression for number density is,

$$n_{g/q} = \frac{g_f}{2\pi^2} \int_0^\infty dk \; k^2 \frac{1}{z_{q/g}^{-1} e^{\frac{\omega_k}{T}} \mp 1}. \tag{2.2}$$

The single particle energy ω_k is approximated to a simple form,

$$\omega_k = \sqrt{k^2 + m_g^2}, \tag{2.3}$$

and

$$\omega_k = \sqrt{k^2 + m_q^2}, \tag{2.4}$$

for gluons and quarks respectively. This approximation is valid at high temperatures only.

It is known that quasiparticles acquire "thermal mass" of order gT at one loop order [115, 127, 128]. In the model that we study here, the thermal mass is defined as proportional to the plasma frequencies as,

$$m_g^2 = \frac{3}{2}\omega_p^2 \quad \text{and} \quad m_q^2 = 2m_f^2, \tag{2.5}$$

for massless particles. For massive quarks m_q^2 is written as,

$$m_q^2 = (m_0 + m_f)^2 + m_f^2. \tag{2.6}$$

21

At zero chemical potential the plasma frequency can be calculated using the density dependent expressions,

$$\omega_p^2 = a_g^2 g^2 \frac{n_g}{T} + a_q^2 g^2 \frac{n_q}{T},$$ (2.7)

for gluons and,

$$m_f^2 = b_q^2 g^2 \frac{n_q}{T},$$ (2.8)

for quarks. Here n_q is the quark number density and n_g is is the gluon number density. $g^2 = 4\pi\alpha_s$ is the QCD running coupling constant. The coefficients a_g, a_q, b_q are determined by demanding that as $T \to \infty$, ω_p and m_f both go to the corresponding perturbative results (see A.3). The motivation for choosing such an expression for plasma frequency is that the plasma frequency for electron-positron plasma is known to be proportional to n/T in the relativistic limit [129, 130]. Since the thermal masses appear in the expression for the density, we need to solve the density equation self-consistently to obtain the thermal mass, which may be used to evaluate the thermodynamic quantities of interest. The result obtained have shown a good fit with lattice data even at temperatures near T_c [124].

The thermodynamic potential in the self-consistent quasiparticle model has the expression,

$$\frac{\Phi}{V} = -P = \pm T g_f \left[\int_0^\infty \frac{d^3k}{(2\pi)^3} \ln\left(1 \mp e^{-\beta\epsilon_k}\right) + \right.$$
$$\left. \int_{T_0}^T \frac{d\tau}{\tau} m \frac{\partial m}{\partial \tau} \int \frac{d^3k}{(2\pi)^3} \frac{1}{\epsilon_k \left(e^{\beta\epsilon_k} \mp 1\right)} \right],$$ (2.9)

where, $\pm$ is for gluons and quarks respectively. Eq. (2.9) is different from the corresponding expression for ideal gas. The second term ensures thermodynamic

consistency so that the relation,

$$\epsilon = T\frac{\partial P}{\partial T} - P,$$ (2.10)

is satisfied.

The quark plasma frequency m_f at non-zero chemical potential may be generalized to [123],

$$m_f^2 = \frac{b_q^2 g^2}{2}\left(\frac{n_q}{T} + \frac{n_{\bar{q}}}{T}\right).$$ (2.11)

Accordingly, the gluon plasma frequency becomes,

$$\omega_p^2 = a_g^2 g^2 \frac{n_g}{T} + a_q^2 g^2 \frac{1}{2}\left(\frac{n_q}{T} + \frac{n_{\bar{q}}}{T}\right).$$ (2.12)

As before, b_q, a_g and a_q can be obained by demanding that at high temperatures the plasma frequencies are equal to the perturbative results.

The self-consistent quasiparticle model has its own ansatz for the thermal masses, and this makes the model easily generalizable, as we shall see in later chapters.

2.3 Thermodynamic consistency problem

We have seen that the simple application of the quasiparticle description leads to thermodynamic inconsistencies. There are many ways in which a quasiparticle model can be made thermodynamically consistent. Gorenstein and Yang suggested reformulating statistical mechanics to make the quasiparticle models thermodynamically consistent. They introduced an ad-hoc term denoted as $B(T)$ so that the thermodynamic relations were satisfied. The physical interpretation of $B(T)$ is somewhat ambiguous. Different authors interpret it differently. They

call it the vacuum energy, the background field, or bag pressure.

Bannur, on the other hand, has shown that thermodynamic consistency can be ensured without any reformulation of statistical mechanics. The self-consistent quasiparticle model described above is an example of a thermodynamically consistent quasiparticle model with standard statistical mechanics. It requires no artificial manipulation of standard statistical mechanics to ensure consistency.

There is no consensus among the community in the solution to the thermodynamic consistency problem in effective mass quasiparticle models. However, we lean towards the solution by Bannur due to its simplicity and the need for no new terms with ambiguous physical interpretation. It requires fewer assumptions than other solutions and hence has the edge over them by the criterion of Occam's razor [131].

2.4   Summary

Quasiparticle models have been quite successful as phenomenological models in the study of the QGP. The simple application of the quasiparticle picture introduces thermodynamic inconsistencies and has to be modified. There are different classes of quasiparticle models which remedy the thermodynamic inconsistency problem in different ways. There exists a class of models that do not require the introduction of additional terms like vacuum energy. One such model, due to Bannur, is straightforward and has fewer assumptions than the models with reformulated statistical mechanics. They are preferable by the Occam's razor principle. The self-consistent quasiparticle model has been quite successful in describing QGP. In the self-consistent model, the quasiparticle masses are defined to be proportional to the number densities. So the only external ingredient needed for this model is the running coupling. The definition of quasiparticle masses in terms of number densities allows for natural generalization to different situations.

Chapter 3

The extended self-consistent quasiparticle model

3.1   Introduction

In the last chapter, we gave a brief outline of the self-consistent quasiparticle model. In this chapter, we present the theoretical formalism of what we call the extended self-consistent quasiparticle model. We modify the self-consistent quasiparticle model to study the effect of the external magnetic field on the equation of state of the QGP. We incorporate the magnetic field by altering the thermal mass using the relativistic Landau levels. Such modified masses in the magnetic field can be used to calculate thermodynamic quantities like energy density, pressure, and entropy density.

3.2 Extension of the self-consistent model in the presence of the magnetic field

The self-consistent quasiparticle model has to be modified to incorporate the effects of the magnetic field. The energy eigenvalues of fermions change in the presence of the magnetic field. Besides, the magnetic field's application makes the momentum of fermions quantized in the transverse direction. We must take both these factors into account. We proceed as follows.

The quantization of fermionic theory in the presence of the uniform magnetic field gives the energy eigenvalues as Landau Levels [132]. In the Landau gauge, $A_y = B_x$ so that $\mathbf{B} = B\hat{z}$ and the energy eigen values are obtained as,

$$E_j = \sqrt{m^2 + k_z^2 + 2j \mid q_f eB \mid}. \tag{3.1}$$

Here, $q_f e$ is the charge of the fermion and $j = 0, 1, 2, ...$ are the Landau energy levels.

The quantization of the momentum in the transverse plane can be incorporated by modifying the integrals over the phase space as [133–137],

$$\int \frac{d^3 k}{(2\pi)^3} \rightarrow \frac{\mid q_f eB \mid}{2\pi} \sum_{j=0}^{\infty} \int \frac{dk_z}{2\pi} \left(2 - \delta_{0j}\right), \tag{3.2}$$

where, $(2 - \delta_{0j})$ is the degeneracy of the jth Landau level [138].

Making these modifications in the self-consistent quasiparticle model allows us to define the quasiparticle mass, which depends on temperature and the magnetic field. We call it the thermomagnetic mass.

We focus primarily on the qualitative thermomagnetic behavior of magnetized QGP. So, the inclusion of the effects of dynamically generated anomalous magnetic moments(AMM) [139], as done in Refs. [87, 140] is out of the scope of our work.

Moreover, it has been demonstrated in Ref. [141], that the effect of AMM is not significant when it comes to the calculation of thermodynamic quantities of charged fermions. In the self-consistent quasiparticle model, the thermomagnetic mass is obtained from the density-dependent expression for plasma frequency. It follows that the contribution from AMM to the thermomagnetic mass is negligible. Since all quantities in this work are expressed in terms of the thermomagnetic mass, it is safe to say that AMM's exclusion does not affect our results in any significant manner.

3.3 Thermomagnetic mass for quarks

We have seen that the quasiparticle masses in the self-consistent quasiparticle model are defined as proportional to the number density. The expression for number density in the presence of the magnetic field can be obtained for a system at zero chemical potential by using Eqs. (3.1) and (3.2).

$$n_q = \frac{g_f q_f eB}{(2\pi)^2} \sum_{j=0}^{\infty} \left[(2 - \delta_{0j}) \int_{-\infty}^{\infty} dk_z \frac{1}{e^{\sqrt{(\frac{k_z}{T})^2 + (\frac{m_{qj}}{T})^2}} + 1} \right], \tag{3.3}$$

where, we have assigned for simplicity,

$$m_{q_j}^2 = m_q^2 + 2j|q_f eB|. \tag{3.4}$$

Defining $k_z/T = x$ and making the substitution, $x = \frac{m_{q_j}}{T} \sinh t$, in Eq. (3.3),

$$n_q = \frac{g_f q_f eB}{(2\pi)^2} \sum_{j=0}^{\infty} \left[(2 - \delta_{0j}) m_{q_j} \int dt \cosh t \frac{1}{e^{\frac{m_{q_j}}{T} \cosh t} + 1} \right]$$

$$= \frac{g_f q_f eB}{(2\pi)^2} \sum_{j=0}^{\infty} \left[(2 - \delta_{0j}) \sum_{l=1}^{\infty} (-1)^{(l-1)} m_{q_j} \int dt \cosh t e^{-l \frac{m_{q_j}}{T} \cosh t} \right]. \tag{3.5}$$

The integral can now be simplified by using the integral representation for the modified Bessel function,

$$K_\nu(z) = \int_0^\infty e^{-z \cosh t} \cosh(\nu t) dt. \tag{3.6}$$

We get,

$$n_q = \frac{T g_f q_f eB}{(2\pi)^2} \sum_{j=0}^\infty \left[(2 - \delta_{0j}) \sum_{l=1}^\infty (-1)^{(l-1)} \frac{m_{q_j}}{T} K_1 \left(l \frac{m_{q_j}}{T} \right) \right]. \tag{3.7}$$

We now define, for later convenience,

$$F_q^2 = \frac{(2\pi)^2}{2g_f |q_f eB|} \frac{n_q}{T^3}. \tag{3.8}$$

Now Eq. (3.7) can be written as,

$$T^2 F_q^2 = \sum_{j=0}^\infty (2 - \delta_{0j}) \sum_{l=1}^\infty (-1)^{(l-1)} \frac{m_{qj}}{T} K_1 \left(l \frac{m_{qj}}{T} \right). \tag{3.9}$$

For massive quarks, m_q can be obtained from Eq. (2.6), with m_f calculated just as in [123],

$$m_f^2 = c_q^2 g^2 \frac{n_q}{T}. \tag{3.10}$$

Or,

$$\begin{aligned} \left(\frac{m_f}{T} \right)^2 &= c_q^2 g^2 \frac{n_q}{T^3} \\ &= \bar{c}_q^2 F_q^2, \end{aligned} \tag{3.11}$$

where,

$$\bar{c}_q^2 = 2c_q^2 g^2 \frac{g_f |q_f eB|}{(2\pi)^2}.$$ (3.12)

Combining Eqs. (2.6), (3.4), and (3.11), we can write,

$$\left(\frac{m_{qj}}{T}\right)^2 = \left[\frac{m_0}{T} + \bar{c}_q Fq\right]^2 + \bar{c}_q^2 F_q^2 + 2j\frac{|q_f eB|}{T^2}.$$ (3.13)

Using (3.13) in Eq. (3.9), and simplifying the Kronecker δ we get,

$$
\begin{aligned}
T^2 F_q^2 = \sum_{l=1}^{\infty} (-1)^{(l-1)} \Bigg[& 2\sum_{j=0}^{\infty} \sqrt{\left[\frac{m_0}{T} + \bar{c}_q Fq\right]^2 + \bar{c}_q^2 F_q^2 + 2j\frac{|q_f eB|}{T^2}} \\
& K_1\left(l\sqrt{\left[\frac{m_0}{T} + \bar{c}_q Fq\right]^2 + \bar{c}_q^2 F_q^2 + 2j\frac{|q_f eB|}{T^2}}\right) \\
& - \sqrt{\left[\frac{m_0}{T} + \bar{c}_q Fq\right]^2 + \bar{c}_q^2 F_q^2}\, K_1\left(l\sqrt{\left[\frac{m_0}{T} + \bar{c}_q Fq\right]^2 + \bar{c}_q^2 F_q^2}\right) \Bigg].
\end{aligned}
$$ (3.14)

We calculate the thermomagnetic mass by solving Eq. (3.14) and then substituting it back in Eq. (3.13). We can now consider the system as a collection of non-interacting quasiparticles with mass depending on both temperature and the magnetic field, allowing us to study thermodynamics.

3.4   Thermomagnetic mass for gluons

The density-dependent expression for plasma frequency for gluons is given by Eq. (2.7). The expression for gluon number density n_g remains unchanged because gluons have no electric charge and are not directly affected by the magnetic field. However, they are indirectly affected by their coupling to the electrically charged quarks. Thus the term n_q changes as explained, and so the gluons also acquire a thermomagnetic mass.

For gluons,

$$\omega_p^2 = a_g g^2 \frac{n_g}{T} + a_q^2 g^2 \frac{n_q}{T}, \tag{3.15}$$

$$m_g^2 = \frac{3}{2}\omega_p^2, \tag{3.16}$$

So,

$$m_g = \frac{3}{2}a_g^2 g^2 \frac{n_g}{T} + \frac{3}{2}a_q^2 g^2 \frac{n_q}{T}. \tag{3.17}$$

Since gluons are chargeless and are not affected by the magnetic field, we have for the number density,

$$n_g = \frac{g_g}{2\pi^2} \int_0^\infty dk k^2 \frac{1}{e^{\omega_k/T} - 1} \tag{3.18}$$

$$= \frac{g_g}{2\pi^2} \int_0^\infty dk k^2 \frac{1}{e^{\frac{1}{T}\sqrt{k^2 + \frac{3}{2}a_g^2 g^2 \frac{n_g}{T} + \frac{3}{2}a_q^2 g^2 \frac{n_q}{T}}} - 1}, \tag{3.19}$$

where,

$$\omega_k = \sqrt{k^2 + m_g^2}. \tag{3.20}$$

Put $x = K/T$; i.e, $dk = Tdx$,

$$n_g = \frac{g_g}{2\pi^2} \int_0^\infty dx x^2 \frac{1}{e^{\sqrt{x^2 + \frac{3}{2}a_g^2 g^2 \frac{n_g}{T^3} + \frac{3}{2}a_q^2 g^2 \frac{n_q}{T^3}}} - 1}. \tag{3.21}$$

Now we define,

$$\frac{2\pi^2}{g_g}\frac{n_g}{T^3} = f_g^2. \tag{3.22}$$

So,

$$\frac{n_g}{T^3} = \frac{g_g}{2\pi^2} f_g^2,$$

$$\text{or,} \quad \frac{3}{2} a_g^2 g^2 \frac{n_g}{T^3} = \frac{3}{2} a_g^2 g^2 \frac{g_g}{2\pi^2} f_g^2 = \bar{a}_g^2 f_g^2 \tag{3.23}$$

where,

$$\bar{a}_g^2 = \frac{3}{4\pi^2} g_g a_g^2 g^2. \tag{3.24}$$

We already have, from equation (3.8),

$$\frac{n_q}{T^3} = \frac{F_q^2 g_f |q_f eB|}{(2\pi)^2}. \tag{3.25}$$

So,

$$\frac{3}{2} a_q^2 g^2 \frac{n_q}{T^3} = \frac{3}{2} a_q^2 g^2 \frac{F_q^2 g_f |q_f eB|}{(2\pi)^2} = \bar{d}_q^2 F_q^2. \tag{3.26}$$

where,

$$\bar{d}_q^2 = \frac{3}{2} \frac{a_q^2 g^2}{(2\pi)^2} g_f |q_f eB|. \tag{3.27}$$

Combining Eqs. (3.22), (3.23) and (3.26) with (3.21) we can write,

$$f_g^2 = \int_0^\infty dx \, x^2 \frac{1}{e^{\sqrt{x^2 + \bar{a}_g^2 f_g^2 + \bar{d}_q^2 F_q^2}} - 1}. \tag{3.28}$$

We make the substitution $x^2 = (\bar{a}_g^2 f_g^2 + \bar{d}_q^2 F_q^2) \sinh^2 t$. Then,

$dx = dt(\bar{a}_g^2 f_g^2 + \bar{d}_q^2 F_q^2)^{\frac{1}{2}} \cosh t$. So,

$$f_g^2 = (\bar{a}_g^2 f_g^2 + \bar{d}_q^2 F_q^2)^{\frac{3}{2}} \int_0^\infty dt \cosh t \sinh^2 t \frac{1}{e^{(\bar{a}_g^2 f_g^2 + \bar{d}_q^2 F_q^2)^{\frac{1}{2}} \cosh t} - 1},$$

$$= (\bar{a}_g^2 f_g^2 + \bar{d}_q^2 F_q^2)^{\frac{3}{2}} \int_0^\infty dt \cosh t \sinh^2 t \sum_{l=1}^\infty e^{-l(\bar{a}_g^2 f_g^2 + \bar{d}_q^2 F_q^2)^{\frac{1}{2}} \cosh t}$$

$$= (\bar{a}_g^2 f_g^2 + \bar{d}_q^2 F_q^2)^{\frac{3}{2}} \sum_{l=1}^\infty \int_0^\infty dt \cosh t [\cosh^2 t - 1] e^{-l(\bar{a}_g^2 f_g^2 + \bar{d}_q^2 F_q^2)^{\frac{1}{2}} \cosh t}.$$

Let us use the notation $F_{gq} = \bar{a}_g^2 f_g^2 + \bar{d}_q^2 F_q^2$, for simplicity. Thus,

$$f_g^2 = F_{gq}^{3/2} \sum_{l=1}^\infty \int_0^\infty dt \left(-\cosh t e^{-lF_{gq}^{1/2} \cosh t} + \cosh^3 t e^{-lF_{gq}^{1/2} \cosh t} \right)$$

$$= F_{gq}^{3/2} \sum_{l=1}^\infty \left(-K_1[lF_{gq}^{1/2}] + \int_0^\infty dt \left(\frac{\cosh 3t + 3\cosh t}{4} \right) e^{-lF_{gq}^{1/2} \cosh t} \right)$$

$$= F_{gq}^{3/2} \sum_{l=1}^\infty \left(-K_1[lF_{gq}^{1/2}] + \frac{1}{4} K_3[lF_{gq}^{1/2}] + \frac{3}{4} K_1[lF_{gq}^{1/2}] \right)$$

$$= F_{gq}^{3/2} \sum_{l=1}^\infty \left(\frac{K_3[lF_{gq}^{1/2}]}{4} - \frac{K_1[lF_{gq}^{1/2}]}{4} \right) . \text{Or,}$$

$$f_g^2 = \frac{(\bar{a}_g^2 f_g^2 + \bar{d}_q^2 F_q^2)^{3/2}}{4} \sum_{l=1}^\infty \left(K_3[l(\bar{a}_g^2 f_g^2 + \bar{d}_q^2 F_q^2)^{1/2}] \right.$$

$$\left. - K_1[l(\bar{a}_g^2 f_g^2 + \bar{d}_q^2 F_q^2)^{1/2}] \right). \tag{3.29}$$

Using the relation

$$K_{\nu-1}(x) - K_{\nu+1}(x) = -\frac{2\nu}{x} K_\nu(x), \tag{3.30}$$

we may further have,

$$f_g^2 = \frac{(\bar{a}_g^2 f_g^2 + \bar{d}_q^2 F_q^2)^{3/2}}{4} \sum_{l=1}^{\infty} \left(\frac{4}{l(\bar{a}_g^2 f_g^2 + \bar{d}_q^2 F_q^2)^{1/2}} K_2[l(\bar{a}_g^2 f_g^2 + \bar{d}_q^2 F_q^2)^{1/2}] \right),$$

or,

$$f_g^2 = (\bar{a}_g^2 f_g^2 + \bar{d}_q^2 F_q^2) \sum_{l=1}^{\infty} \frac{1}{l} K_2[l(\bar{a}_g^2 f_g^2 + \bar{d}_q^2 F_q^2)^{1/2}]. \tag{3.31}$$

F_q is obtained as a solution to (3.14). Now, solving Eq. (3.31) for f_g using the above, we obtain the thermo-magnetic mass using,

$$\left(\frac{m_g}{T} \right)^2 = \bar{a}_g^2 f_g^2 + \bar{d}_q^2 F_q^2. \tag{3.32}$$

The coefficients c_q, a_g and d_q are determined by demanding that as $T \to \infty$ the expression for frequency approaches the corresponding perturbative QCD results.

3.5 QCD Thermodynamics in uniform magnetic field

In this section, we shall obtain the general expressions for energy density, thermodynamic pressure, thermodynamic potential, and entropy density for magnetized QGP within the self-consistent quasiparticle model. These expressions will be used later to make numerical calculations of thermodynamic quantities.

3.5.1 Energy density

We start by calculating the expression for energy density of the magnetized QGP. The quark/antiquark contribution to the energy density get modified in the presence of the magnetic field. Using Eqs. (2.1), (3.1) and (3.2) the contribution

33

to the energy density from quarks becomes,

$$\varepsilon_q = \frac{12 n_q |q_f eB|}{4\pi^2} \sum_{j=0}^{\infty} (2 - \delta_{0j}) \int_{-\infty}^{\infty} dk_z \frac{\omega_{k_{zj}}}{e^{\omega_{k_{zj}}/T} + 1} \tag{3.33}$$

$$= \frac{12 n_q |q_f eB|}{2\pi^2} \sum_{j=0}^{\infty} (2 - \delta_{0j}) I_q,$$

$$I_q = \int_0^{\infty} dk_z \frac{\omega_{k_{zj}}}{e^{\omega_{k_{zj}}/T} + 1}, \tag{3.34}$$

where,

$$\omega_{k_{zj}} = \sqrt{m_q^2 + k_z^2 + 2j|q_f eB|} \tag{3.35}$$

$$= \sqrt{m_{q_j}^2 + k_z^2}. \tag{3.36}$$

The integration in Eq. (3.34) can be simplified as follows.

$$I_q = \int_0^{\infty} dk_z \frac{\omega_{k_{zj}}}{e^{\omega_{k_{zj}}/T} + 1} \tag{3.37}$$

$$= \sum_{l=1}^{\infty} (-1)^{l-1} \int_0^{\infty} dk_z \omega_{k_{zj}} e^{-l\omega_{k_{zj}}/T}$$

$$= \sum_{l=1}^{\infty} (-1)^{l-1} \int_0^{\infty} dk_z \sqrt{k_z^2 + m_{qj}^2} e^{-l\sqrt{(\frac{k_z}{T})^2 + (\frac{m_{qj}}{T})^2}}$$

$$= \sum_{l=1}^{\infty} (-1)^{l-1} \int_0^{\infty} dx T \sqrt{x^2 T^2 + m_{qj}^2} e^{-l\sqrt{x^2 + (\frac{m_{qj}}{T})^2}}$$

$$= T^2 \sum_{l=1}^{\infty} (-1)^{l-1} \int_0^{\infty} dx \sqrt{x^2 + \left(\frac{m_{qj}}{T}\right)^2} e^{-l\sqrt{x^2 + (\frac{m_{qj}}{T})^2}}, \tag{3.38}$$

where we have made the substitution $\frac{k_z}{T} = x$.

Now, further substituting $x^2 = (m_q/T)^2 \sinh^2 t$,

$$
\begin{aligned}
I_q &= T^2 \left(\frac{m_{qj}}{T}\right)^2 \sum_{l=1}^{\infty} (-1)^{l-1} \int_0^{\infty} dt \cosh^2 t\, e^{-l\frac{m_{qj}}{T}\cosh t} \\
&= T^2 \left(\frac{m_{qj}}{T}\right)^2 \sum_{l=1}^{\infty} (-1)^{l-1} \int_0^{\infty} dt \frac{\cosh 2t + 1}{2} e^{-l\frac{m_{qj}}{T}\cosh t} \\
&= \frac{T^2}{2} \left(\frac{m_{qj}}{T}\right)^2 \sum_{l} (-1)^{l-1} \int_0^{\infty} dt \left[\cosh 2t\, e^{-l\left(\frac{m_{qj}}{T}\right)\cosh t} + e^{-l\left(\frac{m_{qj}}{T}\right)\cosh t}\right] \\
&= \frac{T^2}{2} \left(\frac{m_{qj}}{T}\right)^2 \sum_{l} (-1)^{l-1} \left[K_2\left(\frac{m_{qj}}{T}\right) + K_0\left(\frac{m_{qj}}{T}\right)\right].
\end{aligned}
\tag{3.39}
$$

Now, making use of the recurrence relation, Eq. (3.30), we can write,

$$
K_2(x) - K_0(x) = \frac{2}{x} K_1(x)
\tag{3.40}
$$

$$
\Rightarrow K_2(x) + K_0(x) = \frac{2}{x} K_1(x) + 2K_0(x).
\tag{3.41}
$$

Thus,

$$
\begin{aligned}
I_q &= \frac{T^2}{2} \left(\frac{m_{qj}}{T}\right)^2 \sum_{l} (-1)^{l-1} \left[\frac{2}{l\frac{m_{qj}}{T}} K_1\left(l\frac{m_{qj}}{T}\right) + 2K_0\left(l\frac{m_{qj}}{T}\right)\right] \\
&= \frac{T^2}{2} \sum_{l} \frac{(-1)^{l-1}}{l^2} \left[2\left(l\frac{m_{qj}}{T}\right) K_1\left(l\frac{m_{qj}}{T}\right) + 2\left(l\frac{m_{qj}}{T}\right)^2 K_0\left(l\frac{m_{qj}}{T}\right)\right].
\end{aligned}
\tag{3.42}
$$

Thus we have, for quarks,

$$
I_q = \int_0^{\infty} dk_z \frac{\sqrt{m_{qj}^2 + k_z^2}}{e^{\frac{1}{T}\sqrt{m_{qj}^2 + k_z^2}} + 1}
\tag{3.43}
$$

$$
= T^2 \sum_{l=0}^{\infty} \frac{(-1)^{(l-1)}}{l^2} \left[\left(l\frac{m_{qj}}{T}\right) K_1\left(l\frac{m_{qj}}{T}\right) + \left(l\frac{m_{qj}}{T}\right)^2 K_0\left(l\frac{m_{qj}}{T}\right)\right].
\tag{3.44}
$$

With this, and $1/T = \beta$, Eq. (3.33) becomes,

$$\varepsilon_q = \frac{12n_q|q_f eB|}{2\pi^2}\frac{T^2}{2}\sum_{l=0}^{\infty}\frac{(-1)^{(l-1)}}{l^2}\left\{\sum_{j=0}^{\infty}(2-\delta_{0j})\right.$$
$$\left.\times\left[\left(\beta m_{q_j}l\right)K_1\left(\beta m_{q_j}l\right)+\left(\beta m_{q_j}l\right)^2 K_0\left(\beta m_{q_j}l\right)\right]\right. .$$
(3.45)

The expression for the energy density of gluons remains unchanged as they are chargeless. The energy density is indirectly affected by the interaction with quarks, included through the thermomagnetic mass of gluons.

$$\varepsilon_g = \frac{g_g T^4}{2\pi^2}\sum_{l=1}^{\infty}\frac{1}{l^4}\left[\left(\beta m_g l\right)^3 K_1\left(\beta m_g l\right)+3\left(\beta m_g l\right)^2 K_2\left(\beta m_g l\right)\right].$$
(3.46)

The contribution to energy density from quarks and gluons is obtained as

$$\varepsilon = \varepsilon_g + \sum_q \varepsilon_q.$$
(3.47)

3.5.2 Thermodynamic pressure

Here we concern ourselves with the calculation of the thermodynamic pressure or longitudinal pressure. It is the contribution to the total pressure from quarks and gluons. We denote this as P. We shall discuss the pressure anisotropy and the Maxwell contribution to the pressure in the next chapter. The expression for pressure in the self-consistent quasiparticle model is [120],

$$\frac{P_{g/q}}{T} = \mp\frac{g_f}{8\pi^3}\int_0^{\infty}d^3k\ln\left(1\mp e^{-\beta\omega_k}\right)$$
$$+\int d\beta\,\beta\frac{g_f}{8\pi^3}m\frac{dm}{d\beta}\int_0^{\infty}d^3k\frac{1}{\omega_k\left(e^{\beta\omega_k}\mp 1\right)},$$
(3.48)

where $\mp$ for bosons and fermions respectively. The contribution to the thermodynamic pressure from quarks can be obtained by changing the integral and energy

eigenvalues according to Eqs. (3.2) and (3.1). Making these changes, we have,

$$\frac{P_q}{T} = 2\frac{g_f q_f eB}{(2\pi)^2} \sum_{j=0}^{\infty} (2 - \delta_{0j}) \left[I_1 + \int d\beta \beta m_{q_j} \frac{\partial m_{q_j}}{\partial \beta} I_2 \right], \tag{3.49}$$

where,

$$I_1 = \int_0^{\infty} dk_z \ln \left(1 + e^{-\beta \omega_{k_{z_j}}} \right), \tag{3.50}$$

$$I_2 = \int_0^{\infty} dk_z \frac{1}{\omega_{k_{z_j}} \left(e^{\beta \omega_{k_{z_j}}} + 1 \right)}. \tag{3.51}$$

With $\omega_{k_{z_j}}$ from Eq. (3.35),

$$I_1 = \sum_{l=1}^{\infty} \frac{(-1)^{l-1}}{l} \int dk_z e^{-l\beta \sqrt{k_z^2 + m_{q_j}^2}}. \tag{3.52}$$

We have used the relation, $\ln(1 + x) = \sum_{l=1}^{\infty} (-1)^{l-1} x^l / l$. Now, using $x = k_z/T$ and making the substitution $x^2 = (m_q/T)^2 \sinh^2 t$,

$$I_1 = \sum_{l=1}^{\infty} \frac{(-1)^l}{l} m_{q_j} \int dt \cosh t\, e^{-\beta l m_{q_j} \cosh t}$$

$$= \sum_{l=1}^{\infty} \frac{(-1)^l}{l} m_{q_j} K_1(\beta m_{q_j} l). \tag{3.53}$$

We have made use of Eq. (3.6).

Making use of the binomial expansion, $(1 + x)^{-1} = \sum_{l=0}^{\infty} (-1)^l x^l$ and the same substitutions in the calculation of I_1, we get,

$$I_2 = \sum_{l=0}^{\infty} (-1)^{(l)} \int_0^{\infty} dt e^{-\beta m_{q_j} \cosh t} e^{-\beta l m_{q_j} \cosh t}$$

$$= \sum_{l=1}^{\infty} (-1)^{(l-1)} \int_0^{\infty} dt e^{-\beta l m_{q_j} \cosh t}, \tag{3.54}$$

37

which, using Eq. (3.6) gives,

$$I_2 = \sum_{l=1}^{\infty} (-1)^{l-1} K_0(\beta l m_{q_j}).$$

(3.55)

Using Eqs. (3.53) and Eq. (3.55) in Eq. (3.49) gives,

$$\beta P_q = \frac{g_f |q_f e B|}{2\pi^2} \sum_{l=1}^{\infty} \frac{(-1)^{l-1}}{l} \sum_{j=0}^{\infty} (2 - \delta_{0j})$$
$$\left[\frac{1}{\beta l} (\beta m_{q_j} l) K_1(\beta m_{q_j} l) + \int d\beta \, \frac{\partial m_{q_j}}{\partial \beta} (\beta m_{q_j} l) K_0(\beta m_{q_j} l) \right].$$

(3.56)

The contribution to the pressure from gluons can be obtained by replacing the thermal mass by thermo-magnetic mass. From Eq. (3.48), we can write the contribution from gluons as,

$$\frac{P_g}{T} = \frac{g_g}{2\pi^2} \sum_{l=1}^{\infty} \frac{1}{l^4} \left[T^3 (\beta m_g l)^2 K_2(\beta m_g l) \right.$$
$$\left. + \int d\beta \, \frac{\beta}{m_g} \frac{\partial m_g}{\partial \beta} \frac{1}{\beta^4} (\beta m_g l)^3 K_1(\beta m_g l) \right].$$

(3.57)

3.5.3 Entropy Density

Another important quantity is the entropy density. It can be calculated from the relations for energy density and pressure using the following thermodynamic relation,

$$s = \frac{\varepsilon + P}{T}.$$

(3.58)

38

Using Eqs. (3.45) and (3.56) we get for quarks,

$$s_q = \frac{g_f|q_f eB|}{2\pi^2\beta} \sum_{l=1}^{\infty} \frac{(-1)^{l-1}}{l^2} \sum_{j=0}^{\infty}(2 - \delta_{0j})$$

$$\left[\frac{3}{2}(\beta m_{q_j}l)K_1(\beta m_{q_j}l) + (\beta m_{q_j}l)^2 K_0(\beta m_{q_j}l)\right.$$

$$\left. + \beta \int d\beta \frac{\partial(m_{q_j}l)}{\partial\beta}(\beta m_{q_j}l)K_0(\beta m_{q_j}l)\right]. \tag{3.59}$$

The expression for entropy density for gluons can be found using Eqs. (3.58), (3.46), and (3.58).

$$s_g = \frac{g_g}{2\pi^2\beta^3} \sum_{l=1}^{\infty} \left[4\left(\beta m_g l\right)^2 K_2\left(\beta m_g l\right) + (\beta m_g l)^3 K_1(\beta m_g l)\right.$$

$$\left. \beta^3 \int d\beta \frac{\beta}{m_g} \frac{\partial m_g}{\partial\beta} \frac{1}{\beta^4}(\beta m_g l)^3 K_1(\beta m_g l)\right]. \tag{3.60}$$

3.5.4 Grand canonical potential

The grand canonical potential for magnetized QGP within the self-consistent quasiparticle model for quarks is,

$$\frac{\Phi_q}{V} = -P_q = -T\frac{g_f q_f|eB|}{2\pi^2} \sum_{l=1}^{\infty}(-1)^{l-1} \sum_{j=0}^{\infty}(2 - \delta_{0j})\left[\frac{T}{l^2}\frac{m_{q_j}l}{T}K_1\left(\frac{m_{q_j}l}{T}\right)\right.$$

$$\left. + \int_{T_0}^{T} \frac{d\tau}{\tau}\, m_{q_j}\frac{\partial m_{q_j}}{\partial\tau}K_0\left(\frac{m_{q_j}l}{\tau}\right)\right]. \tag{3.61}$$

The contribution from gluons is,

$$\frac{\Phi_g}{V} = -P_g = -T\frac{g_f}{2\pi^2} \sum_{l=1}^{\infty} \frac{1}{l^4}\left[T^3\left(\frac{m_g l}{T}\right)^2 K_2\left(\frac{m_g l}{T}\right)\right.$$

$$\left. + \int_{T_0}^{T} \frac{d\tau}{m_g}\,\tau^3 \frac{\partial m_g}{\partial\tau}\left(\frac{m_g l}{\tau}\right)^3 K_1\left(\frac{m_g l}{\tau}\right)\right]. \tag{3.62}$$

Here, T_0 is some reference temperature, suitably chosen. We have considered a system with zero chemical potential ($\mu = 0$). Note that in the self-consistent quasiparticle model, the relationship between the grand canonical potential and the grand partition function is more complicated. The relation,

$$\Phi = -KT \log \mathcal{Z}, \tag{3.63}$$

between the grand canonical potential and the grand partition function $\mathcal{Z}$ does not hold. There is an additional term due to the temperature dependence of the masses, ensuring thermodynamic consistency, as shown in Ref. [120].

3.5.5 Speed of sound

The velocity of sound is a fundamental quantity that is used in the description of hot QCD medium. The velocity of sound square c_s^2 is given by,

$$c_s^2 = \frac{\partial P}{\partial \varepsilon} = \frac{dP/dT}{d\varepsilon/dT}, \tag{3.64}$$

where, ε is the energy density which can be found using Eq. (3.45). Alternatively, it can be obtained from the pressure using the thermodynamic relation,

$$\varepsilon = T\frac{\partial P}{\partial T} - P. \tag{3.65}$$

The speed of sound in magnetized QGP medium can be calculated using these equations.

3.6 Energy scale hierarchy

The lowest Landau level (LLL) approximation can be used in the strong magnetic field limit, $T \ll \sqrt{|q_f eB|}$. For a more realistic regime $gT \ll \sqrt{|q_f eB|}$ the higher Landau level (HLL) are significant and have to be included in the calculations [94].

3.7 Thermodynamic consistency of the extended self-consistent quasiparticle model

It remains to be shown that the self-consistent quasiparticle model, when extended to include the effects of the external magnetic field, stays thermodynamically consistent. The gluon case is straightforward as the expressions for energy density and pressure are the same as those in the self-consistent quasiparticle model. We need to show that the expressions for energy density and pressure for quarks obey the thermodynamic consistency relation,

$$\varepsilon = T\frac{\partial P}{\partial T} - P, \tag{3.66}$$

$$= -\frac{\partial}{\partial \beta}(\beta P). \tag{3.67}$$

We start by differentiating Eq. (3.56) with respect to β,

$$\frac{\partial(\beta P_q)}{\partial \beta} = \frac{g_f |q_f eB|}{2\pi^2} \sum_{l=1}^{\infty} \frac{(-1)^{l-1}}{l} \sum_{j=0}^{\infty}(2 - \delta_{0j})\left[D_1 + D_2\right], \tag{3.68}$$

where,

$$D_1 = \frac{\partial}{\partial \beta}\left[m_{q_j}K_1(\beta m_{q_j}l)\right], \tag{3.69}$$

and

$$D_2 = \frac{\partial}{\partial \beta} \left[\int d\beta \, \frac{\partial m_{q_j}}{\partial \beta} (\beta m_{q_j} l) K_0(\beta m_{q_j} l) \right]. \tag{3.70}$$

We simplify the derivative D_1 using the relation,

$$\frac{\partial K_\nu(z)}{\partial z} = \frac{\nu}{z} K_\nu(z) - K_{\nu+1}(z), \tag{3.71}$$

to get,

$$\begin{aligned}
D_1 &= K_1(\beta m_{q_j} l) \frac{\partial m_{q_j}}{\partial \beta} - K_0(\beta m_{q_j} l) \left[\frac{m_{q_j}^2 l}{2} + \frac{\beta m_{q_j} l}{2} \frac{\partial m_{q_j}}{\partial \beta} \right] \\
&\quad - K_2(\beta m_{q_j} l) \left[\frac{m_{q_j}^2 l}{2} + \frac{\beta m_{q_j} l}{2} \frac{\partial m_{q_j}}{\partial \beta} \right] \\
&= K_1(\beta m_{q_j} l) \frac{\partial m_{q_j}}{\partial \beta} \\
&\quad - \left[\frac{m_{q_j}^2 l}{2} + \frac{\beta m_{q_j} l}{2} \frac{\partial m_{q_j}}{\partial \beta} \right] \left[K_0(\beta m_{q_j} l) + K_2(\beta m_{q_j} l) \right].
\end{aligned}$$

Making use of Eq. (3.41),

$$\begin{aligned}
D_1 &= K_1(\beta m_{q_j} l) \frac{\partial m_{q_j}}{\partial \beta} \\
&\quad - \left[\frac{m_{q_j}^2 l}{2} + \frac{\beta m_{q_j} l}{2} \frac{\partial m_{q_j}}{\partial \beta} \right] \left[\frac{2}{\beta m_{q_j} l} K_1(\beta m_{q_j} l) + 2 K_0(\beta m_{q_j} l)) \right]. \tag{3.72}
\end{aligned}$$

We also have,

$$D_2 = \frac{\partial m_{q_j}}{\partial \beta} (\beta m_{q_j} l) K_0(\beta m_{q_j} l). \tag{3.73}$$

Substituting Eqs. (3.72) and (3.73) in Eq. (3.68), and simplifying, we get,

$$-\frac{\partial}{\partial\beta}(\beta P) = \frac{g_f|q_f eB|}{2\pi^2}\frac{T^2}{2}\sum_{l=1}^{\infty}\frac{(-1)^{(l-1)}}{l^2}\left\{\sum_{j=0}^{\infty}(2-\delta_{0j})\right.$$
$$\left.\times\left[\left(\beta m_{q_j}l\right)K_1\left(\beta m_{q_j}l\right)+\left(\beta m_{q_j}l\right)^2 K_0\left(\beta m_{q_j}l\right)\right]\right\},\qquad(3.74)$$

which is exactly the expression for energy density in Eq. (3.45). Thus, we have shown that the extended self-consistent quasiparticle model is thermodynamically consistent. So, the thermodynamic pressure can also be obtained from the energy density. Solving Eq. (3.66),

$$\frac{P}{T} = \frac{P_0}{T_0} + \int_{T_0}^{T}d\tau\frac{\varepsilon}{\tau^2}.\qquad(3.75)$$

Here, P_0 and T_0 are pressure and temperature at some reference points [121].

3.8   Summary

The extended self-consistent quasiparticle model is a modification of the self-consistent quasiparticle model to incorporate the magnetic field's effects. In the modified model, the quasiparticle mass becomes a function of both temperature and the magnetic field. Landau level quantization, together with the modification of phase space integrals in the magnetic field, allows for calculating the thermomagnetic mass and the various thermodynamic quantities. The extended self-consistent quasiparticle model satisfies the thermodynamic consistency relation.

Chapter 4

Thermodynamics of 2 and $(2+1)$ flavor magnetized QGP

4.1   Introduction

In this chapter, we use the formalism developed in Ch. 3 to study the thermodynamic behavior of the magnetized QGP. We will study the energy density, pressure, entropy density, and speed of sound and examine how the thermodynamics are affected by the external magnetic field. The only external ingredient we need to obtain the thermodynamics using our model is the thermomagnetic coupling. We shall make use of two of different parametrizations available in the literature.

We organize this chapter as follows. Sec. 4.2 gives the different parametrizations of the thermomagnetic coupling that we use. Sec. 4.3 we study the thermodynamic behavior of the magnetize QGP. We begin with studying the thermodynamics of a 2flavor magnetized QGP in Sec. 4.3.1 by looking at the behavior of energy density, pressure, and entropy density. We also look at how the difference between these quantities with the corresponding zero-magnetic field results evolve. In Sec. 4.3.2 we go on to study the thermodynamics of a magnetized,

$(2 + 1)$ flavor, QGP. We study thermodynamics by examining the behavior of the thermodynamic pressure, entropy density, and speed of sound. We summarize the chapter in Sec. 4.4.

4.2 The thermomagnetic Coupling

The thermomagnetic coupling is a coupling that depends on both temperature and the magnetic field. It has been well known that the coupling constant is affected by the magnetic field [142, 143]. Different ansatzes for the dependence of coupling constant on the magnetic field, in the presence of the magnetic field, have been proposed [104, 144–146]. We use two parametrizations for the running coupling constant available in the literature to study the thermodynamic behavior of the 2 and $(2 + 1)$ flavor magnetized QGP.

4.2.1 Thermomagnetic Coupling 1

In Ref. [146] the coupling constant depending on both temperature and the magnetic field was introduced in the SU(2) Nambu-Jona-Lasinio (NJL) models as,

$$G(B, T) = c(B) \left[1 - \frac{1}{1 + e^{\beta(B)[T_a(B) - T]}} \right] + s(B), \qquad (4.1)$$

where, the four parameters c, β, T_a, and s were obtained by fitting the lattice data. This parametrization does not show the functional dependence of the coupling on the magnetic field. The parameters have to be chosen differently for different strengths of the magnetic field.

4.2.2 Thermomagnetic coupling 2

For studying the thermodynamics of the magnetized $(2+1)$ flavor QGP we make use of a different thermomagnetic coupling from Ref. [143]. The coupling that evolves with both momentum transfer and the magnetic field is,

$$\alpha_s(\Lambda^2, \mid eB \mid) = \frac{\alpha_s(\Lambda^2)}{1 + b_1 \alpha_s(\Lambda^2) \log\left(\frac{\Lambda^2}{\Lambda^2 + |eB|}\right)}. \tag{4.2}$$

The one-loop running coupling in the absence of a magnetic field at the renormalization scale is given by,

$$\alpha_s(\Lambda^2) = \frac{1}{b_1 \log(\Lambda^2/\Lambda_{\overline{MS}}^2)}, \tag{4.3}$$

where, $b_1 = (11N_c - 2N_f)/12\pi$ and following Ref. [89], $\overline{MS} = .176 GeV$ at $\alpha_s(1.5 GeV) = 0.326$, for $N_f = 3$.

It is to be noted that the above thermomagnetic coupling has been obtained using the LLL approximation suitable in a strong magnetic field limit $(eB \gg T^2)$. In this limit, the coupling is split into terms dependent on the momentum parallel and perpendicular to the magnetic field separately [142]. The coupling dependent on the transverse momentum does not depend on the magnetic field at all. We are interested in how the system responds to the magnetic field, and so we make use of the longitudinal part of the coupling constant. The coupling is obtained in the one-loop order, and so this may be appropriate only at high temperatures. We use this coupling as an approximation, and so our results are bound to be qualitative. A two-loop thermomagnetic coupling, which includes the contribution from HLLs, is expected to give quantitatively reliable results.
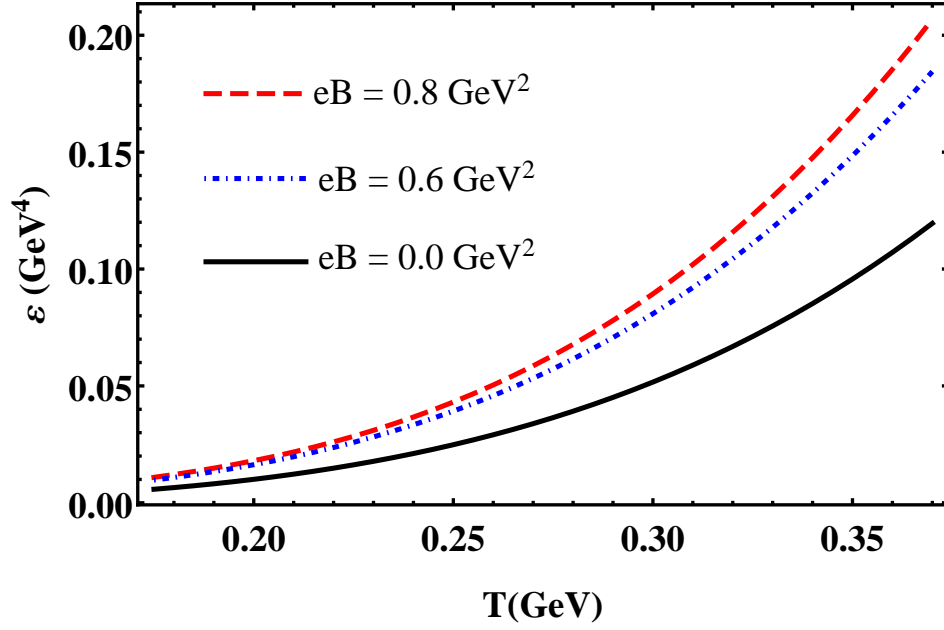
Figure 4.1: Energy density for different strengths of the magnetic field as a function of temperature.
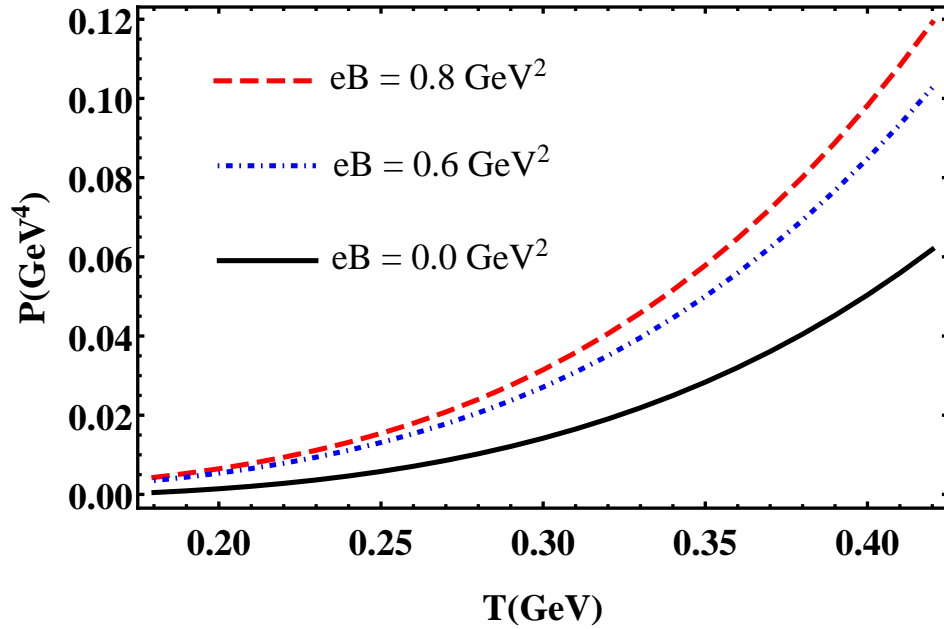
Figure 4.2: Pressure for different strengths of the magnetic field as a function of temperature.
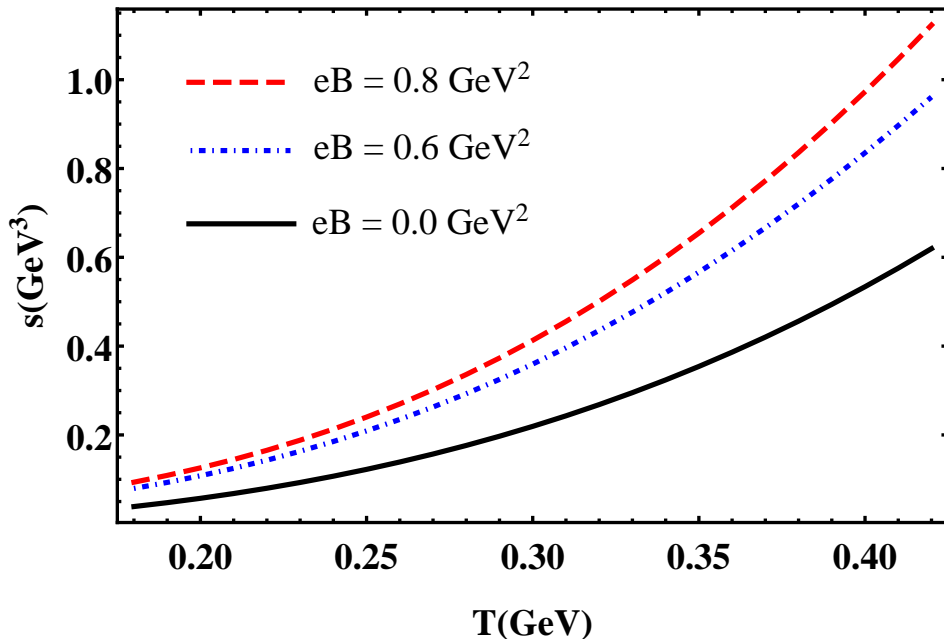
Figure 4.3: Entropy density for different strengths of the magnetic field as a function of temperature.

4.3 The thermodynamics of magnetized QGP

Using the formalism developed in the previous chapter, we study thermodynamics for the 2 flavor, and (2+1) flavor system at zero chemical potential in the presence the magnetic field. We calculate the thermomagnetic mass as explained in Secs. 3.3 and 3.4 using a suitable parametrization of the thermomagnetic coupling.

4.3.1 2 flavor magnetized QGP

We make use of the thermomagnetic coupling in Eq. (4.1) for the study of the magnetized 2 flavor QGP.

We have shown the temperature dependence of different thermodynamic quantities at different strengths of the magnetic field in Figures 4.1 - 4.3. We use Eqs. (3.45) and (3.46) to find the total energydensity. Figure 4.1 shows that the energy density increases, at a given temperature, as the magnetic field increases. This is expected as, in the presence of magnetic field the total energy density

Figure 4.4: $\Delta\varepsilon/T^4$ for two different strengths of the magnetic field, plotted as a function of temperature.
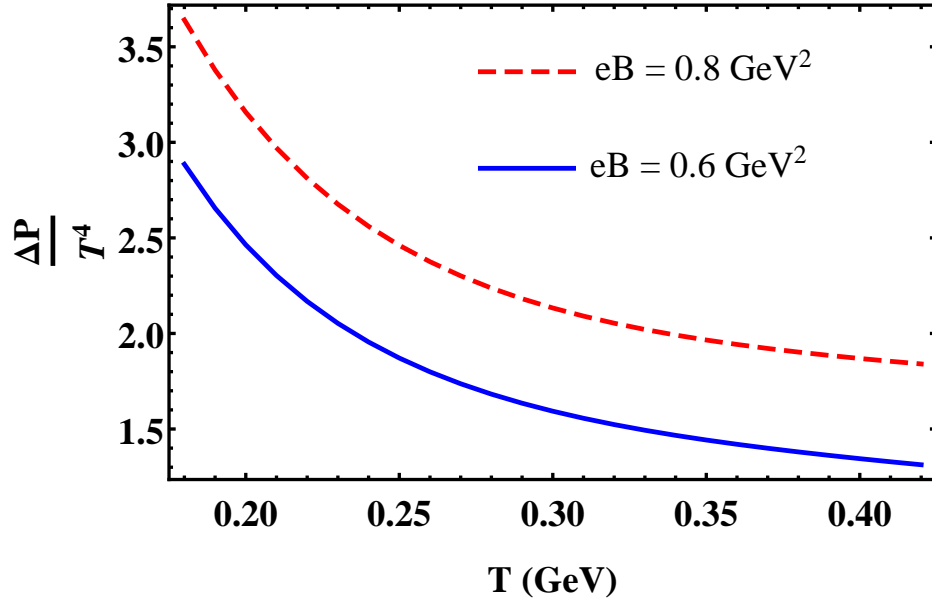
Figure 4.5: $\Delta P/T^4$ for two different strengths of the magnetic field, plotted as a function of temperature.
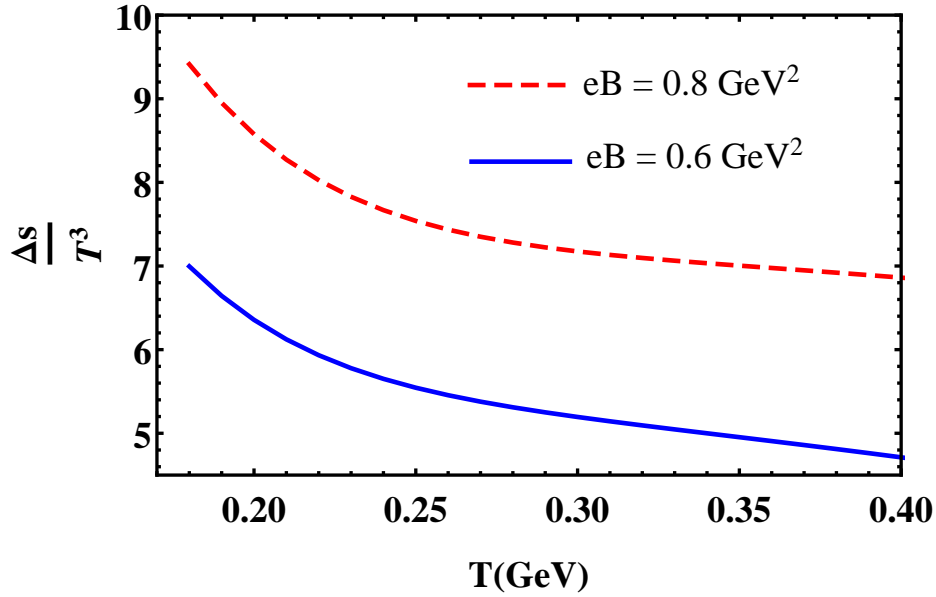
Figure 4.6: $\Delta s/T^3$ for two different strengths of the magnetic field, plotted as a function of temperature.
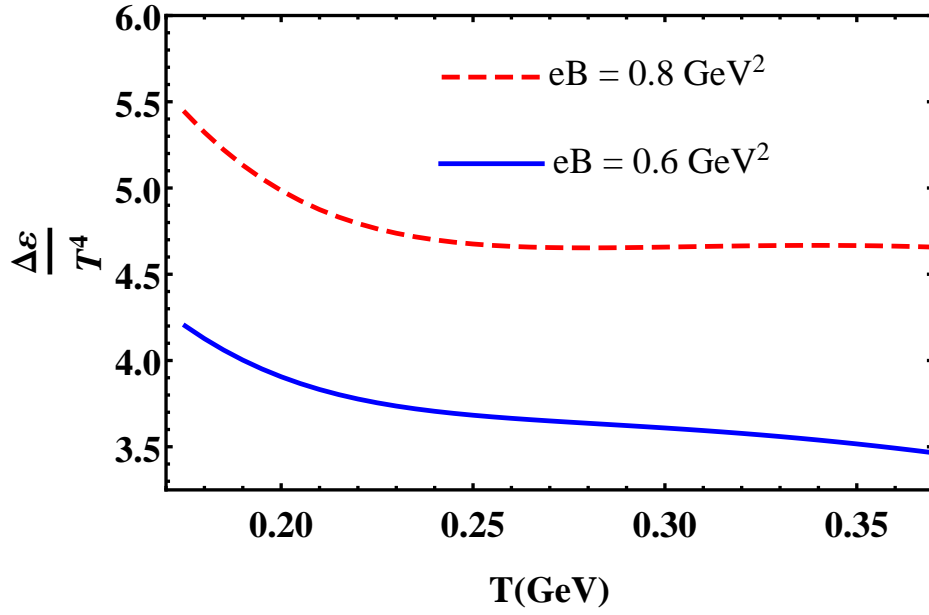
goes as $\varepsilon_{total} = \varepsilon + q\mathbf{M} \cdot \mathbf{B}$, where $\mathbf{M}$ is the magnetization [147]. We notice that the plots show correct qualitative behavior.

Calculation of quarks and gluons' contribution to the thermodynamic pressure using Eqs. (3.56) and (3.57), requires a value of P at some fixed temperature of T_0. If lattice data is available, P_0 can be chosen as the value of pressure at transition temperature T_c. Here we have chosen the value of thermodynamic pressure at T_c from Ref. [146]. We can make use of the relation in Eq. 3.58 to plot the variation of entropy density. The quark/gluon contribution to the thermodynamic pressure, energy density, and entropy density increase with the increase in eB. This behavior is consistent with that obtained using lattice QCD simulations [148] and [98]. The same behavior has been obtained using an effective fugacity quasiparticle model [147], within the SU(2) NJL model [146], and using the Bag Model [133]. The QCD equation of state in the presence of the magnetic field has been studied numerically [149, 150]. The effect of the magnetic field on QCD thermodynamics has been studied using the hard-thermal-loop (HTL)

perturbation theory both at strong [151] and in weak [152] magnetic field.

$\Delta\varepsilon$ is the difference between energy density in the presence of the magnetic field with that in the absence of any magnetic field. This depicts the increment of energy density in the presence of the magnetic field. The temperature dependence of $\Delta\varepsilon/T$ has been plotted in Figure 4.4. In addition, we have plotted $\Delta P/T^4$ and $\Delta s/T^3$ as functions of temperature, in Figure 4.5 and, Figure 4.6, respectively. As expected, the higher the magnetic field, the higher their values are too.

4.3.2 $(2+1)$ flavor magnetized QGP

In this section, we shall examine the thermodynamic behavior of the $(2+1)$ flavor QGP in the presence of an external magnetic field. We use the thermomagnetic coupling in Eq. (4.2). For all calculations, we have taken the physical masses of strange quarks as $.15 GeV$ and those of the light quarks as $\frac{1}{28.15}$ times the strange quark mass [124].

We have plotted the variation of longitudinal pressure with temperature, for different strengths of the magnetic field in Figure 4.7. Figure 4.8 shows the variation of pressure with the magnetic field for different temperatures. The increase in pressure with a magnetic field at a given temperature, as seen in our equation of state, is consistent with lattice QCD results [148], perturbative QCD results [89] and other works [147]. At this point, we do not make a quantitative comparison with the lattice data because the coupling constant used here is calculated in the LLL approximation. The one-loop thermomagnetic coupling we used may be reliable at high temperatures only. In Figure 4.9, using Eq. (3.64), we have plotted C_s^2 as a function of temperature, for different magnetic field strengths. The speed of sound is seen to reach the Stefan-Boltzmann limit of 1/3, asymptotically. This behavior is consistent with the behavior of P/ε in lattice QCD results [148] and with the behavior of sound velocity using an effective
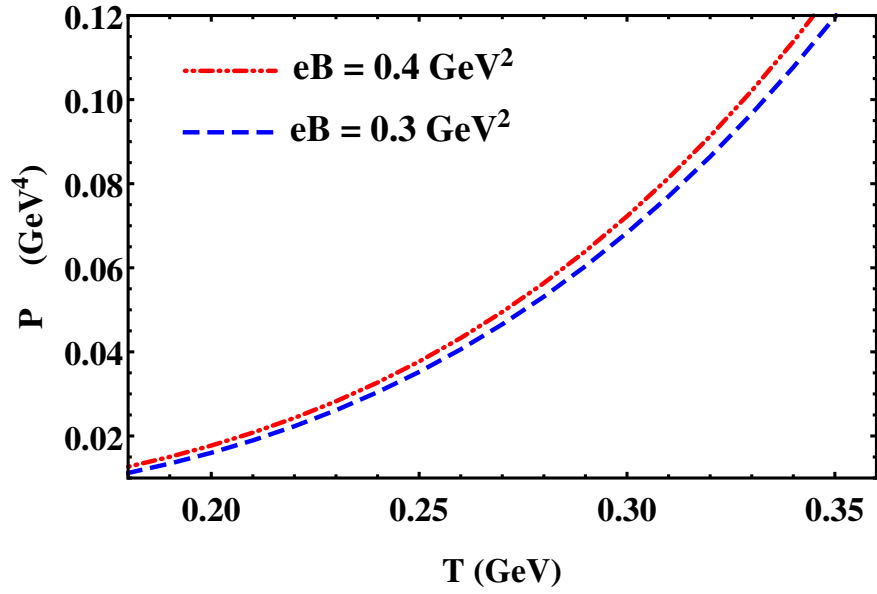
Figure 4.7: Thermodynamic Pressure as a function of temperature for different strengths of the magnetic field.
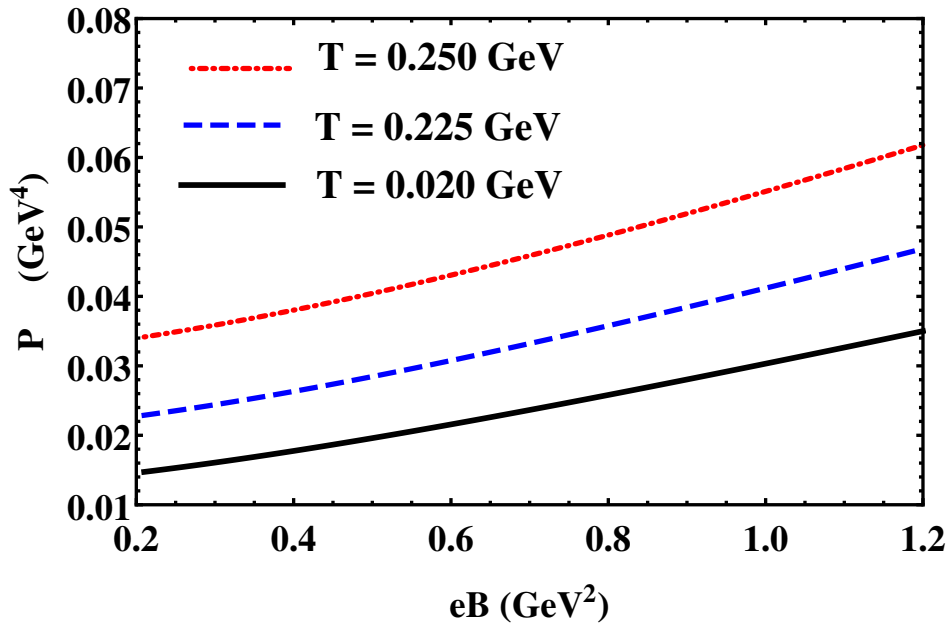
Figure 4.8: Thermodynamic Pressure for different temperatures as a function of magnetic field.

53
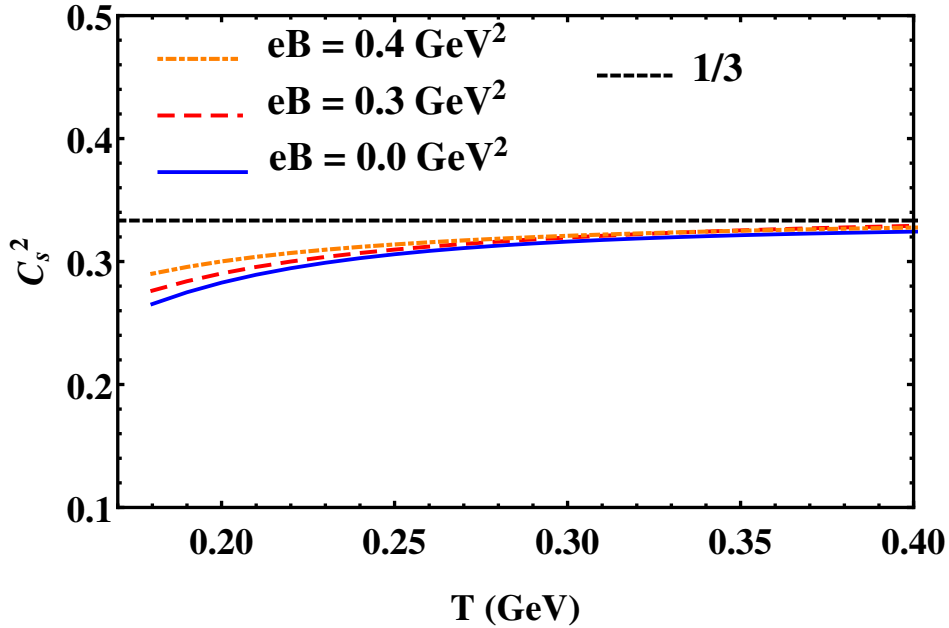
Figure 4.9: Velocity of sound as a function of temperature for different strengths of the magnetic field

fugacity quasiparticle model [147].

The qualitative behavior of our results is consistent with the results using an effective-fugacity quasiparticle model [147]. We show this in Figure 4.10 where we plotted our results for the energy density with the corresponding results from Ref. [147]. The results do not match exactly. To show the qualitative comparison, we have multiplied our result by a factor of 1.37. The plot shows that the predicted behavior of energy density in the presence of the magnetic field as obtained by these two different models is similar. We denote our model by "eqqgp" and the effective-fugacity model as "eqpm".

4.4   Summary

When applied to the study of the 2 and (2+1) flavor magnetized QGP, the extended self-consistent quasiparticle model shows that the thermodynamic quantities are enhanced in the presence of the magnetic field. The qualitative comparison of
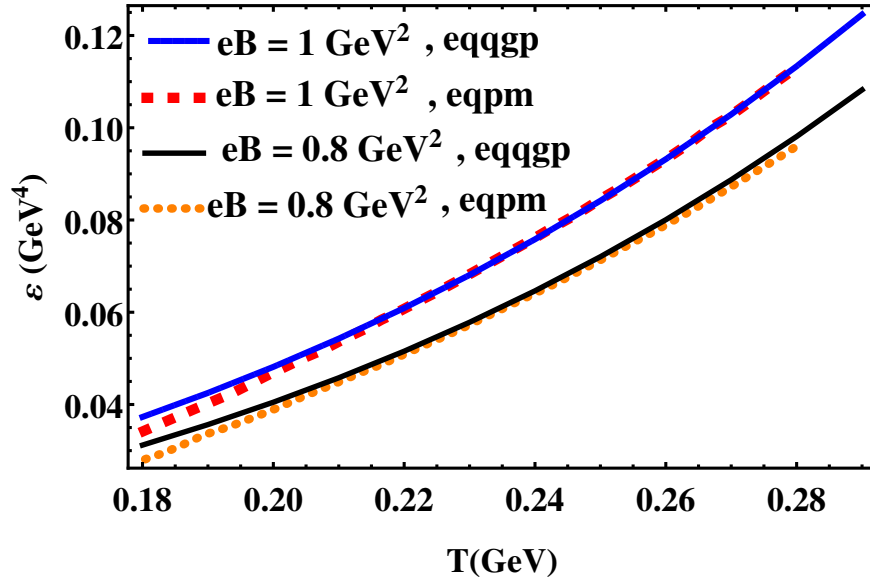
Figure 4.10: Energy density in our model (eqqgp) ($\times 1.37$) plotted with the result from effective fugacity quasiparticle model (eqpm)

our results with other results in the area underlines the effectiveness of using a quasiparticle description to study the magnetized QGP. The self-consistent quasiparticle model, in particular, allows a natural extension to include the effects of the magnetic field and proves to be successful in predicting the qualitative behavior of the magnetized QGP.

Chapter 5

Pressure anisotropy and Debye screening mass for the magnetized QGP

5.1 Introduction

In this chapter, we make use of the extended self-consistent quasiparticle model (Ch. 3) to study the pressure anisotropy and the Debye Screening mass for magnetized $(2+1)$ flavor QGP. We start by examining the magnetic response of QGP by finding the magnetization and showing that it exhibits paramagnetic behavior. Using the calculated magnetization, we study the anisotropy between longitudinal and transverse pressures caused by the magnetization acquired by the system along the field direction. We bring out the dependence of transverse pressure on temperature and the magnetic field. We study the total longitudinal and transverse pressure behavior, including the pure field or Maxwell contributions. Finally, we look at the screening properties of magnetized QGP in the longitudinal direction by calculating the Debye screening mass. As a consistency check, we compare the Debye mass obtained within our formalism with a similar result

using perturbation techniques and examine how well they agree, especially at high temperatures.

We organize this chapter as follows. In Sec. 5.2 we study the magnetic response of the system by calculating the magnetization. Sec. 5.3 focuses on the pressure anisotropy in the system caused by the magnetization. In Sec. 5.4, we include the pure field contributions and see how the pure field contributions modify the transverse and longitudinal pressures. Sec. 5.5 is the study of screening properties of magnetized QGP. We discuss our results in Sec. 5.6 and summarize in Sec. 5.7.

5.2 Magnetization

Magnetization quantifies the magnetic response of the system. We can calculate magnetization from the grand canonical potential Φ.

$$\mathcal{M} = -\frac{1}{V}\frac{\partial \Phi}{\partial (eB)}.$$ (5.1)

We confine our calculation to the region where eB is greater than zero. Note that the equation for magnetization in the self-consistent quasiparticle model is not related to the partition function as given in Ref. [148]. This is because of the additional terms in Eqs. (3.61) and (3.62), which ensure thermodynamic consistency.

From Eqs. (3.61), and (5.1), we get, for quarks,

$$\mathcal{M}_q = \frac{Tg_f q_f}{2\pi^2} \sum_{l=1}^{\infty} (-1)^l \sum_j (2 - \delta_{0j}) \left\{ \left[\frac{T}{l^2} \left(\frac{m_{qj}l}{T} \right) K_1 \left(\frac{m_{qj}l}{T} \right) \right. \right.$$
$$+ \int_{T_0}^{T} \frac{d\tau}{\tau} \, m_{q_j} \frac{\partial m_{q_j}}{\partial \tau} K_0 \left(\frac{m_{q_j}l}{\tau} \right) \Bigg]$$
$$- eB \left[\frac{T}{l^2} \left(\frac{m_{qj}l}{T} \right) K_0 \left(\frac{m_{qj}l}{T} \right) \frac{\partial}{\partial(eB)} \left(\frac{m_{qj}l}{T} \right) \right.$$
$$\left. \left. - \frac{\partial}{\partial(eB)} \left(\int_{T_0}^{T} \frac{d\tau}{\tau} \, m_{q_j} \frac{\partial m_{q_j}}{\partial \tau} K_0 \left(\frac{m_{q_j}l}{\tau} \right) \right) \right] \right\}. \quad (5.2)$$

In the above calculation we have made use of Eq. (3.71) and the relation,

$$\frac{\partial K_0(z)}{\partial z} = -K_1(z). \quad (5.3)$$

In a similar manner, we obtain the expression for magnetization of gluons from Eq. (3.62) as,

$$\mathcal{M}_g = \frac{Tg_f}{2\pi^2} \sum_{l=1}^{\infty} \left[\frac{\partial}{\partial(eB)} \int_{T_0}^{T} \frac{d\tau}{m_g} \tau^3 \frac{\partial m_g}{\partial \tau} \left(\frac{m_g l}{\tau} \right)^3 K_1 \left(\frac{m_g l}{\tau} \right) \right.$$
$$\left. - T^3 \left(\frac{m_g l}{T} \right)^2 K_1 \left(\frac{m_g l}{T} \right) \frac{\partial}{\partial(eB)} \left(\frac{m_g l}{T} \right) \right]. \quad (5.4)$$

By obtaining the magnetization using the above equations, we can go on to study the pressure anisotropy of QGP in the presence of the magnetic field.

5.3 Pressure anisotropy

It has been known that the presence of the magnetic field breaks the $O(3)$ rotational symmetry resulting in a pressure anisotropy [138, 153–155]. There have also been arguments suggesting that the total pressure is indeed isotropic and the issue has been subject to some debate [156–158]. The scheme dependence

of pressure anisotropy has been discussed [148, 159], where the authors have distinguished between two schemes. The $B-$scheme, which corresponds to a setup in which the magnetic field B is kept constant during the compression, and the Φ-scheme corresponding to a setup in which the magnetic flux is kept constant during the compression. They showed that pressure anisotropy appears only in the Φ-scheme, i.e., $P_\perp^{(B)} = P^{(B)}$ and $P_\perp^{(\Phi)} \neq P^{(\Phi)}$, where $P_\perp$ and P denote the transverse and longitudinal pressure respectively. They also showed that the longitudinal pressure is scheme independent. Thus, $P^{(\Phi)} = P^{(B)}$. In the Φ scheme the longitudinal and transverse pressures were found to be related by,

$$P_T = P - eB \cdot \mathcal{M}. \tag{5.5}$$

Using Eqs. (3.61) and (5.2) the transverse pressure becomes,

$$
\begin{aligned}
\frac{(P_T)_q}{T} =& \frac{g_f q_f (eB)^2}{2\pi^2} \sum_{l=1}^{\infty} (-1)^l \sum_j (2 - \delta_{0j}) \\
& \left[\frac{T}{l^2} \left(\frac{m_{qj}l}{T} \right) K_0 \left(\frac{m_{qj}l}{T} \right) \frac{\partial}{\partial(eB)} \left(\frac{m_{qj}l}{T} \right) \right. \\
& \left. - \frac{\partial}{\partial(eB)} \left(\int_{T_0}^{T} \frac{d\tau}{\tau} m_{q_j} \frac{\partial m_{q_j}}{\partial \tau} K_0 \left(\frac{m_{q_j}l}{\tau} \right) \right) \right],
\end{aligned} \tag{5.6}
$$

for quarks, and

$$
\begin{aligned}
\frac{(P_T)_g}{T} =& \frac{g_f}{2\pi^2} \sum_{l=1}^{\infty} \frac{1}{l^4} \left\{ T^3 \left(\frac{m_g l}{T} \right)^2 K_2 \left(\frac{m_g l}{T} \right) \right. \\
& + \int_{T_0}^{T} \frac{d\tau}{m_g} \tau^3 \frac{\partial m_g}{\partial \tau} \left(\frac{m_g l}{\tau} \right)^3 K_1 \left(\frac{m_g l}{\tau} \right) \\
& - eB \left[\frac{\partial}{\partial(eB)} \int_{T_0}^{T} \frac{d\tau}{m_g} \tau^3 \frac{\partial m_g}{\partial \tau} \left(\frac{m_g l}{\tau} \right)^3 K_1 \left(\frac{m_g l}{\tau} \right) \right. \\
& \left. \left. - T^3 \left(\frac{m_g l}{T} \right)^2 K_1 \left(\frac{m_g l}{T} \right) \frac{\partial}{\partial(eB)} \left(\frac{m_g l}{T} \right) \right] \right\},
\end{aligned} \tag{5.7}
$$

for gluons.

5.4 Pure field contributions

So far we concentrated only on the contributions to the thermodynamic quantities from quarks and gluons. The total pressure of magnetized QGP involves one another contribution namely the pure field or Maxwell contribution [153, 158, 160–162]. These contributions are again different in the parallel and perpendicular directions as the magnetic field breaks rotational symmetry. The total pressure in the transverse direction is,

$$
\begin{aligned}
P_T^{total} &= P_T + (P_T)_m \\
&= P_T + \frac{B^2}{2}.
\end{aligned}
\tag{5.8}
$$

The total pressure in the longitudinal direction is given by,

$$
\begin{aligned}
P^{total} &= P + P_m \\
&= P - \frac{B^2}{2},
\end{aligned}
\tag{5.9}
$$

where, $(P_T)_m$ and P_m are the pure field contributions in the transverse and longitudinal directions, respectively. Using these we can calculate the total longitudinal and transverse pressures.

5.5 Longitudinal Debye screening mass

At the leading order, Debye screening mass parameterizes the dynamically generated screening of chromo-electric fields, due to the strong interactions of hot QCD [163]. The ability of QGP to shield out the chromoelectric potential can be measured in terms of the Debye screening length, which is the inverse of the Debye mass (m_D). Calculations of the higher-order contributions to the

Debye screening [164, 165] are beyond the scope of this work. The presence of an external magnetic field causes an anisotropy, and we study the Debye mass in the longitudinal direction.

The conventional definition for Debye mass can be obtained either from the small momentum limit of the gluon self energy [27, 166–169] or the semiclassical transport theory [147, 170, 171].

5.5.1 Debye mass at zero magnetic field

In the zero magnetic field case, the Debye mass can be defined as [97, 147, 167],

$$m_D^2 = -g_n g^2 \int \frac{d^3 k}{(2\pi)^3} \frac{\partial}{\partial \omega_k} f(\omega_k), \tag{5.10}$$

where $f(\omega_k)$ are the quasi-gluon, quasi-quark/antiquark distribution functions with,

$$\omega_k = \sqrt{m(T)^2 + k^2}, \tag{5.11}$$

and g_n the degeneracy factor. In the self-consistent quasiparticle model, all the medium effects are captured by the thermal masses of the quasiparticles $m(T)$. The distribution functions (in zero chemical potential) are,

$$f_g(\omega_k) = \frac{1}{e^{\beta \omega_k} - 1}, \text{ and, } f_q(\omega_k^f) = \frac{1}{e^{\beta \omega_k^f} + 1}, \tag{5.12}$$

for gluons and quark/antiquark flavor f, respectively. Hereafter we shall drop the flavor index on the quasiparticle mass and energies of quarks, to avoid cluttering.

The gluonic contribution to the Debye mass can be calculated using Eqs. (5.10), (5.11), the first relation in Eq. (5.12), and $g_n = 2N_c$.

We have,

$$\frac{\partial}{\partial \omega_k} f(\omega_k) = \frac{\partial}{\partial \omega_k} \left(\frac{1}{e^{\beta \omega_k} - 1} \right)$$

$$= \frac{e^{-\beta \sqrt{k^2 + m_g^2}}}{\left(1 - e^{-\beta \sqrt{k^2 + m_g^2}} \right)^2}. \tag{5.13}$$

Using Eq. (5.13) in Eq. (5.10),

$$m_{Dg}^2 = \frac{N_c g^2}{\pi^2 T} \int_0^\infty dk k^2 \frac{e^{-\beta \sqrt{k^2 + m_g^2}}}{\left(1 - e^{-\beta \sqrt{k^2 + m_g^2}} \right)^2}. \tag{5.14}$$

Defining $x = K/T$ and making the substitution, $x = m_g/T \sinh t$, and binomially expanding the denominator, the above integral yields,

$$m_{Dg}^2 = \frac{N_c g^2 T^2}{\pi^2} \left[\sum_{l=1}^\infty \frac{1}{l^2} \left(\frac{l m_g}{T} \right)^2 K_2 \left(\frac{l m_g}{T} \right) \right]. \tag{5.15}$$

The calculations are very similar to what we did in the last chapter and so we do not repeat all the steps here.

At zero magnetic field, Eq. (5.10), with the quark distribution function in Eq. (5.12), can also be written as,

$$m_{Dq}^2 = \frac{g^2}{T} g_n \int \frac{d^3 k}{(2\pi)^3} f(\omega_k) \left[1 - f(\omega_k) \right]. \tag{5.16}$$

With $g_n = 2 \times 2 \times N_c$(quark-antiquark, spin and color), and for a single quark flavor,

$$m_{Dq}^2 = \frac{4 N_c g^2}{T} \int \frac{d^3 k}{(2\pi)^3} \frac{e^{-\beta \sqrt{k^2 + m_q^2}}}{\left(1 + e^{-\beta \sqrt{k^2 + m_q^2}} \right)^2}. \tag{5.17}$$

The integral can be simplified by making the same substitutions as in the previous

63

case and also expanding the denominator binomially. The algebra is straightforward and we get,

$$m_{Dq}^2 = \frac{2N_c g^2 T^2}{\pi^2} \sum_{l=1}^{\infty} \frac{(-1)^{l-1}}{l^2} \left(\frac{lm_q}{T}\right)^2 K_2\left(\frac{lm_q}{T}\right). \tag{5.18}$$

5.5.2 Debye mass at non-zero magnetic field

The gluon Debye mass is associated with the gluon and ghost loops contribution to the gluon self-energy. In the presence of the magnetic field, the expression of Debye mass for gluons remains the same as the magnetic field does not change the ghost and gluon loops [89]. The expression for gluon Debye mass in the self-consistent quasiparticle model also remains the same as Eq. (5.15). However, the thermomagnetic mass of gluons, 'm_g', depends on the magnetic field through the quark contribution to the gluon plasma frequency. The gluon plasma frequency in Eq. (2.7) is defined in such a way that it approaches the corresponding values in perturbative QCD (pQCD) at high temperatures, ensuring consistency. So we can consider the dependence of the gluon Debye mass on the magnetic field, through the quark plasma frequency, as a correction to the perturbative result due to medium-effects caused by the strong interaction.

The debye mass for quarks is associated with the quark loop contribution to the gluon self-energy. This changes in the presence of an external magnetic field. The expression of Debye mass for quarks in the presence of the magnetic field can be obtained by replacing the thermal masses by thermomagnetic masses, changing the dispersion relation in accordance with Eq. (3.1) and modifying the momentum integration according to Eq. (3.2) in Eq. (5.16). This gives [167],

$$m_{Dq}^2(eB) = \frac{\mid q_f eB \mid g^2}{2\pi^2} \sum_{j=0}^{\infty} g_j \int_0^{\infty} \frac{dk_z}{T} f_q(\omega_{k_z}^j) \left(1 - f_q(\omega_{k_z}^j)\right), \tag{5.19}$$

64

where,

$$f_q(\omega_{k_z}^j) = \frac{1}{e^{\beta\omega_{k_z}^j} + 1}, \tag{5.20}$$

and,

$$\omega_{k_z}^j = \sqrt{k_z^2 + m_{q_j}^2}, \tag{5.21}$$

where g_j in Eq. (5.19) is the degeneracy of the jth Landau level and is dependent on the Landau level index j. Along with these and adding up the contributions from all flavors, we get from Eq. (5.19),

$$m_{Dq}^2 = \sum_f \frac{|\, q_f eB \,|\, g^2}{2\pi^2} \sum_{j=0}^{\infty} g_j \int_0^{\infty} \frac{dk_z}{T} \frac{e^{-\beta\sqrt{k_z^2 + m_{q_j}^2}}}{\left(1 + e^{-\beta\sqrt{k_z^2 + m_{q_j}^2}}\right)^2}. \tag{5.22}$$

With $g_j = 2N_c \times (2 - \delta_{0j})$ [167], Eq. (5.22) simplifies to,

$$m_{Dq}^2(eB) = \frac{N_c g^2}{\pi^2} \sum_f |\, q_f eB \,| \sum_{l=1}^{\infty} (-1)^{l-1} \sum_{j=0}^{\infty} (2 - \delta_{0j})$$
$$\left(\frac{l m_{q_j}}{T}\right) K_1\left(\frac{l m_{q_j}}{T}\right). \tag{5.23}$$

5.6   Results and discussions

For all the calculations we make use of the thermomagnetic coupling Eq. (4.2).

The variation of magnetization with temperature for different strengths of the magnetic field is plotted in Figure 5.1. We see that the magnetization has a positive value for all values of temperature above T_c. This shows that QGP has a paramagnetic nature.

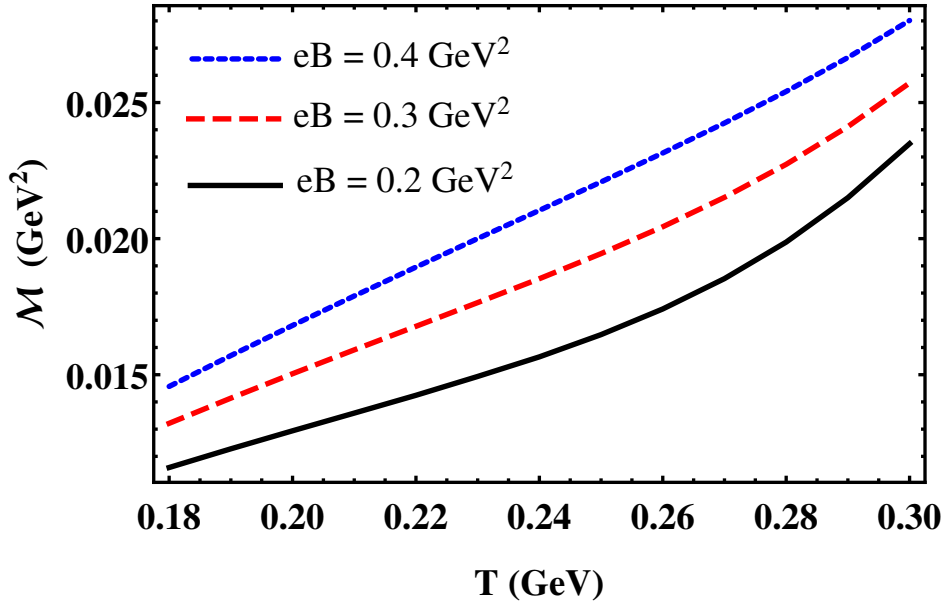In Figure 5.2, we have plotted the variation of magnetization with the magnetic

Figure 5.1: Magnetization for different strengths of the magnetic field as a function of temperature.
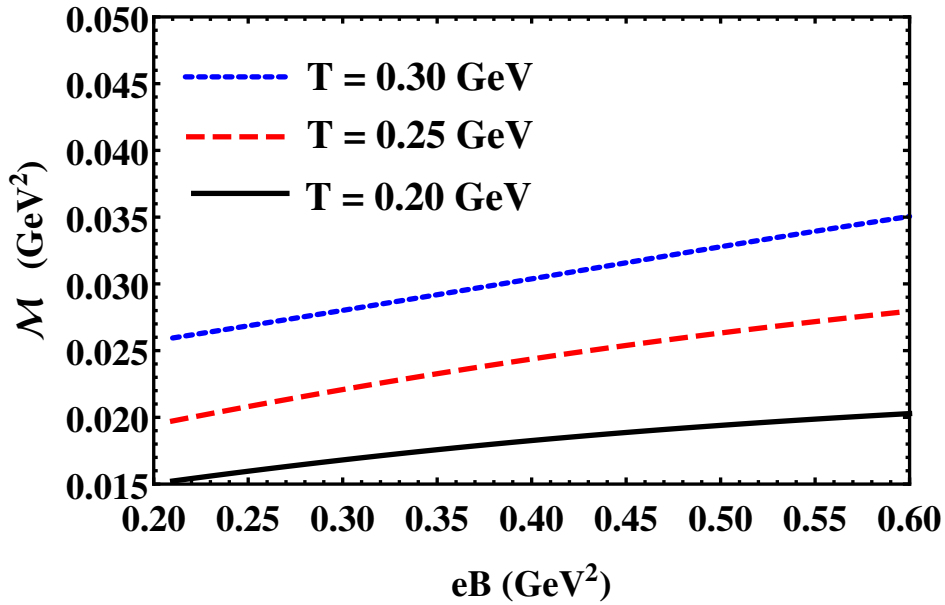

Figure 5.2: Magnetization for different temperatures as a function of the magnetic field.

field for different temperatures. It is seen that the magnetization increases with the magnetic field. The behavior of magnetization of QGP, as seen in our work, is qualitatively consistent with lattice QCD results [172] and with results from HTL perturbation theory [89]. We have included HLLs, whereas, in [89] the LLL approximation has been used.

In Figure 5.3, we have plotted the variation of transverse pressure with temperature for different strengths of the magnetic field. In Figure 5.4, we show the variation of transverse pressure with the magnetic field for different temperatures. Since magnetization increases with temperature, the transverse pressure tends to decrease with an increase in the magnetic field. This behavior, too, is qualitatively consistent with the pQCD results [89], and the lattice QCD results [148, 172].

Including the Maxwell contribution to the total pressure, we see that the parallel or longitudinal pressure decreases and the transverse pressure increases with increase in the magnetic field strength. The behavior of the total longitudinal and transverse pressure is plotted in Figures 5.5 - 5.8. Figure 5.5 shows that for a given magnetic field, the total longitudinal pressure increases with temperature. Toward the lower values of temperature the value of total longitudinal pressure is negative. Figure 5.6 shows that the total longitudinal pressure decreases and becomes negative as the magnetic field strength is increased. The negative value of total longitudinal pressure can produce instabilities to the system and this aspect deserves to be studied carefully. The total transverse pressure (Figure 5.8) increases with increase in magnetic field and remains positive.

We study the screening effect in magnetized QGP using our model by calculating the Debye mass. At $B = 0$, the Debye mass increases with temperature. We have plotted the variation of Debye mass with temperature for different strengths of the magnetic field in Figure 5.9. The Debye screening mass variation
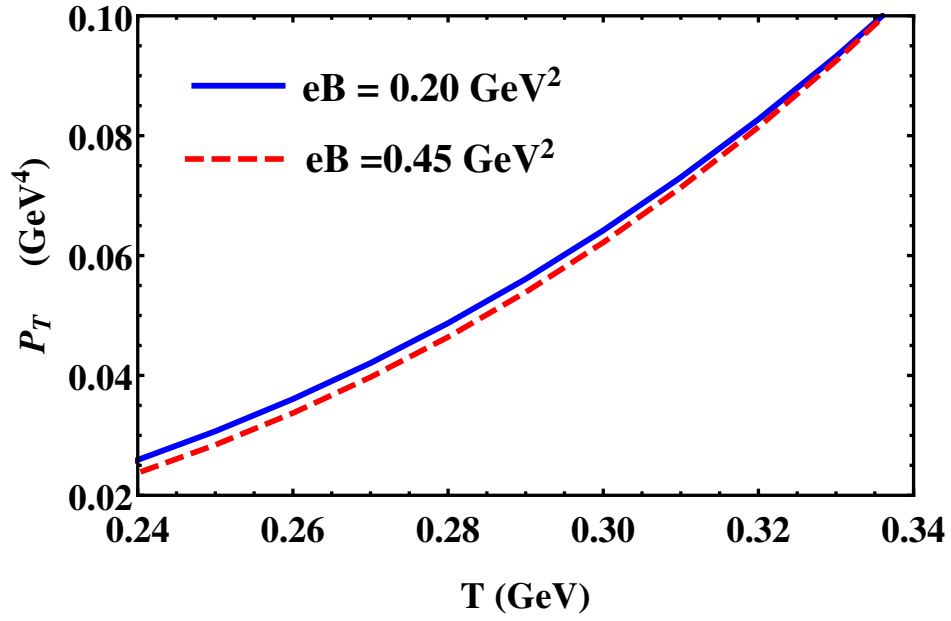
Figure 5.3: Transverse pressure for different strengths of the magnetic field as a function of temperature.
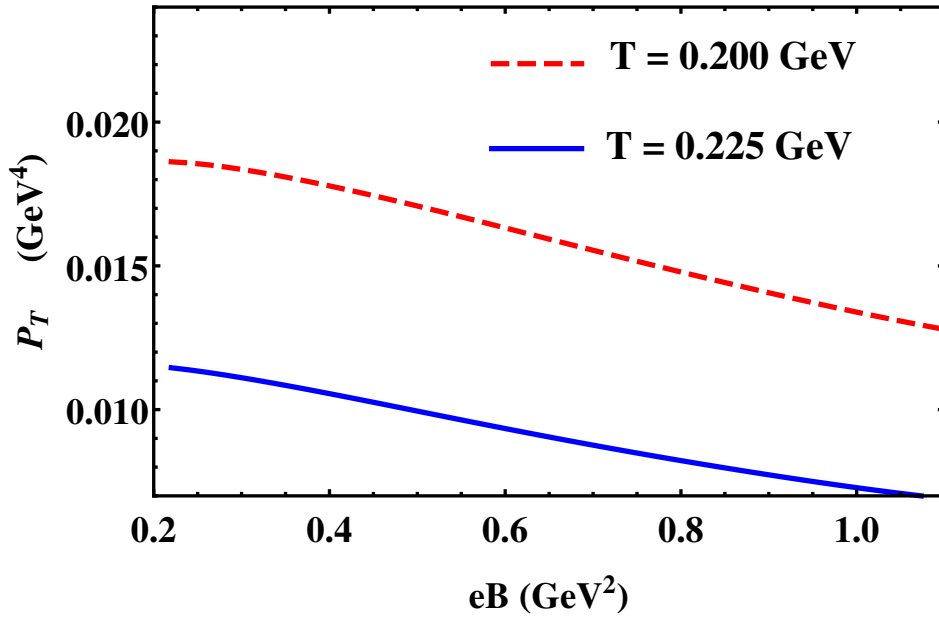
Figure 5.4: Transverse pressure for different temperatures as a function of magnetic field.
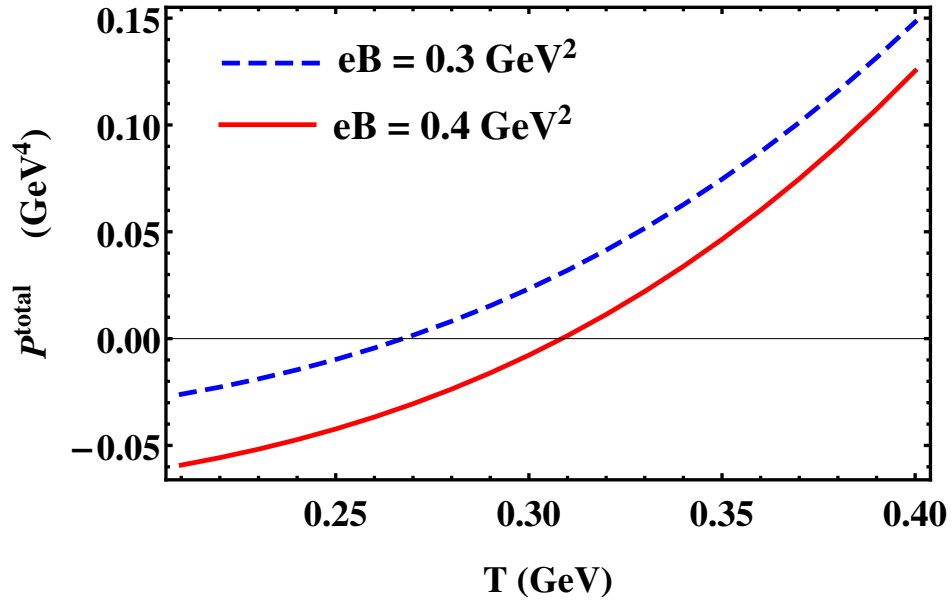
Figure 5.5: Variation of total longitudinal pressure $(P + P_m)$ with temperature for different strengths of the magnetic field.
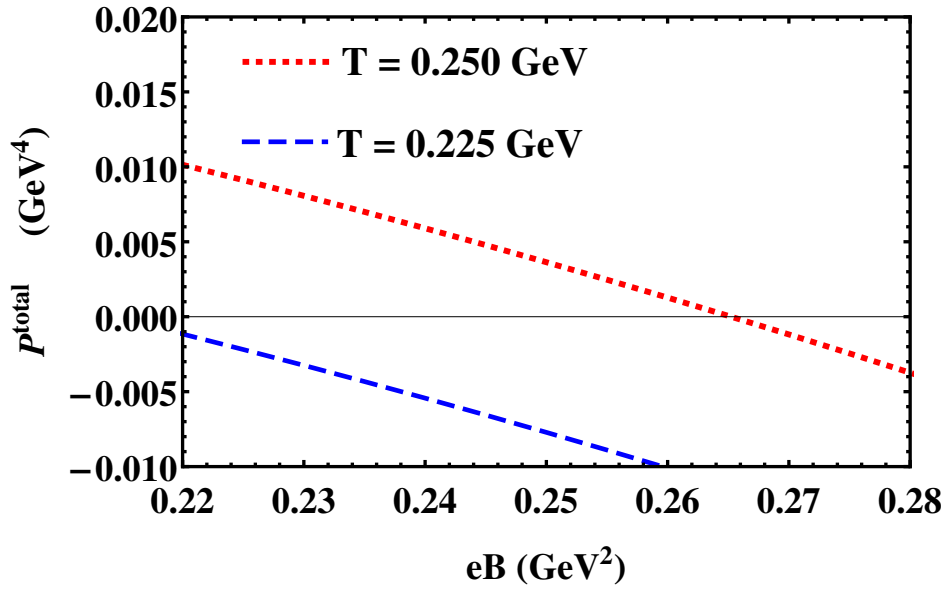
Figure 5.6: Variation of total longitudinal pressure with magnetic field for different temperatures.
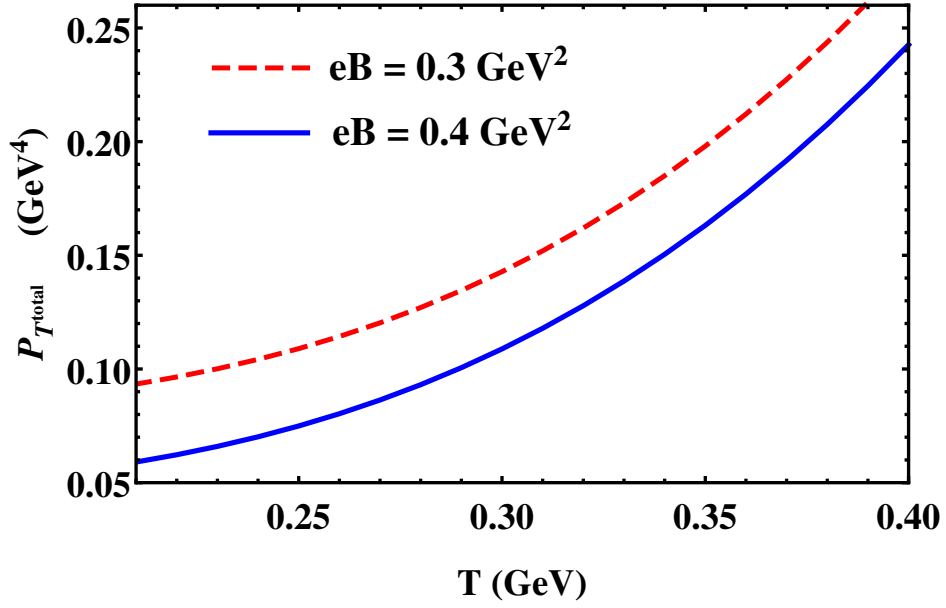
Figure 5.7: Variation of total transverse pressure $(P_T + (P_T)_m)$ with temperature for different strengths of the magnetic field.
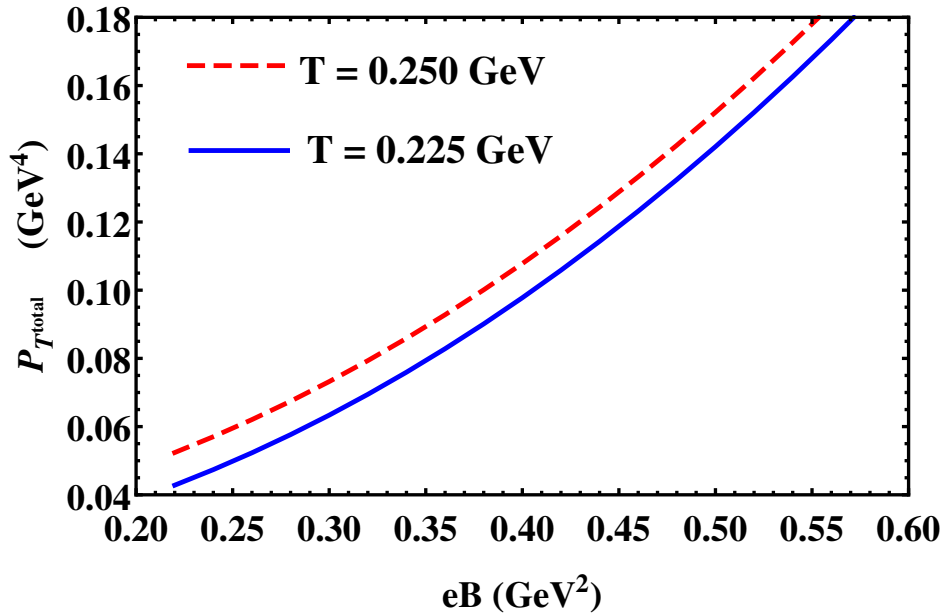
Figure 5.8: Variation of total transverse pressure with the magnetic field for different temperatures.
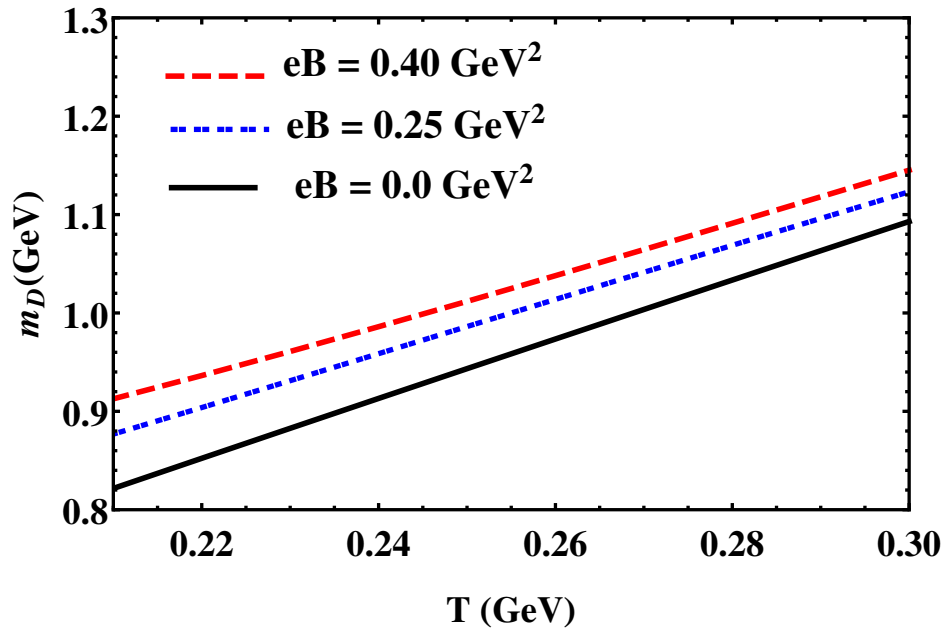
Figure 5.9: Debye mass as a function of temperature for different strengths of the magnetic field.
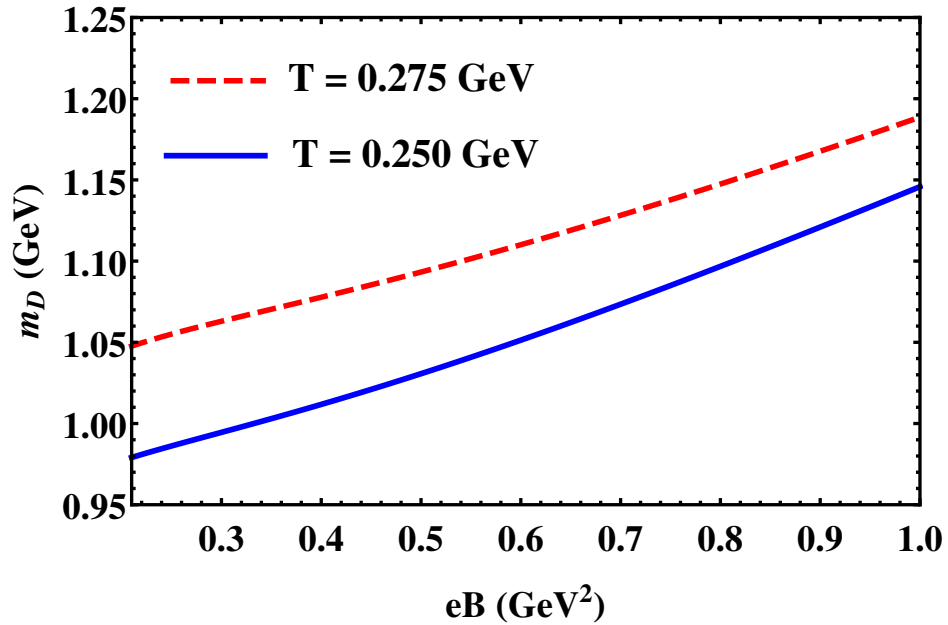
Figure 5.10: Debye mass as a function of magnetic field for different temperatures.
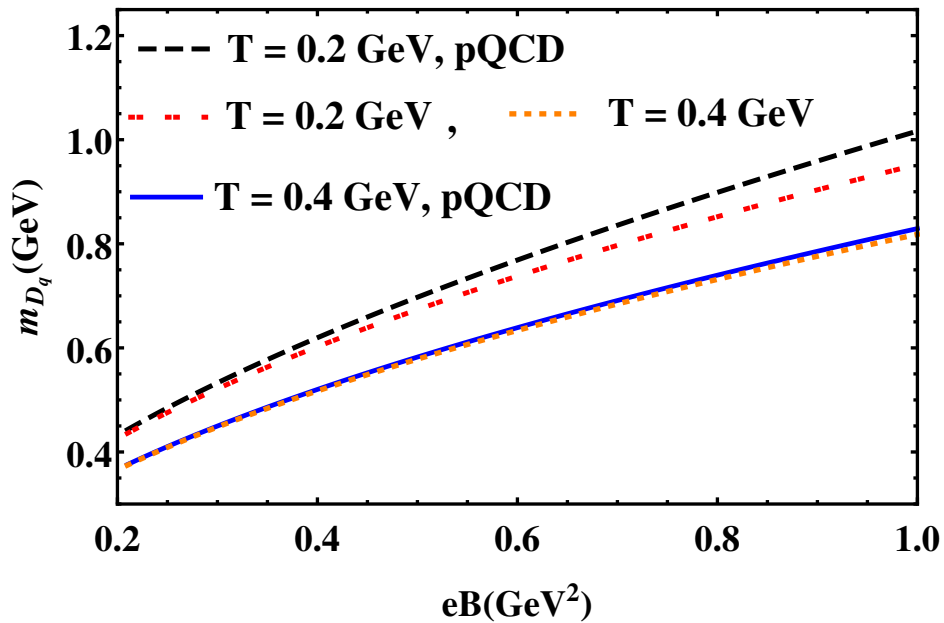
Figure 5.11: Contribution of quarks to the Debye mass plotted against the magnetic field compared with pQCD result.

with the magnetic field is plotted for different temperatures in Figure 5.10. The enhancement of Debye screening mass in the presence of external magnetic field agrees with the findings using Lattice QCD simulations [165], and the results using perturbative calculations [95, 101, 173]. Similar results are also obtained in Ref. [147] and Ref. [167].

In Figure 5.11, we plot our result for the contribution of quarks to the Debye mass along with the corresponding result from pQCD. The expression for the debye mass of quarks obtained from the gluon self-energy tensor in the strong magnetic field limit and with massless quarks [151, 152, 174], is,

$$m_D^2 = \frac{g^2}{4\pi^2} \sum_f \mid q_f eB \mid .$$ (5.24)

We have corrected for a factor of 2 overlooked in Ref. [151] as pointed out in [152]. We plot the quark Debye mass of Eq. (5.24) in Figure 5.11, after including the appropriate degeneracy factor $g_n = 2N_c$ [167]. We have used $g^2 = 4\pi\alpha_s$, with

the thermomagnetic coupling α_s given in Eq. (4.2). The plots are denoted as 'pQCD'.

Along with the pQCD results in Figure 5.11, we have plotted the quark Debye mass calculated using Eq. (5.23) in the LLL approximation and neglecting the physical quark masses ($m_0 = 0$). The quasiparticles, however, are still massive with masses depending on temperature and the magnetic field.

At $T = 0.2 GeV$ our results deviate from the pQCD results. The deviation is expected because QGP is strongly interacting at these temperatures, and pQCD may not be suitable. In our model, the strong interaction is taken into account through the temperature and magnetic field dependence of the quasiparticle masses.

The results from these different approaches match reasonably well at a higher temperature of $T = 0.4 GeV$, as shown in the plot. The agreement shows that our results approach the results obtained through a perturbative calculation at high temperatures. The proportionality constants in Eq. (2.7) and (2.8) are obtained by demanding that the expressions for plasma frequency approach the corresponding pQCD results at high temperature. So the comparison plot shows that our approach is consistent.

The expression for Debye mass of massive quarks in Ref. [151], after correcting for the missing factor of 2 and multiplying by the degeneracy factor is,

$$m_D^2 = \frac{N_c g^2}{\pi^2} \sum_f \mid q_f eB \mid \int_0^\infty \frac{dk_z}{T} \frac{e^{\beta\sqrt{k_z^2+m_0^2}}}{\left(1 + e^{\beta\sqrt{k_z^2+m_0^2}}\right)^2}, \tag{5.25}$$

where, m_0 is the physical quark mass (we have dropped the flavor index for convenience.) We note that Eq. (5.22), obtained from the self-consistent quasiparticle model, reduces to Eq. (5.25) in the LLL approximation and when quarks and gluons are considered as non-interacting ($m_{q_j} = m_0$). Interacting quarks

and gluons acquire thermomagnetic mass and stronger the interaction, more significant the deviation from the ideal gas result.

5.7 Summary

QGP has a paramagnetic nature. The existence of a positive magnetization causes anisotropy in pressure. The full QGP pressure (thermodynamic+ pure field) shows that there may be an instability in the system at specific strengths of the magnetic field and temperatures. This area deserves more study. The study of screening properties of magnetized QGP reveals that the screening mass increases in the presence of the magnetic field. The results from the extended self-consistent quasiparticle model compare well with the corresponding pQCD results at high temperatures.

Chapter 6

The extended self-consistent quasiparticle model at finite chemical potential

6.1   Introduction

In the previous chapters, we studied the magnetized QGP at zero chemical potential. We successfully extended the self-consistent quasiparticle model to incorporate the magnetic field's effect and studied both 2 flavor and $(2+1)$ flavor QGP using the extended model. In this chapter, we intend to generalize the model further to include the effects of the chemical potential. The generalization of the extended quasiparticle model to include the effects of chemical potential will make it suitable in the context of strongly magnetized neutron stars and magnetars [82–86]. The presence of magnetic field breaks the rotational symmetry. The thermodynamic quantities we calculate are hence generally different in the longitudinal and transverse directions. In this chapter we shall focus solely on the longitudinal quantities without explicitly stating so.

6.2 Thermomagnetic mass at finite chemical potential

We can generalize the expression for plasma frequencies in the previous chapters to introduce thermomagnetic mass that depends on chemical potential. Using Eqs. (3.2) and (3.1) n_q and $n_{\bar{q}}$ become in the presence of the magnetic field,

$$n_q = \frac{g_f q_f eB}{(2\pi)^2} \sum_{j=0}^{\infty} \left[(2 - \delta_{0j}) \int_{-\infty}^{\infty} dk_z \frac{1}{z^{-1} e^{\sqrt{(\frac{k_z}{T})^2 + (\frac{m_{qj}}{T})^2}} + 1} \right], \qquad (6.1)$$

and,

$$n_{\bar{q}} = \frac{g_f q_f eB}{(2\pi)^2} \sum_{j=0}^{\infty} \left[(2 - \delta_{0j}) \int_{-\infty}^{\infty} dk_z \frac{1}{z e^{\sqrt{(\frac{k_z}{T})^2 + (\frac{m_{qj}}{T})^2}} + 1} \right], \qquad (6.2)$$

where $z = e^{\beta \mu}$ is the fugacity.

The expression for plasma frequencies at non-zero chemical potentials was given in Eq. (2.11). From Eqs. (6.1) and (6.2) we get,

$$\frac{1}{2} \left(\frac{n_q + n_{\bar{q}}}{T} \right) = \frac{2 g_f q_f eB}{(2\pi)^2} \sum_{j=0}^{\infty} \left[(2 - \delta_{0j}) \right.$$
$$\left. \sum_{l=1}^{\infty} (-1)^{l-1} \left(\frac{m_{qj}}{T} \right) K_1 \left(l \frac{m_{qj}}{T} \right) \cosh \left(l \frac{\mu}{T} \right) \right]$$

$$= \frac{2 g_f q_f eB}{(2\pi)^2} T^2 F_q^2. \qquad (6.3)$$

Now Eq. (2.11) can be written as,

$$\left(\frac{m_f}{T} \right)^2 = \bar{b}_q^2 F_q^2, \qquad (6.4)$$

76

where,

$$\bar{b}_q^2 = \frac{2b_q^2 g^2 g_f \mid q_f eB \mid}{(2\pi)^2}. \tag{6.5}$$

Using Eq. (6.4) with Eq. (2.6), we get,

$$\left(\frac{m_q}{T}\right)^2 = \left(\frac{m_0}{T} + \bar{b}_q F_q\right)^2 + \bar{b}_q^2 F_q^2. \tag{6.6}$$

Eq. (6.6) can now be substituted in Eq. (6.3) and solved for F_q, to obtain the thermomagnetic mass at finite chemical potential using Eq. (6.6).

6.3 The QCD coupling

An essential ingredient to our model is the thermomagnetic coupling at finite chemical potential. We use the one-loop running coupling constant that evolves with both the momentum transfer and the magnetic field [143] as,

$$\alpha_s(\Lambda^2, \mid eB \mid) = \frac{\alpha_s(\Lambda^2)}{1 + b_1 \alpha_s(\Lambda^2) \ln\left(\frac{\Lambda^2}{\Lambda^2 + |eB|}\right)}. \tag{6.7}$$

The one-loop running coupling in the absence of a magnetic field at the renormalization scale is given by,

$$\alpha_s(\Lambda^2) = \frac{1}{b_1 \ln(\Lambda^2/\Lambda_{\overline{MS}}^2)}, \tag{6.8}$$

where, $b_1 = (11N_c - 2N_f)/12\pi$, and $\overline{MS} = .176 GeV$ at $\alpha_s(1.5 GeV) = 0.326$ for $N_f = 3$.

For non-zero chemical potential, following [152] we need to choose different renormalization scales for gluons, $\Lambda = \Lambda_g$, and quarks $\Lambda = \Lambda_q$. We choose $\Lambda_g = 2\pi T$ and $\Lambda_q = 2\pi \sqrt{T^2 + \mu^2/\pi^2}$.

6.4 Number density and susceptibility

The net quark flavor number density is,

$$N_q = \frac{g_f \mid q_f eB \mid}{(2\pi)^2} \sum_{j=0}^{\infty} (2 - \delta_{0j}) \int_{-\infty}^{\infty} dk_z \left(\frac{1}{z^{-1} e^{\frac{\omega_j(k_z)}{T}} + 1} - \frac{1}{z e^{\frac{\omega_j(k_z)}{T}} + 1} \right),$$

(6.9)

where, $\omega_j(k_z)^2 = k_z^2 + m_{q_j}^2$. After some algebra, we have,

$$\frac{N_q}{T^3} = \frac{g_f}{2\pi^2} \sum_{j=0}^{\infty} (2 - \delta_{0j}) \sum_{l=1}^{\infty} \frac{(-1)^{l-1}}{l^3} \left(l \frac{m_{q_j}}{T} \right)^2 K_2 \left(l \frac{m_{q_j}}{T} \right) \sinh \left(l \frac{\mu}{T} \right).$$

(6.10)

The number suceptibility is the measure of fluctuations in N_q and can be obtained from N_q.

$$\chi_q = \frac{\partial N_q}{\partial \mu} \mid_{\mu=0} .$$

(6.11)

6.5 Energy density

The quark-contribution to the energy density of magnetized QGP at finite chemical potential is given by,

$$\varepsilon_q = \frac{g_f |q_f eB|}{4\pi^2} \sum_{j=0}^{\infty} (2 - \delta_{0j}) \int_{-\infty}^{\infty} dk_z \frac{\omega_{k_{zj}}}{z^{-1} e^{\omega_{k_{zj}}/T} + 1}.$$

(6.12)

The contribution from antiquarks is,

$$\varepsilon_{\bar{q}} = \frac{g_f |q_f eB|}{4\pi^2} \sum_{j=0}^{\infty} (2 - \delta_{0j}) \int_{-\infty}^{\infty} dk_z \frac{\omega_{k_{zj}}}{z e^{\omega_{k_{zj}}/T} + 1}.$$

(6.13)

The contribution from the quarks and antiquarks of a particular flavor can be obtained by adding (6.12) and (6.13) to get,

$$\varepsilon_f = \frac{2g_f|q_f eB|}{2\pi^2}\frac{T^2}{2}\sum_{l=0}^{\infty}\frac{(-1)^{(l-1)}}{l^2}\left\{\sum_{j=0}^{\infty}(2-\delta_{0j})\right.$$
$$\left.\left[\left(\beta m_{q_j}l\right)K_1\left(\beta m_{q_j}l\right) + \left(\beta m_{q_j}l\right)^2 K_0\left(\beta m_{q_j}l\right)\right]\cosh\left(l\frac{\mu}{T}\right)\right\}. \quad (6.14)$$

The expression for the contribution from gluons remains the same as Eq. (3.46) because gluons have chemical potential zero. The gluon energy density depends on the quark chemical potential through the thermomagnetic mass of gluons, which depends on the quark chemical potential.

6.6   Pressure

Following [123], we can find the pressure from the energy density by the relation,

$$\frac{P(T,B,\mu)}{T} = \frac{P(T_0,B,\mu)}{T_0} + \int_{T_0}^{T} d\tau \frac{\varepsilon - \mu N_q}{\tau^2}. \quad (6.15)$$

The difference between the pressures at non-zero chemical potential and zero chemical potential for quarks can be obtained by the relation,

$$\Delta P \equiv P(T,B,\mu) - P(T,B,0) = \int_0^{\mu} N_q d\mu. \quad (6.16)$$

6.7   Debye mass

The distribution function of quasiparticles in Eq. (5.20) becomes,

$$f_q(\omega_{k_z}^j) = \frac{1}{z^{-1}e^{\beta\omega_k} + 1}, \quad (6.17)$$

for quarks, and

$$f_{\bar{q}}(\omega_k) = \frac{1}{ze^{\beta\omega_k} + 1},\tag{6.18}$$

for antiquarks. These expressions along with Eq. (5.16) gives the quark-antiquark contribution, for $B = 0$,

$$m_D^2 = \frac{2N_c g^2 T^2}{\pi^2} \sum_{l=1}^{\infty} \frac{(-1)^{l-1}}{l^2} \left(\frac{lm_q}{T}\right)^2 K_2\left(\frac{lm_q}{T}\right) \cosh\left(l\frac{\mu}{T}\right).\tag{6.19}$$

In the presence of an external magnetic field, the distribution functions for quarks and antiquarks become,

$$f_q(\omega_{k_z}^j) = \frac{1}{z^{-1}e^{\beta\omega_{k_z}^j} + 1},\tag{6.20}$$

and

$$f_{\bar{q}}(\omega_{k_z}^j) = \frac{1}{ze^{\beta\omega_{k_z}^j} + 1}.\tag{6.21}$$

Using these distribution functions in Eq. (5.19) and adding the contributions from quarks and antiquarks, we get,

$$m_D^2(eB) = \frac{N_c g^2}{\pi^2} \sum_f \mid q_f eB \mid \sum_{l=1}^{\infty} (-1)^{l-1} \sum_{j=0}^{\infty} (2 - \delta_{0j})$$
$$\left(\frac{lm_{q_j}}{T}\right) K_1\left(\frac{lm_{q_j}}{T}\right) \cosh\left(l\frac{\mu}{T}\right).\tag{6.22}$$
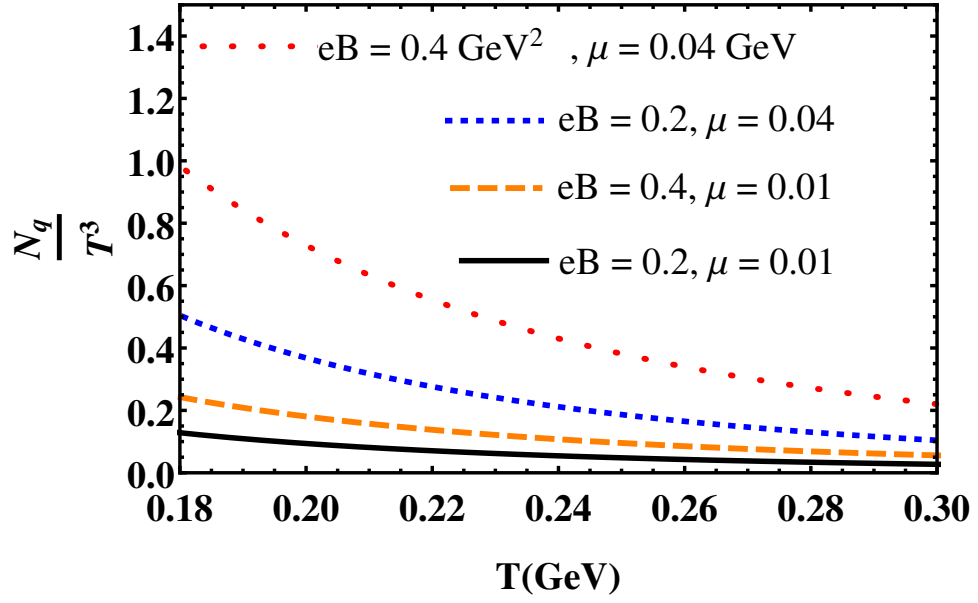
Figure 6.1: The variation of scaled quark number density with temperature for different combinations of μ and eB
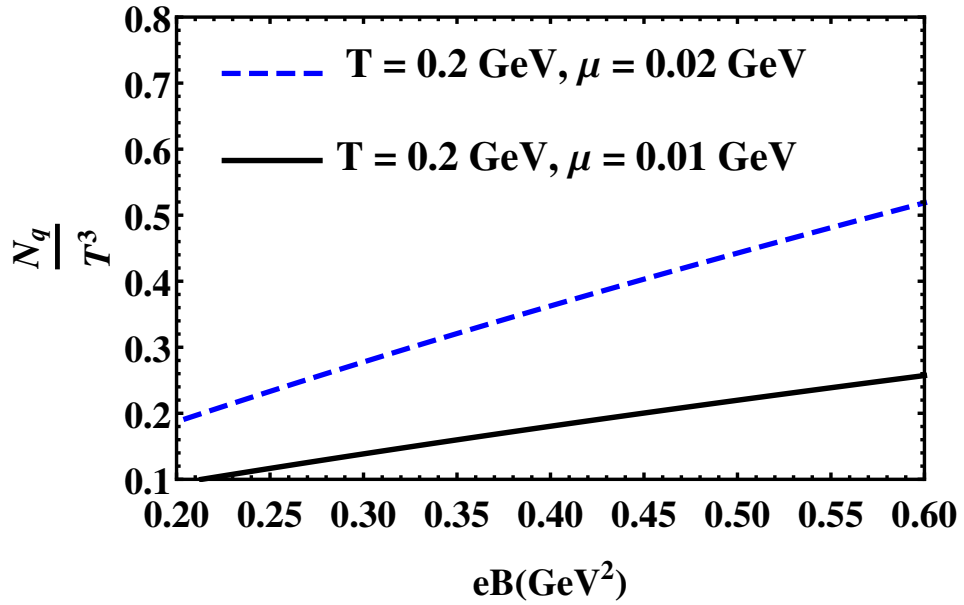
Figure 6.2: The variation of scaled quark number density with magnetic field for different chemical potentials.
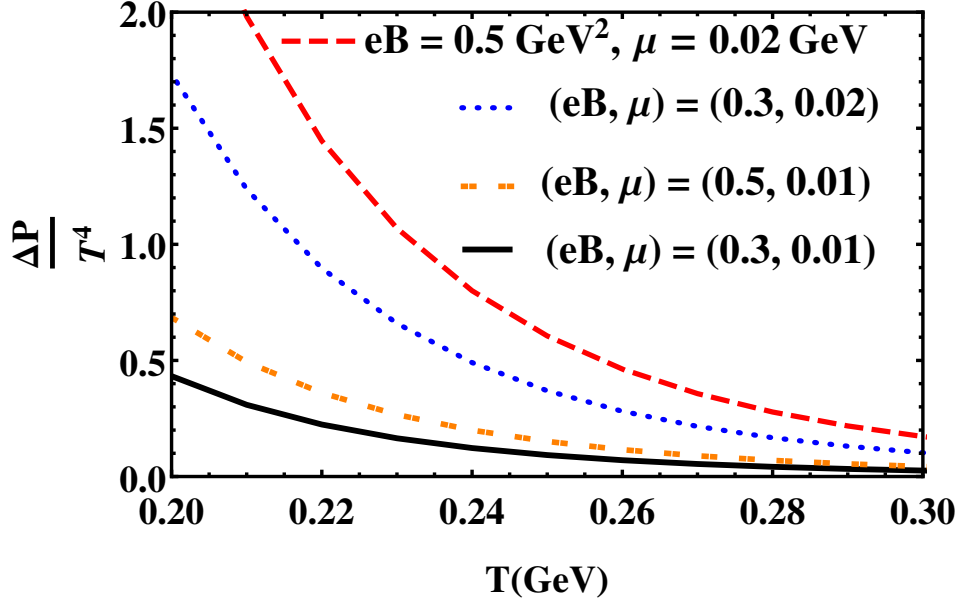
Figure 6.3: Variation of $\Delta P/T^4$ with temperature for different strengths of the magnetic field and chemical potentials

6.8 Results and discussions

For simplicity, we confine our calculations to the LLL approximation applicable to the strong magnetic field ($T \ll \sqrt{|q_f eB|}$). The expressions we have obtained, however, are general and include the HLL effects too. Besides, the running coupling we use is valid only in the LLL approximation.

We plot the scaled net Baryon number density, Eq. (6.10), in Figures 6.1 and 6.2. We see that the number-density increases with both the magnetic field and chemical potential.

In Figures 6.3 and 6.4 we see the behavior of $\Delta P/T^4$ as a function of the temperature strength of the magnetic field respectively. As expected, the pressure difference is enhanced as the chemical potential increases. The pressure also increases with the magnetic field, which are in accordance with our previous chapters' results.

The quark number susceptibility is enhanced in the presence of both chemical
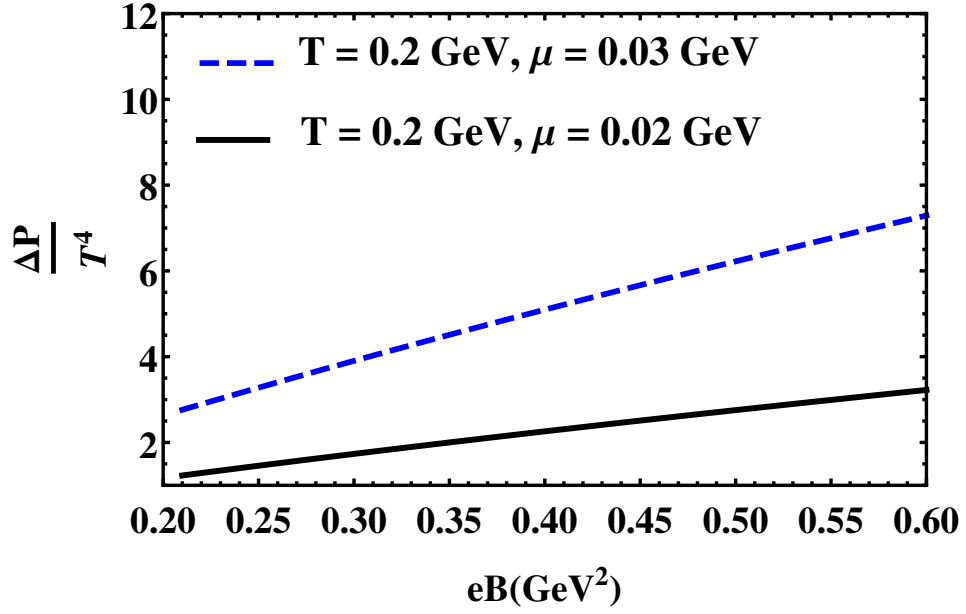
Figure 6.4: Variation of $\Delta P/T^4$ with magnetic field for different chemical potentials.
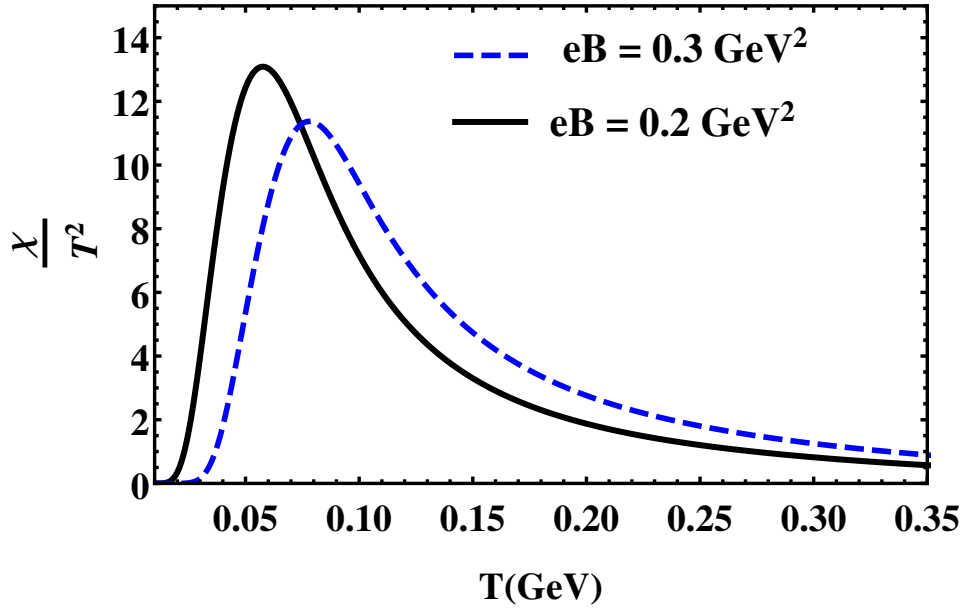
Figure 6.5: The scaled number susceptibility χ/T^2 for two different strengths of the magnetic field, plotted as a function of temperature.
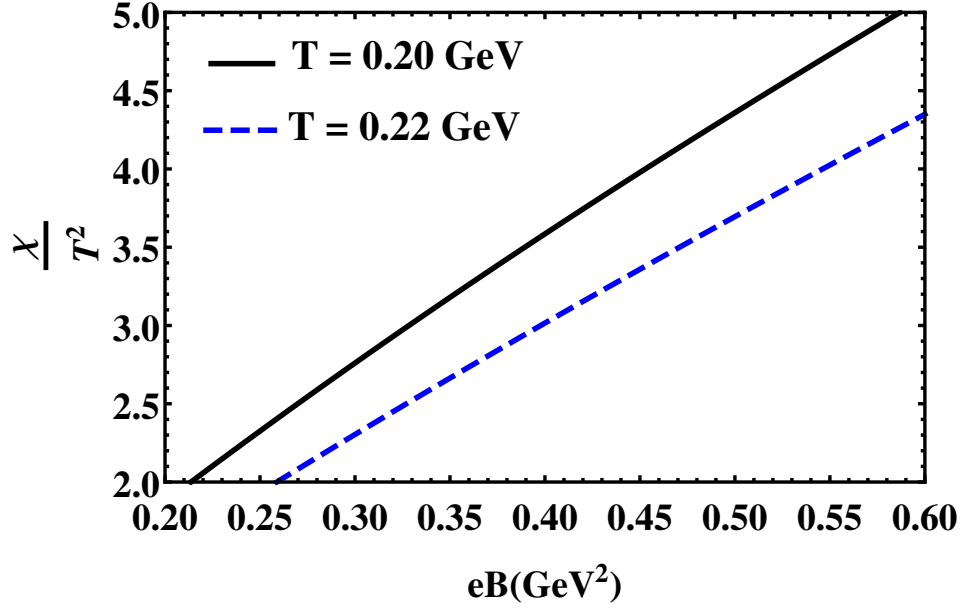
Figure 6.6: The variation of scaled number susceptibility (χ/T^2) with magnetic field for two different temperatures.
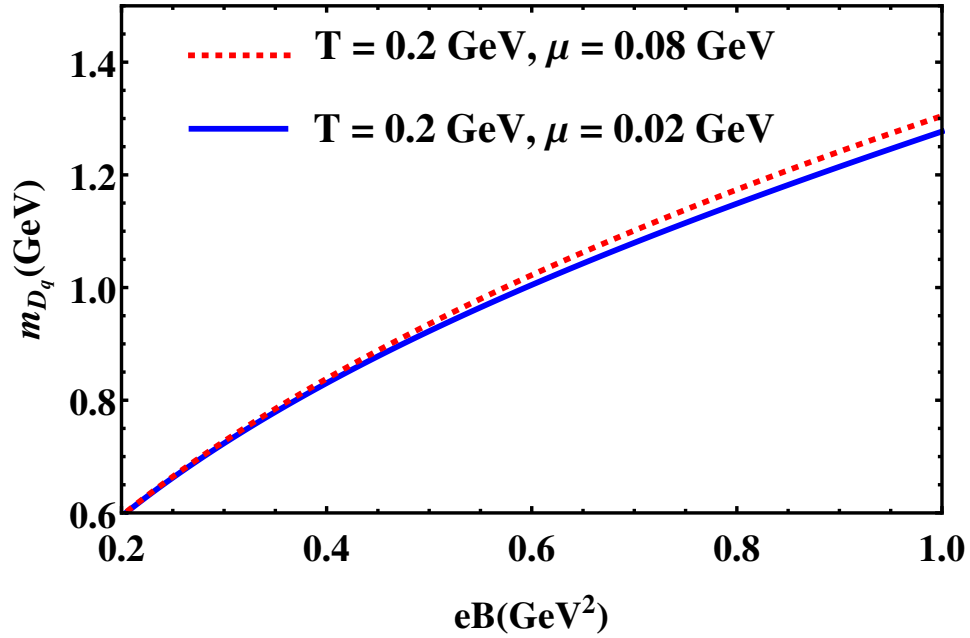
Figure 6.7: The variation of quark Debye mass with magnetic field for different chemical potentials.
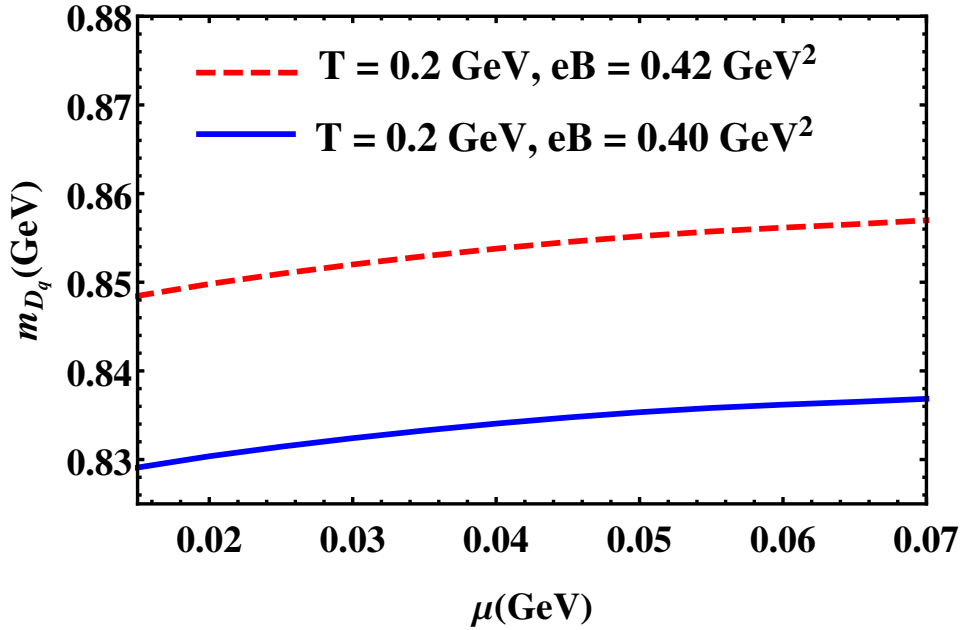
Figure 6.8: The variation of quark Debye mass with chemical potential for different strengths of the magnetic field.

potential and the magnetic field, as seen from Figures 6.5 and 6.6. The behavior of the susceptibility obtained using our model is consistent with the results obtained using holographic QCD [175].

From Figures 6.7 and 6.8, we see that the quark Debye mass increases with both magnetic field and chemical potential. The change in the Debye mass with chemical potential is small.

6.9 Summary

The generalization of the extended quasiparticle model facilitates the study of magnetized QGP at finite densities. Such generalization allows us to calculate the net baryon density, quark number susceptibility, and the pressure difference and examine the variation of these quantities with the magnetic field and temperature. The quark contribution to the Debye mass shows a small increase as the chemical potential increases.

Chapter 7

Conclusions and future plans

QGP, the state of matter believed to have existed shortly after the big bang, has been successfully created in high energy collisions. It is known that a large magnetic field is produced during off-central collisions involving charged particles. A strong magnetic field is estimated to have existed right after the big bang and in the interior of strongly magnetized neutron stars. The investigation of the behavior of magnetized QGP is, therefore, of importance. The theoretical tools used to study the QGP need modifications to incorporate the effects of the external magnetic field, and much research has been going on in this area.

In this work, we have constructed a phenomenological model to study the effect of the magnetic field on the QGP behavior. We adopted the quasiparticle approach and considered magnetized QGP as a system of quasiparticles with mass depending on both temperature and the magnetic field. Along with the modification of thermal mass under the external magnetic field, we took into account the quantization of momentum perpendicular to the magnetic field direction. We found that the so-called self-consistent quasiparticle model is particularly suitable to be generalized to incorporate the external magnetic field. So, in chapter 2, we studied the self-consistent quasiparticle model with the necessary details.

In chapter 3, we have extended the self-consistent quasiparticle model for hot QCD in the presence of the magnetic field to understand the behavior of magnetized quark matter. The definition of thermal mass in the self-consistent model can be modified to define the thermomagnetic mass of quasiparticles. The thermodynamic quantities are evaluated by starting with the modified momentum distributions and the energy dispersion relations. The modification of these quantities has been brought about by incorporating relativistic Landau levels.

In chapter 4 we studied the thermodynamics of both 2 and $(2 + 1)$ flavor magnetized QGP using the modified quasiparticle model. We examined the behavior of energy density, pressure, entropy density and speed of sound in the temperature range 170-400 MeV. To this end, we made use of two separate parametrizations of the coupling constant that depends both on temperature and the magnetic field. We found that the energy density, pressure, and entropy density increase in the presence of the magnetic field as expected. Our results are qualitatively consistent with the results obtained using other approaches, including lattice QCD simulations.

The correct behavior of the equation of state shows that the self-consistent quasiparticle model allows an extension to study the thermodynamics of QGP in the presence of the magnetic field.

In chapter 5, we used the extended self-consistent quasiparticle model to study the magnetic response, pressure anistropy, and screening properties of $(2 + 1)$-flavor QGP. The magnetic response of QGP was investigated by our model, and the variation of magnetization with temperature and the magnetic field examined. We found that QGP has a paramagnetic nature. It has a small but positive magnetization at all temperatures above the transition temperature. We also noted that magnetization makes the system anisotropic, causing different pressures

in directions parallel and perpendicular to the magnetic field. We evaluated the transverse pressure and plotted its variation with both the magnetic field and temperature. The equation of state and anisotropic pressure calculated here can be used as an input for magnetohydrodynamic calculations and analysis of the elliptic flow of QGP formed in heavy-ion collisions. We see that the total longitudinal pressure (thermodynamic + pure field) becomes negative, indicating instability in the system in this region. The full transverse pressure remains positive and increases with the magnetic field in the range of the magnetic field and temperatures considered in this work. Finally, we studied the screening properties of magnetized QGP by examining the behavior of Debye screening mass in the longitudinal direction. We saw that the screening mass increases with the magnetic field. Our results showed the same qualitative behavior as those obtained from Lattice QCD calculations and HTL perturbation theory approach and those obtained using other phenomenological models. The quark contribution to Debye mass as calculated and plotted using our model agrees reasonably well with the corresponding results from perturbative QCD at high temperatures.

In Chapter 6, we further generalized our model to finite chemical potentials. We studied the net quark-number density (n_μ), the pressure difference (ΔP), and the number susceptibility (χ_q) at different temperatures, different values of the magnetic field, and chemical potentials. We also examined the behavior of the quark Debye mass using our generalized model. Our results are qualitatively consistent with corresponding results obtained in other works.

We have seen that the extension of the self-consistent quasiparticle model to include the effects of the magnetic field is quite successful. It provides a phenomenological description of magnetized QGP and allows the study of the thermodynamic and thermomagnetic properties of the de-confined QCD matter in the presence of the magnetic field. The model is simple and is capable of

incorporating the HLLs without any modification. The only missing ingredient is a more reliable thermomagnetic coupling, which includes the effects of HLLs.

Our next interest is to predict results that can be quantitatively compared with Lattice QCD and experimental results. The present results could be improved and made quantitatively reliable with a two-loop order thermomagnetic coupling, which also includes the contributions from HLLs. We like to apply our model to study the transport coefficients of magnetized QGP with the equation of state obtained using the extended self-consistent quasiparticle model. Yet another potential area of investigation is the application of our model to the study of strongly magnetized neutron stars and magnetars.

Bibliography

[1] T. Muta. *Foundations of quantum chromodynamics : an introduction to perturbative methods in gauge theories.* World Scientific, Singapore Hackensack, N.J, 2010.

[2] M. Gell-Mann. A schematic model of baryons and mesons. *Physics Letters*, 8(3):214–215, Feb. 1964.

[3] G. Zweig. *An SU(3) model for strong interaction symmetry and its breaking. Version 2*, pages 22–101. CERN-TH-412, 2 1964.

[4] J. D. Bjorken. Asymptotic sum rules at infinite momentum. *Physical Review*, 179(5):1547–1553, Mar. 1969.

[5] M. Breidenbach, J. I. Friedman, H. W. Kendall, E. D. Bloom, D. H. Coward, H. DeStaebler, J. Drees, L. W. Mo, and R. E. Taylor. Observed behavior of highly inelastic electron-proton scattering. *Physical Review Letters*, 23(16):935–939, Oct. 1969.

[6] J. D. Bjorken and E. A. Paschos. Inelastic electron-proton and γ-proton scattering and the structure of the nucleon. *Physical Review*, 185(5):1975–1982, Sept. 1969.

[7] R. P. Feynman. Very high-energy collisions of hadrons. *Physical Review Letters*, 23(24):1415–1417, Dec. 1969.

[8] A. Zee. Study of the renormalization group for small coupling constants. *Physical Review D*, 7(12):3630–3636, June 1973.

[9] C. N. Yang and R. L. Mills. Conservation of isotopic spin and isotopic gauge invariance. *Physical Review*, 96(1):191–195, Oct. 1954.

[10] G. 't Hooft and M. Veltman. Regularization and renormalization of gauge fields. *Nuclear Physics B*, 44(1):189–213, July 1972.

[11] D. J. Gross and F. Wilczek. Ultraviolet behavior of non-abelian gauge theories. *Physical Review Letters*, 30(26):1343–1346, June 1973.

[12] H. D. Politzer. Reliable perturbative results for strong interactions? *Physical Review Letters*, 30(26):1346–1349, June 1973.

[13] S. Coleman and D. J. Gross. Price of asymptotic freedom. *Physical Review Letters*, 31(13):851–854, Sept. 1973.

[14] G. 't Hooft. Renormalization of massless yang-mills fields. *Nuclear Physics B*, 33(1):173–199, Oct. 1971.

[15] M. Y. Han and Y. Nambu. Three-triplet model with Double SU(3) symmetry. *Physical Review*, 139(4B):B1006–B1010, Aug. 1965.

[16] M. Gell-Mann. Quarks. In *Elementary Particle Physics*, pages 733–761. Springer Vienna, 1972.

[17] O. W. Greenberg. Spin and unitary-spin independence in a paraquark model of baryons and mesons. *Physical Review Letters*, 13(20):598–602, Nov. 1964.

[18] Y. Ohnuki and S. Kamefuchi. Parafermi field theory. *Progress of Theoretical Physics*, 50(1):258–276, July 1973.

[19] H. Fritzsch, M. Gell-Mann, and H. Leutwyler. Advantages of the color octet gluon picture. *Physics Letters B*, 47(4):365–368, Nov. 1973.

[20] D. J. Gross and F. Wilczek. Asymptotically free gauge theories. i. *Physical Review D*, 8(10):3633–3652, Nov. 1973.

[21] D. J. Gross and F. Wilczek. Asymptotically free gauge theories. II. *Physical Review D*, 9(4):980–993, Feb. 1974.

[22] H. Georgi and H. D. Politzer. Electroproduction scaling in an asymptotically free theory of strong interactions. *Physical Review D*, 9(2):416–420, Jan. 1974.

[23] Y. Watanabe, L. N. Hand, S. Herb, A. Russell, C. Chang, K. K. W. Chen, D. J. Fox, A. Kotlewski, P. F. Kunz, S. C. Loken, M. Strovink, and W. Vernon. Test of scale invariance in ratios of muon scattering cross sections at 150 and 56 GeV. *Physical Review Letters*, 35(14):898–901, Oct. 1975.

[24] C. Chang, K. W. Chen, D. J. Fox, A. Kotlewski, P. F. Kunz, L. N. Hand, S. Herb, A. Russell, Y. Watanabe, S. C. Loken, M. Strovink, and W. Vernon. Observed deviations from scale invariance in high-energy muon scattering. *Physical Review Letters*, 35(14):901–904, Oct. 1975.

[25] R. Hagedorn. Statistical thermodynamics of strong interactions at high-energies. *Nuovo Cimento, Supplemento*, 3:147–186, 1965.

[26] N. Cabibbo and G. Parisi. Exponential hadronic spectrum and quark liberation. *Physics Letters B*, 59(1):67–69, Oct. 1975.

[27] E. Shuryak. Quark-gluon plasma and hadronic production of leptons, photons and psions. *Physics Letters B*, 78(1):150–153, Sept. 1978.

[28] U. Heinz. The strongly coupled quark–gluon plasma created at RHIC. *Journal of Physics A: Mathematical and Theoretical*, 42(21):214003, May 2009.

[29] K. Aamodt et al. Elliptic flow of charged particles in pb-pb collisions atsNN=2.76 TeV. *Physical Review Letters*, 105(25), Dec. 2010.

[30] G. Aad et al. Observation of a centrality-dependent dijet asymmetry in lead-lead collisions atsNN=2.76 TeVwith the ATLAS detector at the LHC. *Physical Review Letters*, 105(25), Dec. 2010.

[31] M. D. Schwartz. *Quantum Field Theory and the Standard Model.* Cambridge University Pr., 2014.

[32] R. A. Schneider. *QCD Phenomenology at High Temperatures.* PhD thesis, Technische Universität München, 2002.

[33] G. Martinez. Advances in quark gluon plasma. *arXiv:1304.1452v1 [nucl-ex]*, 2013.

[34] T. Kugo and I. Ojima. Local covariant operator formalism of non-abelian gauge theories and quark confinement problem. *Progress of Theoretical Physics Supplement*, 66:1–130, 1979.

[35] D. V. S. Michael E. Peskin. *An Introduction To Quantum Field Theory.* Taylor & Francis Inc, 1995.

[36] C. Becchi, A. Rouet, and R. Stora. Renormalization of gauge theories. *Annals of Physics*, 98(2):287–321, June 1976.

[37] M. Z. Iofa and I. V. Tyutin. Gauge invariance of spontaneously broken non-abelian theories in the bogolyubov-parasyuk-hepp-zimmermann method. *Theoretical and Mathematical Physics*, 27(1):316–322, Apr. 1976.

[38] D. Griffiths. *Introduction to Elementary Particles.* Wiley, Dec. 1987.

[39] A. Zee. *Quantum Field Theory in a Nutshell.* Princeton Univers. Press, 2010.

[40] C. Gattringer and C. B. Lang. *Quantum Chromodynamics on the Lattice.* Springer Berlin Heidelberg, 2010.

[41] J. I. Kapusta and C. Gale. *Finite-Temperature Field Theory.* Cambridge University Press, 2006.

[42] L. McLerran. The quark gluon plasma and the color glass condensate: 4 lectures. *arXiv:hep-ph/0311028v1*, 2003.

[43] G. Aarts. Introductory lectures on lattice QCD at nonzero baryon number. *Journal of Physics: Conference Series*, 706:022004, Apr. 2016.

[44] K. Rajagopal and F. Wilczek. The condensed matter physics of QCD. In *At The Frontier of Particle Physics*, pages 2061–2151. World Scientific, Apr. 2001.

[45] V. Koch. Aspects of chiral symmetry. *International Journal of Modern Physics E*, 06(02):203–249, June 1997.

[46] A. Chodos, R. L. Jaffe, K. Johnson, C. B. Thorn, and V. F. Weisskopf. New extended model of hadrons. *Physical Review D*, 9(12):3471–3495, June 1974.

[47] T. DeGrand, R. L. Jaffe, K. Johnson, and J. Kiskis. Masses and other parameters of the light hadrons. *Physical Review D*, 12(7):2060–2076, Oct. 1975.

[48] V. M. Bannur. Equation of state for a non-ideal quark gluon plasma. *Physics Letters B*, 362(1-4):7–10, Nov. 1995.

[49] B. Sheikholeslami-Sabzevari. Equation of state for hot quark-gluon plasma transitions to hadrons with full QCD potential. *Physical Review C*, 65(5), Apr. 2002.

[50] K. M. Udayanandan, P. Sethumadhavan, and V. M. Bannur. Equation of

state of a quark-gluon plasma using the cornell potential. *Physical Review C*, 76(4), Oct. 2007.

[51] V. M. Bannur. Quark–gluon plasma as a strongly coupled color-coulombic plasma. *The European Physical Journal C*, 11(1):169–171, Oct. 1999.

[52] V. M. Bannur. Strongly coupled quark gluon plasma (SCQGP). *Journal of Physics G: Nuclear and Particle Physics*, 32(7):993–1002, May 2006.

[53] P. Lévai and U. Heinz. Massive gluons and quarks and the equation of state obtained from SU(3) lattice QCD. *Physical Review C*, 57(4):1879–1890, Apr. 1998.

[54] A. Dumitru and R. D. Pisarski. Degrees of freedom and the deconfining phase transition. *Physics Letters B*, 525(1-2):95–100, Jan. 2002.

[55] K. Fukushima. Chiral effective model with the polyakov loop. *Physics Letters B*, 591(3-4):277–284, July 2004.

[56] S. K. Ghosh, T. K. Mukherjee, M. G. Mustafa, and R. Ray. Susceptibilities and speed of sound from the polyakov-nambu-jona-lasinio model. *Physical Review D*, 73(11), June 2006.

[57] H. Abuki and K. Fukushima. Gauge dynamics in the PNJL model: Color neutrality and casimir scaling. *Physics Letters B*, 676(1-3):57–62, June 2009.

[58] H.-M. Tsai and B. Müller. Phenomenology of the three-flavor PNJL model and thermal strange quark production. *Journal of Physics G: Nuclear and Particle Physics*, 36(7):075101, Apr. 2009.

[59] M. D'Elia, A. D. Giacomo, and E. Meggiolaro. Field strength correlators in full QCD. *Physics Letters B*, 408(1-4):315–319, Sept. 1997.

[60] P. Castorina and M. Mannarelli. Effective degrees of freedom of the quark–gluon plasma. *Physics Letters B*, 644(5-6):336–339, Jan. 2007.

[61] P. Castorina and M. Mannarelli. Effective degrees of freedom and gluon condensation in the high temperature deconfined phase. *Physical Review C*, 75(5), May 2007.

[62] N. Su and K. Tywoniuk. Massless mode and positivity violation in hot QCD. *Physical Review Letters*, 114(16), Apr. 2015.

[63] V. Chandra and V. Ravishankar. Quasi-particle model for lattice QCD: quark–gluon plasma in heavy ion collisions. *The European Physical Journal C*, 64(1):63–72, Sept. 2009.

[64] V. Chandra and V. Ravishankar. Quasiparticle description of (2+1)- flavor lattice QCD equation of state. *Physical Review D*, 84(7), Oct. 2011.

[65] B. Back et al. The phobos perspective on discoveries at rhic. *Nuclear Physics A*, 757(1):28 – 101, 2005. First Three Years of Operation of RHIC.

[66] Z. Yang, Y. Chun-Bin, C. Xu, and F. Sheng-Qin. Spatial distributions of magnetic field in the rhic and lhc energy regions. *Chinese Physics C*, 39(10):104105, 2015.

[67] K. Adcox et al. Formation of dense partonic matter in relativistic nucleus–nucleus collisions at rhic: Experimental evaluation by the phenix collaboration. *Nuclear Physics A*, 757(1):184 – 283, 2005. First Three Years of Operation of RHIC.

[68] I. Arsene et al. Quark–gluon plasma and color glass condensate at RHIC? The perspective from the BRAHMS experiment. *Nuclear Physics A*, 757(1):1 – 27, 2005. First Three Years of Operation of RHIC.

[69] V. V. Skokov, A. Y. Illarionov, and V. D. Toneev. Estimate of the magnetic field strength in heavy-ion collisions. *International Journal of Modern Physics A*, 24(31):5925–5932, Dec. 2009.

[70] K. Tuchin. Synchrotron radiation by fast fermions in heavy-ion collisions. *Phys. Rev. C*, 82:034904, Sept. 2010.

[71] K. Marasinghe and K. Tuchin. Quarkonium dissociation in quark-gluon plasma via ionization in a magnetic field. *Phys. Rev. C*, 84:044908, Oct. 2011.

[72] K. Tuchin. Photon decay in a strong magnetic field in heavy-ion collisions. *Phys. Rev. C*, 83:017901, Jan. 2011.

[73] K. Fukushima and J. M. Pawlowski. Magnetic catalysis in hot and dense quark matter and quantum fluctuations. *Physical Review D*, 86:076013, Oct. 2012.

[74] V. Gusynin, V. Miransky, and I. Shovkovy. Catalysis of dynamical flavor symmetry breaking by a magnetic field in $2 + 1$ dimensions. *Physical Review Letters*, 73(26):3499–3502, 1994.

[75] *Strongly Interacting Matter in Magnetic Fields*. Springer Berlin Heidelberg, 2013.

[76] V. Gusynin, V. Miransky, and I. Shovkovy. Dimensional reduction and catalysis of dynamical symmetry breaking by a magnetic field. *Nuclear Physics B*, 462(2-3):249–290, Mar. 1996.

[77] K. Fukushima and Y. Hidaka. Magnetic catalysis versus magnetic inhibition. *Physical Review Letters*, 110(3), Jan. 2013.

[78] K. Fukushima, D. E. Kharzeev, and H. J. Warringa. Chiral magnetic effect. *Physical Review D*, 78:074033, Oct. 2008.

[79] D. E. Kharzeev, L. D. McLerran, and H. J. Warringa. The effects of topological charge change in heavy ion collisions: "event by event p and cp violation". *Nuclear Physics A*, 803(3):227 – 253, 2008.

[80] D. E. Kharzeev. The chiral magnetic effect and anomaly-induced transport. *Progress in Particle and Nuclear Physics*, 75:133 – 151, 2014.

[81] D. Grasso and H. R. Rubinstein. Magnetic fields in the early universe. *Physics Reports*, 348(3):163–266, July 2001.

[82] R. C. Duncan and C. Thompson. Formation of very strongly magnetized neutron stars - implications for gamma-ray bursts. *The Astrophysical Journal*, 392:L9, June 1992.

[83] A. Broderick, M. Prakash, and J. M. Lattimer. The equation of state of neutron star matter in strong magnetic fields. *The Astrophysical Journal*, 537(1):351–367, July 2000.

[84] C. Y. Cardall, M. Prakash, and J. M. Lattimer. Effects of strong magnetic fields on neutron star structure. *The Astrophysical Journal*, 554(1):322–339, June 2001.

[85] A. Rabhi, C. Providência, and J. D. Providência. Stellar matter with a strong magnetic field within density-dependent relativistic models. *Journal of Physics G: Nuclear and Particle Physics*, 35(12):125201, Oct. 2008.

[86] A. Rabhi, P. K. Panda, and C. Providência. Warm and dense stellar matter under strong magnetic fields. *Physical Review C*, 84(3), Sept. 2011.

[87] M. Strickland, V. Dexheimer, and D. P. Menezes. Bulk properties of a fermi gas in a magnetic field. *Physical Review D*, 86(12), Dec. 2012.

[88] S. S. Avancini, V. Dexheimer, R. L. S. Farias, and V. S. Timóteo. Anisotropy in the equation of state of strongly magnetized quark matter within the nambu–jona-lasinio model. *Physical Review C*, 97(3), Mar. 2018.

[89] B. Karmakar, R. Ghosh, A. Bandyopadhyay, N. Haque, and M. G. Mustafa. Anisotropic pressure of deconfined QCD matter in presence of strong magnetic field within one-loop approximation. *Physical Review D*, 99(9), May 2019.

[90] M. Kurian and V. Chandra. Bulk viscosity of a hot QCD medium in a strong magnetic field within the relaxation-time approximation. *Physical Review D*, 97(11), June 2018.

[91] M. Kurian, S. K. Das, and V. Chandra. Heavy quark dynamics in a hot magnetized QCD medium. *Physical Review D*, 100(7), Oct. 2019.

[92] M. Kurian and V. Chandra. Longitudinal conductivity of hot magnetized collisional QCD medium in the inhomogeneous electric field. *Physical Review D*, 99(11), June 2019.

[93] A. Mukherjee, S. Ghosh, M. Mandal, S. Sarkar, and P. Roy. Effect of external magnetic fields on nucleon mass in a hot and dense medium: Inverse magnetic catalysis in the walecka model. *Physical Review D*, 98(5), Sept. 2018.

[94] M. Kurian, S. Mitra, S. Ghosh, and V. Chandra. Transport coefficients of hot magnetized QCD matter beyond the lowest landau level approximation. *The European Physical Journal C*, 79(2), Feb. 2019.

[95] A. Bandyopadhyay, C. A. Islam, and M. G. Mustafa. Electromagnetic spectral properties and debye screening of a strongly magnetized hot medium. *Physical Review D*, 94(11), Dec. 2016.

[96] G. Endrődi. QCD equation of state at nonzero magnetic fields in the hadron resonance gas model. *Journal of High Energy Physics*, 2013(4), Apr. 2013.

[97] M. Y. Jamal, S. Mitra, and V. Chandra. Collective excitations of hot QCD medium in a quasiparticle description. *Physical Review D*, 95(9), May 2017.

[98] L. Levkova and C. DeTar. Quark-gluon plasma in an external magnetic field. *Physical Review Letters*, 112(1), Jan. 2014.

[99] S. Ghosh and V. Chandra. Scattering cross-section under external magnetic field using the optical theorem. *The European Physical Journal A*, 56(7), July 2020.

[100] A. Bandyopadhyay, S. Ghosh, R. L. Farias, J. Dey, and G. Krein. Anisotropic electrical conductivity of magnetized hot quark matter. *Physical Review D*, 102(11):114015, Dec. 2020.

[101] A. Bandyopadhyay, R. L. S. Farias, B. S. Lopes, and R. O. Ramos. Quantum chromodynamics axion in a hot and magnetized medium. *Physical Review D*, 100(7), Oct. 2019.

[102] S. K. Das, S. Plumari, S. Chatterjee, J. Alam, F. Scardina, and V. Greco. Directed flow of charm quarks as a witness of the initial strong magnetic field in ultra-relativistic heavy ion collisions. *Physics Letters B*, 768:260–264, May 2017.

[103] S. S. Avancini, R. L. Farias, N. N. Scoccola, and W. R. Tavares. NJL-type models in the presence of intense magnetic fields: The role of the regularization prescription. *Physical Review D*, 99(11), June 2019.

[104] R. L. S. Farias, K. P. Gomes, G. Krein, and M. B. Pinto. Importance of asymptotic freedom for the pseudocritical temperature in magnetized quark matter. *Physical Review C*, 90(2), Aug. 2014.

[105] R. Rougemont, R. Critelli, and J. Noronha. Holographic calculation of the QCD crossover temperature in a magnetic field. *Physical Review D*, 93(4), Feb. 2016.

[106] S. Fayazbakhsh and N. Sadooghi. Phase diagram of hot magnetized two-flavor color-superconducting quark matter. *Physical Review D*, 83(2), Jan. 2011.

[107] S. Fayazbakhsh and N. Sadooghi. Color neutral two-flavor superconducting phase of cold and dense quark matter in the presence of constant magnetic fields. *Physical Review D*, 82(4), Aug. 2010.

[108] B. Singh, L. Thakur, and H. Mishra. Heavy quark complex potential in a strongly magnetized hot QGP medium. *Physical Review D*, 97(9), May 2018.

[109] S. Acharya et al. Probing the effects of strong electromagnetic fields with charge-dependent directed flow in pb-pb collisions at the LHC. *Physical Review Letters*, 125(2), July 2020.

[110] S. Bhadury, M. Kurian, V. Chandra, and A. Jaiswal. First order dissipative hydrodynamics and viscous corrections to the entropy four-current from an effective covariant kinetic theory. *Journal of Physics G: Nuclear and Particle Physics*, 47(8):085108, July 2020.

[111] T. S. Biró, P. Lévai, and B. Müller. Strangeness production with "massive" gluons. *Physical Review D*, 42(9):3078–3087, Nov. 1990.

[112] V. Goloviznin and H. Satz. The refractive properties of the gluon plasma in SU(2) gauge theory. *Zeitschrift für Physik C Particles and Fields*, 57(4):671–675, Dec. 1993.

[113] A. Peshier, B. Kämpfer, O. Pavlenko, and G. Soff. An effective model of the quark-gluon plasma with thermal parton masses. *Physics Letters B*, 337(3-4):235–239, Oct. 1994.

[114] M. I. Gorenstein and S. N. Yang. Gluon plasma with a medium-dependent dispersion relation. *Physical Review D*, 52(9):5206–5212, Nov. 1995.

[115] A. Peshier, B. Kämpfer, O. P. Pavlenko, and G. Soff. Massive quasiparticle model of the SU(3) gluon plasma. *Physical Review D*, 54(3):2399–2402, Aug. 1996.

[116] R. A. Schneider and W. Weise. Quasiparticle description of lattice QCD thermodynamics. *Physical Review C*, 64(5), Oct. 2001.

[117] A. Peshier, B. Kämpfer, and G. Soff. From QCD lattice calculations to the equation of state of quark matter. *Physical Review D*, 66(9), Nov. 2002.

[118] A. Rebhan and P. Romatschke. Hard-thermal-loop quasiparticle models of deconfined QCD at finite chemical potential. *Physical Review D*, 68(2), July 2003.

[119] V. M. Bannur. Self-consistent quasiparticle model for quark-gluon plasma. *Physical Review C*, 75(4), Apr. 2007.

[120] V. M. Bannur. Comments on quasiparticle models of quark–gluon plasma. *Physics Letters B*, 647(4):271–274, Apr. 2007.

[121] V. M. Bannur. Quasi-particle model for QGP with nonzero densities. *Journal of High Energy Physics*, 2007(09):046–046, Sept. 2007.

[122] V. M. Bannur. Revisiting the quasi-particle model of the quark–gluon plasma. *The European Physical Journal C*, 50(3):629–634, Feb. 2007.

[123] V. M. Bannur. Self-consistent quasiparticle model for 2, 3, and (2+1) flavor QGP. *Physical Review C*, 78(4), Oct. 2008.

[124] V. M. Bannur. Thermodynamics of (2+1) flavor qgp in quasiparticle model. *International Journal of Modern Physics E*, 21(11):1250090, Nov. 2012.

[125] F. Gardim and F. Steffens. Thermodynamics of quasi-particles. *Nuclear Physics A*, 797(1-2):50–66, Dec. 2007.

[126] F. Gardim and F. Steffens. Thermodynamics of quasi-particles at finite chemical potential. *Nuclear Physics A*, 825(3-4):222–244, July 2009.

[127] R. D. Pisarski. Scattering amplitudes in hot gauge theories. *Physical Review Letters*, 63(11):1129–1132, Sept. 1989.

[128] R. D. Pisarski. Damping rates for moving particles in hot QCD. *Physical Review D*, 47(12):5589–5600, June 1993.

[129] M. V. Medvedev. Thermodynamics of photons in relativistic $e+e-\gamma$ plasmas. *Physical Review E*, 59(5):R4766–R4768, May 1999.

[130] V. M. Bannur. Self-consistent quasiparticle model results for ultrarelativistic electron-positron thermodynamic plasma. *Physical Review E*, 73(6), June 2006.

[131] P. U. Colin Howson. *Scientific Reasoning*. Open Court Publishing Co ,U.S., 2006.

[132] F. Bruckmann, G. Endrődi, M. Giordano, S. D. Katz, T. G. Kovács, F. Pittler, and J. Wellnhofer. Landau levels in QCD in an external magnetic field. *EPJ Web of Conferences*, 175:07014, 2018.

[133] E. S. Fraga and L. F. Palhares. Deconfinement in the presence of a strong magnetic background: An exercise within the MIT bag model. *Physical Review D*, 86(1), July 2012.

[134] A. J. Mizher, M. N. Chernodub, and E. S. Fraga. Phase diagram of hot QCD in an external magnetic field: Possible splitting of deconfinement and chiral transitions. *Physical Review D*, 82(10), Nov. 2010.

[135] S. Chakrabarty. Quark matter in a strong magnetic field. *Physical Review D*, 54(2):1306–1316, July 1996.

[136] F. Bruckmann, G. Endrődi, M. Giordano, S. Katz, T. Kovács, F. Pittler, and J. Wellnhofer. Landau levels in QCD. *Physical Review D*, 96(7), Oct. 2017.

[137] A. N. Tawfik. Transport coefficients and quark-hadron phase transition(s) from PLSM in vanishing and finite magnetic field. *Journal of Physics: Conference Series*, 668:012082, Jan. 2016.

[138] K. Kohri, S. Yamada, and S. Nagataki. Anisotropic kinetic pressure in ideal MHD and application to entropy production in neutrino-driven wind in supernovae. *Astroparticle Physics*, 21(4):433–441, July 2004.

[139] E. J. Ferrer and V. de la Incera. Dynamically generated anomalous magnetic moment in massless QED. *Nuclear Physics B*, 824(1-2):217–238, Jan. 2010.

[140] N. Chaudhuri, S. Ghosh, S. Sarkar, and P. Roy. Effects of quark anomalous magnetic moment on the thermodynamical properties and mesonic excitations of magnetized hot and dense matter in PNJL model. *The European Physical Journal A*, 56(8), Aug. 2020.

[141] E. Ferrer, V. de la Incera, D. M. Paret, A. P. Martínez, and A. Sanchez. Insignificance of the anomalous magnetic moment of charged fermions for

the equation of state of a magnetized and dense medium. *Physical Review D*, 91(8), Apr. 2015.

[142] E. Ferrer, V. de la Incera, and X. Wen. Quark antiscreening at strong magnetic field and inverse magnetic catalysis. *Physical Review D*, 91(5), Mar. 2015.

[143] A. Ayala, C. Dominguez, S. Hernandez-Ortiz, L. Hernandez, M. Loewe, D. M. Paret, and R. Zamora. Thermomagnetic evolution of the QCD strong coupling. *Physical Review D*, 98(3), Aug. 2018.

[144] V. A. Miransky and I. A. Shovkovy. Magnetic catalysis and anisotropic confinement in QCD. *Physical Review D*, 66(4), Aug. 2002.

[145] M. Ferreira, P. Costa, O. Lourenço, T. Frederico, and C. Providência. Inverse magnetic catalysis in the(2+1)-flavor nambu–jona-lasinio and polyakov–nambu–jona-lasinio models. *Physical Review D*, 89(11), June 2014.

[146] R. L. S. Farias, V. S. Timóteo, S. S. Avancini, M. B. Pinto, and G. Krein. Thermo-magnetic effects in quark matter: Nambu-jona-lasinio model constrained by lattice QCD. *The European Physical Journal A*, 53(5), May 2017.

[147] M. Kurian and V. Chandra. Effective description of hot QCD medium in strong magnetic field and longitudinal conductivity. *Physical Review D*, 96(11), Dec. 2017.

[148] G. S. Bali, F. Bruckmann, G. Endrödi, S. D. Katz, and A. Schäfer. The QCD equation of state in background magnetic fields. *Journal of High Energy Physics*, 2014(8), Aug. 2014.

[149] C. Bonati, M. D'Elia, M. Mariti, F. Negro, and F. Sanfilippo. Magnetic susceptibility of strongly interacting matter across the deconfinement transition. *Physical Review Letters*, 111(18), Oct. 2013.

[150] C. Bonati, M. D'Elia, M. Mariti, F. Negro, and F. Sanfilippo. Magnetic susceptibility and equation of state of Nf=2+1 QCD with physical quark masses. *Physical Review D*, 89(5), Mar. 2014.

[151] S. Rath and B. K. Patra. One-loop QCD thermodynamics in a strong homogeneous and static magnetic field. *Journal of High Energy Physics*, 2017(12), Dec. 2017.

[152] A. Bandyopadhyay, B. Karmakar, N. Haque, and M. G. Mustafa. Pressure of a weakly magnetized hot and dense deconfined QCD matter in one-loop hard-thermal-loop perturbation theory. *Physical Review D*, 100(3), Aug. 2019.

[153] E. J. Ferrer, V. de la Incera, J. P. Keith, I. Portillo, and P. L. Springsteen. Equation of state of a dense and magnetized fermion system. *Physical Review C*, 82(6), Dec. 2010.

[154] A. P. Martínez, H. P. Rojas, and H. J. M. Cuesta. Magnetic collapse of a neutron gas: Can magnetars indeed be formed? *The European Physical Journal C*, 29(1):111–123, July 2003.

[155] M. Chaichian, S. S. Masood, C. Montonen, A. P. Martínez, and H. P. Rojas. Quantum magnetic collapse. *Physical Review Letters*, 84(23):5261–5264, June 2000.

[156] A. Y. Potekhin and D. G. Yakovlev. Comment on "equation of state of a dense and magnetized fermion system". *Physical Review C*, 85(3), Mar. 2012.

[157] E. J. Ferrer, V. de la Incera, J. P. Keith, I. Portillo, and P. L. Springsteen. Reply to "comment on 'equation of state of a dense and magnetized fermion system'". *Physical Review C*, 85(3), Mar. 2012.

[158] V. Dexheimer, D. P. Menezes, and M. Strickland. The influence of strong magnetic fields on proto-quark stars. *Journal of Physics G: Nuclear and Particle Physics*, 41(1):015203, Dec. 2013.

[159] G. S. Bali, F. Bruckmann, G. Endrődi, F. Gruber, and A. Schäfer. Magnetic field-induced gluonic (inverse) catalysis and pressure (an)isotropy in QCD. *Journal of High Energy Physics*, 2013(4), Apr. 2013.

[160] R. D. Blandford and L. Hernquist. Magnetic susceptibility of a neutron star crust. *Journal of Physics C: Solid State Physics*, 15(30):6233–6243, Oct. 1982.

[161] D. P. Menezes, M. B. Pinto, S. S. Avancini, A. P. Martínez, and C. Providência. Quark matter under strong magnetic fields in the nambu–jona-lasinio model. *Physical Review C*, 79(3), Mar. 2009.

[162] P.-C. Chu, X. Wang, L.-W. Chen, and M. Huang. Quark magnetar in the three-flavor nambu–jona-lasinio model with vector interactions and a magnetized gluon potential. *Physical Review D*, 91(2), Jan. 2015.

[163] I. Ghisoiu, J. Möller, and Y. Schröder. Debye screening mass of hot yang-mills theory to three-loop order. *Journal of High Energy Physics*, 2015(11), Nov. 2015.

[164] P. Arnold and L. G. Yaffe. Non-abelian debye screening length beyond leading order. *Physical Review D*, 52(12):7208–7219, Dec. 1995.

[165] C. Bonati, M. D'Elia, M. Mariti, M. Mesiti, F. Negro, A. Rucci, and

F. Sanfilippo. Screening masses in strong external magnetic fields. *Physical Review D*, 95(7), Apr. 2017.

[166] A. K. Rebhan. Non-abelian debye mass at next-to-leading order. *Physical Review D*, 48(9):R3967–R3970, Nov. 1993.

[167] S. Ghosh and V. Chandra. Electromagnetic spectral function and dilepton rate in a hot magnetized QCD medium. *Physical Review D*, 98(7), Oct. 2018.

[168] P. Silva, O. Oliveira, P. Bicudo, and N. Cardoso. Gluon screening mass at finite temperature from the landau gauge gluon propagator in lattice QCD. *Physical Review D*, 89(7), Apr. 2014.

[169] R. A. Schneider. Debye screening at finite temperature reexamined. *Physical Review D*, 66(3), Aug. 2002.

[170] S. Mrowczynski. Topics in the transport theory of quark-gluon plasma. *Physics of Particles and Nuclei*, 30(4):419, July 1999.

[171] K. Yagi, T. Hatsuda, and Y. Miake. *Quark-gluon plasma: From big bang to little bang*, volume 23 of *Camb.Monogr.Part.Phys.Nucl.Phys.Cosmol.* Cambridge, UK:Univ.Pr, 2005.

[172] G. Bali, F. Bruckmann, G. Endrődi, and A. Schäfer. Paramagnetic squeezing of QCD matter. *Physical Review Letters*, 112(4), Jan. 2014.

[173] J. Alexandre. Vacuum polarization in thermal QED with an external magnetic field. *Physical Review D*, 63(7), Mar. 2001.

[174] B. Karmakar, A. Bandyopadhyay, N. Haque, and M. G. Mustafa. General structure of gauge boson propagator and its spectra in a hot magnetized medium. *The European Physical Journal C*, 79(8), Aug. 2019.

[175] Y. Kim, Y. Matsuo, W. Sim, S. Takeuchi, and T. Tsukioka. Quark number susceptibility with finite chemical potential in holographic QCD. *Journal of High Energy Physics*, 2010(5), May 2010.

Appendix

Appendix A

The self-consistent quasiparticle model

A.1 Calculation of quark thermal masses

Here we write down a general method to obtain the quark thermal masses, which can be used for both massive and massless quarks. We start with the ansatz,

$$m_f^2 = b_g^2 g^2 \frac{n_q}{T},$$ (A.1)

where,

$$n_q = \frac{g_f}{2\pi^2} \int_0^\infty dk k^2 \frac{1}{z^{-1} e^{\omega_k/T} + 1},$$ (A.2)

where,

$$\omega_k = \sqrt{k^2 + m_q^2}.$$ (A.3)

Thus,

$$n_q = \frac{g_f}{2\pi^2} \int_0^\infty dk k^2 \frac{1}{e^{\sqrt{k^2+m_q^2}} + 1}. \tag{A.4}$$

We need to remember that m_q is dependent on n_q and hence we have to solve the above equation self consistently. The exact dependence of m_q on n_q, we will substitute in the end. For now we continue with m_q. with $x = \frac{k}{T}$, equation (A.4) becomes, $(z = 1$ case)

$$f_q^2 = \frac{2\pi^2}{g_f} \frac{n_q}{T^3} = \int_0^\infty dx x^2 \frac{1}{e^{\sqrt{x^2 + \left(\frac{m_q}{T}\right)^2}} + 1}. \tag{A.5}$$

Now, put

$$x^2 = \left(\frac{m_q}{T}\right)^2 \sinh^2 t \quad \Rightarrow dx = \frac{m_q}{T} \cosh t dt. \tag{A.6}$$

Then,

$$\begin{aligned} f_q^2 &= \int_0^\infty dt \left(\frac{m_q}{T}\right)^2 \sinh^2 t \frac{m_q}{T} \cosh t \frac{1}{e^{\frac{m_q}{T} \cosh t} + 1} \\ &= \sum_{l=1}^\infty (-1)^{l-1} \left(\frac{m_q}{T}\right)^3 \int_0^\infty dt \cosh t [\cosh^2 t - 1] e^{-l\frac{m_q}{T} \cosh t} \\ &= \sum_{l=1}^\infty (-1)^{l-1} \left(\frac{m_q}{T}\right)^3 \int_0^\infty dt \left[\frac{\cosh 3t - \cosh t}{4}\right] e^{-l\frac{m_q}{T} \cosh t}. \end{aligned} \tag{A.7}$$

Making use of the well known integral representation for the modified Bessell function,

$$K_\nu(z) = \int_0^\infty e^{-z \cosh t} \cosh(\nu t) dt, \tag{A.8}$$

114

$$f_q^2 = \sum_{l=1}^{\infty} (-1)^{l-1} \left(\frac{m_q}{T}\right)^3 \frac{K_3(l\frac{m_q}{T}) - K_1(l\frac{m_q}{T})}{4}. \tag{A.9}$$

This can be further simplified using the relation,

$$K_{\nu-1}(x) - K_{\nu+1}(x) = -\frac{2\nu}{x} K_\nu(x), \tag{A.10}$$

$$
\begin{aligned}
f_q^2 &= \sum_{l=1}^{\infty} (-1)^{l-1} \left(\frac{m_q}{T}\right)^3 \frac{4}{l\frac{m_q}{T}} \frac{K_2(l\frac{m_q}{T})}{4} \\
&= \sum_{l=1}^{\infty} (-1)^{l-2} \left(\frac{m_q}{T}\right)^2 K_2(l\frac{m_q}{T}).
\end{aligned}
\tag{A.11}
$$

A.1.1 Thermal mass for massless quarks

For massless quarks,

$$m_q^2 = 2m_f^2, \tag{A.12}$$

$$m_f^2 = b_q^2 g^2 \frac{n_q}{T}, \tag{A.13}$$

$$m_q^2 = 2b_q^2 g^2 \frac{n_q}{T}. \tag{A.14}$$

With,

$$
\begin{aligned}
f_q^2 &= \frac{2\pi^2}{g_f} \frac{n_q}{T^3}, \\
\left(\frac{m_q}{T}\right)^2 &= 2b_q^2 g^2 \frac{g_f}{2\pi^2} f_q^2 \\
&= 2\bar{b}_q^2 f_q^2 \\
\bar{b}_q^2 &= \frac{g_f}{2\pi^2} b_q^2 g^2.
\end{aligned}
\tag{A.15}
$$

So the thermal mass can be determined by solving the following equation self consistently.

$$f_q^2 = \sum_{l=1}^{\infty} (-1)^{l-2} \left(2\bar{b}_q f_q\right)^2 K_2(l2\bar{b}_q f_q). \tag{A.16}$$

A.1.2 Thermal mass for massive quarks

For massive quarks,

$$m_q^2 = (m_0 + m_f)^2 + m_f^2 \tag{A.17}$$

$$\left(\frac{m_q}{T}\right)^2 = \left(\frac{m_0}{T} + \frac{m_f}{T}\right)^2 + \left(\frac{m_f}{T}\right)^2. \tag{A.18}$$

The ansatz for m_f is,

$$m_f^2 = b_q^2 g^2 \frac{n_q}{T}. \tag{A.19}$$

We have already defined,

$$f_q = \frac{2\pi^2}{g_f} \frac{n_q}{T^3} \tag{A.20}$$

$$\Rightarrow \frac{n_q}{T} = \frac{g_f}{2\pi^2} f_q^2 T^2. \tag{A.21}$$

Now, $m_f^2 = b_q^2 g^2 \frac{g_f}{2\pi^2} f_q^2 T^2$

$$\left(\frac{m_f}{T}\right)^2 = b_q^2 g^2 \frac{g_f}{2\pi^2} f_q^2$$

$$= \bar{b}_q^2 f_q^2, \tag{A.22}$$

where,

$$\bar{b}^2 = \frac{g_f}{2\pi^2} b_q^2 g^2. \tag{A.23}$$

$$\Rightarrow \left(\frac{m_q}{T}\right)^2 = \left[\frac{m_0}{T} + \bar{b}_q f_q\right]^2 + \bar{b}_q^2 f_q^2. \tag{A.24}$$

116

Substituting (A.24) in equation (A.11), the equation to be solved self consistently in order to obtain quark mass becomes,

$$f_q^2 = \sum_{l=1}^{\infty} (-1)^{l-2} \left(\left[\frac{m_0}{T} + \bar{b}_q f_q \right]^2 + \bar{b}_q^2 f_q^2 \right)$$

$$K_2 \left(l \left\{ \left[\frac{m_0}{T} + \bar{b}_q f_q \right]^2 + \bar{b}_q^2 f_q^2 \right\}^{1/2} \right). \tag{A.25}$$

A.2   Thermal mass for gluons

For Gluons we have,

$$\omega_p^2 = a_g g^2 \frac{n_g}{T} + a_q^2 g^2 \frac{n_q}{T}$$

$$m_g^2 = \frac{3}{2} \omega_p^2, \tag{A.26}$$

So,

$$m_g^2 = \frac{3}{2} a_g g^2 \frac{n_g}{T} + \frac{3}{2} a_q^2 g^2 \frac{n_q}{T} \tag{A.27}$$

$$\omega_k = \sqrt{k^2 + m_g^2}. \tag{A.28}$$

Thus, the number density for gluons,

$$n_g = \frac{g_g}{2\pi^2} \int_0^{\infty} dk k^2 \frac{1}{e^{\omega_k/T} - 1}$$

$$= \frac{g_g}{2\pi^2} \int_0^{\infty} dk k^2 \frac{1}{e^{\frac{1}{T} \sqrt{k^2 + \frac{3}{2} a_g g^2 \frac{n_g}{T} + \frac{3}{2} a_q^2 g^2 \frac{n_q}{T}}} - 1}. \tag{A.29}$$

Now we redefine,

$$\frac{2\pi^2}{g_g} \frac{n_g}{T^3} = f_g^2; \quad \frac{n_g}{T^3} = \frac{g_g}{2\pi^2} f_g^2 \; \Rightarrow \; \frac{3}{2} a_g^2 g^2 \frac{n_q}{T^3} = \frac{3}{2} a_q^2 g^2 \frac{g_g}{2\pi^2} f_g^2 = \bar{a}_g^2 f_g^2. \tag{A.30}$$

117

where,

$$\bar{a}_g^2 = \frac{3}{4\pi^2} g_g a_g^2 g^2. \tag{A.31}$$

We already have, from equation (A.21),

$$\frac{n_q}{T^3} = \frac{g_f}{2\pi^2} f_q^2 T^2. \tag{A.32}$$

So,

$$\frac{3}{2} a_q^2 g^2 \frac{n_q}{T^3} = \frac{3}{2} a_q^2 g^2 \frac{g_f}{2\pi^2} f_q^2 T^2 = \bar{a}_q^2 f_q^2, \tag{A.33}$$

where,

$$\bar{a}_q^2 = \frac{3}{2} \frac{g_f}{2\pi^2} a_q^2 g^2. \tag{A.34}$$

Thus,

$$f_g^2 = \int_0^\infty dx x^2 \frac{1}{e^{\sqrt{x^2 + \bar{a}_g^2 f_g^2 + \bar{a}_q^2 f_q^2}} - 1}. \tag{A.35}$$

Let's make the substitution $x^2 = (\bar{a}_g^2 f_g^2 + \bar{a}_q^2 f_q^2) \sinh^2 t$. Then, $dx = (\bar{a}_g^2 f_g^2 + \bar{a}_q^2 f_q^2)^{\frac{1}{2}} \cosh t dt$. So,

$$
\begin{aligned}
f_g^2 &= (\bar{a}_g^2 f_g^2 + \bar{a}_q^2 f_q^2)^{\frac{3}{2}} \int_0^\infty dt \cosh t \sinh^2 t \frac{1}{e^{(\bar{a}_g^2 f_g^2 + \bar{a}_q^2 f_q^2)^{\frac{1}{2}} \cosh t} - 1}, \\
&= (\bar{a}_g^2 f_g^2 + \bar{a}_q^2 f_q^2)^{\frac{3}{2}} \int_0^\infty dt \cosh t \sinh^2 t \sum_{l=1}^\infty e^{-l(\bar{a}_g^2 f_g^2 + \bar{a}_q^2 f_q^2)^{\frac{1}{2}} \cosh t} \\
&= (\bar{a}_g^2 f_g^2 + \bar{a}_q^2 f_q^2)^{\frac{3}{2}} \sum_{l=1}^\infty \int_0^\infty dt \cosh t [\cosh^2 t - 1] \times
\end{aligned}
$$

$$e^{-l(\bar{a}_g^2 f_g^2 + \bar{a}_q^2 f_q^2)^{\frac{1}{2}} \cosh t}. \tag{A.36}$$

We shall use the notation $f_{gq} = \bar{a}_g^2 f_g^2 + \bar{d}_q^2 F_q^2$, for simplicity. Thus,

$$f_g^2 = f_{gq}^{3/2} \sum_{l=1}^{\infty} \int_0^{\infty} dt \left(-\cosh t\, e^{-l f_{gq}^{1/2} \cosh t} + \cosh^3 t\, e^{-l f_{gq}^{1/2} \cosh t} \right)$$

$$= f_{gq}^{3/2} \sum_{l=1}^{\infty} \left(-K_1[l f_{gq}^{1/2}] + \frac{1}{4} K_3[l f_{gq}^{1/2}] + \frac{3}{4} K_1[l f_{gq}^{1/2}] \right)$$

$$= f_{gq}^{3/2} \sum_{l=1}^{\infty} \left(\frac{K_3[l f_{gq}^{1/2}]}{4} - \frac{K_1[l f_{gq}^{1/2}]}{4} \right) . \text{Or,}$$

$$f_g^2 = \frac{(\bar{a}_g^2 f_g^2 + \bar{a}_q^2 f_q^2)^{3/2}}{4} \sum_{l=1}^{\infty} \left(K_3[l(\bar{a}_g^2 f_g^2 + \bar{a}_q^2 f_q^2)^{1/2}] \right.$$

$$\left. - K_1[l(\bar{a}_g^2 f_g^2 + \bar{a}_q^2 f_q^2)^{1/2}] \right). \qquad \text{(A.37)}$$

Solving this equation by using already obtained solution for f_q, we can obtain f_g and hence $m_g(T)$.

$$\left(\frac{m_g}{T} \right)^2 = \bar{a}_g^2 f_g^2 + \bar{a}_q^2 f_q^2. \qquad \text{(A.38)}$$

A.3   Evaluation of a_q, b_q, a_g

a_q, b_q and a_g are evaluated by demanding that the density dependent expressions for ω_p, m_f approach the perturbative QCD result as $T \to \infty$. The perturbative QCD results are,

$$\omega_p^2 = \frac{g^2 T^2}{18}(6 + n_f), \qquad \text{(A.39)}$$

and,

$$m_f^2 = \frac{g^2 T^2}{6}, \qquad \text{(A.40)}$$

where g is the QCD running coupling constant and n_f is the number of flavors with the same mass.

We have, for gluons,

$$f_g(T \to \infty) = \int_0^\infty dx x^2 \frac{1}{e^x - 1} = 2\zeta(3), \tag{A.41}$$

where, $x = k/T$. We have used the integral representation for Riemann Zeta function,

$$\zeta(x) = \frac{1}{\Gamma(x)} \int_0^\infty \frac{u^{x-1}}{e^u - 1} du, \tag{A.42}$$

Similarly as $T \to \infty$ we have for quarks,

$$f_q(T \to \infty) = \int_0^\infty dx x^2 \frac{1}{e^x + 1} = 2\eta(3) = \frac{3}{2}\zeta(3). \tag{A.43}$$

Here we have used the integral representation for eta function

$$\eta(s) = \frac{1}{\Gamma(s)} \int_0^\infty \frac{x^{s-1}}{e^x + 1} dx, \tag{A.44}$$

and the relation $\eta(s) = (1 - 2^{(1-s)})\zeta(s)$. Thus, $\eta(3) = \frac{3}{4}\zeta(3)$.

Now, from equation (A.38) we have,

$$\omega_p^2 = a_g^2 g^2 T^2 \frac{g_g}{2\pi^2} f_g^2 + a_q^2 g^2 T^2 \frac{g_q}{2\pi^2} f_q^2, \tag{A.45}$$

and from equation (A.22),

$$m_f^2 = b_q^2 g^2 T^2 \frac{g_q}{2\pi^2} f_q^2. \tag{A.46}$$

Now, taking the limit $T \to \infty$ in (A.46) and equating to the pQCD result in

equation (A.40), we have,

$$b_q^2 g^2 T^2 \frac{g_q}{2\pi^2} \frac{3}{2} \zeta(3) = \frac{g^2 T^2}{6},$$
(A.47)

or,

$$b_q^2 = \frac{2\pi^2}{9 g_q \zeta(3)}.$$
(A.48)

Thus

$$b_u^2 = b_d^2 = \frac{2\pi^2}{9 \times 12 \zeta(3)},$$
(A.49)

$$b_s^2 = \frac{2\pi^2}{9 \times 6 \zeta(3)}.$$
(A.50)

where we have used $g_q = 6 n_f$. n_f is the number of flavors with the same mass.

Similarly, equating the high temperature limit of equation (A.45) with equation (A.39), we get,

$$a_g^2 g^2 T^2 \frac{g_g}{2\pi^2} 2\zeta(3) + a_q^2 g^2 T^2 \frac{g_q}{2\pi^2} \frac{3}{2} \zeta(3) = \frac{g^2 T^2}{18}(6 + n_f).$$
(A.51)

or, equating the contributions separately,

$$a_g^2 g^2 T^2 \frac{g_g}{2\pi^2} 2\zeta(3) = \frac{g^2 T^2}{3},$$
(A.52)

$$a_{u/d}^2 g^2 T^2 \frac{12}{2\pi^2} \frac{3}{2} \zeta(3) = \frac{g^2 T^2}{9},$$
(A.53)

$$a_s^2 g^2 T^2 \frac{6}{2\pi^2} \frac{3}{2} \zeta(3) = \frac{g^2 T^2}{18}.$$
(A.54)

From equation (A.52),(A.53) and (A.54) with $g_g = 16$, we get,

$$a_g^2 = \frac{\pi^2}{48\zeta(3)}, \tag{A.55}$$

$$a_{u/d}^2 = \frac{\pi^2}{81\zeta(3)}, \tag{A.56}$$

$$a_s^2 = \frac{\pi^2}{81\zeta(3)}. \tag{A.57}$$

Thus, a_q^2 has the same value for all three quarks.

A.4   General expression for energy density using quasi-particle model

The energy density can be written as,

$$\varepsilon = \frac{g_g}{2\pi^2} \underbrace{\int_0^\infty dk k^2 \frac{\omega_k}{e^{\omega_k/T} - 1}}_{I_1} + \sum_f \frac{12 n_f}{2\pi^2} \underbrace{\int_0^\infty dk k^2 \frac{\omega_k^f}{e^{\omega_k^f/T} + 1}}_{I_q}. \tag{A.58}$$

Now,

$$\begin{aligned} I_1 &= \int_0^\infty dk k^2 \frac{\omega_k}{e^{\omega_k/T} - 1} \\ &= \int_0^\infty dk k^2 \frac{\omega_k}{e^{\omega_k/T} \left[1 - e^{-\omega_k/T} \right]} \\ &= \sum_{l=0}^\infty \int_0^\infty dk k^2 \omega_k e^{-l\frac{\omega_k}{T}} e^{-\frac{\omega_k}{T}} \\ &= \sum_{l=1}^\infty \int_0^\infty dk k^2 \omega_k e^{-l\frac{\omega_k}{T}}. \end{aligned} \tag{A.59}$$

With $\omega_k = \sqrt{k^2 + m_g^2}$, we get,

$$I_1 = \sum_{l=1}^\infty \int_0^\infty dk k^2 \sqrt{k^2 + m_g^2} e^{-l\frac{\sqrt{k^2 + m_g^2}}{T}}. \tag{A.60}$$

Substituting $x = k/T \to dk = Tdx$,

$$I_1 = T^4 \sum_{l=1}^{\infty} \int_0^{\infty} dx x^2 \sqrt{x^2 + \left(\frac{m_g}{T}\right)^2} e^{-l\sqrt{x^2 + \left(\frac{m_g}{T}\right)^2}}. \tag{A.61}$$

Put $x^2 = \left(\frac{m_g}{T}\right)^2 \sinh^2 t$ then,

$$I_1 = T^4 \left(\frac{m_g}{T}\right)^4 \sum_{l=1}^{\infty} \int_0^{\infty} dt \cosh^2 t \sinh^2 t e^{-l\left(\frac{m_g}{T}\right)\cosh t}. \tag{A.62}$$

Using the relation $\cosh t \sinh t = \sinh 2t/2$,

$$\begin{aligned} I_1 &= T^4 \left(\frac{m_g}{T}\right)^4 \sum_{l=1}^{\infty} \int_0^{\infty} dt \left(\frac{\sinh 2t}{2}\right)^2 e^{-l\left(\frac{m_g}{T}\right)\cosh t} \\ &= \frac{T^4}{4} \left(\frac{m_g}{T}\right)^4 \sum_{l=1}^{\infty} \int_0^{\infty} dt \frac{\cosh 4t - 1}{2} e^{-l\left(\frac{m_g}{T}\right)\cosh t} \\ &= \frac{T^4}{8} \left(\frac{m_g}{T}\right)^4 \sum_{l=1}^{\infty} \int_0^{\infty} dt \left[\cosh 4t e^{-l\left(\frac{m_g}{T}\right)\cosh t} - e^{-l\left(\frac{m_g}{T}\right)\cosh t}\right]. \end{aligned} \tag{A.63}$$

We can now make use of the integral representation for modified Bessel function,

$$K_\nu(z) = \int_0^{\infty} e^{-z\cosh t} \cosh(\nu t) dt, \tag{A.64}$$

and I_1 becomes,

$$I_1 = \frac{T^4}{8} \left(\frac{m_g}{T}\right)^4 \sum_{l=1}^{\infty} \left[K_4\left(l\frac{m_g}{T}\right) - K_0\left(l\frac{m_g}{T}\right)\right]. \tag{A.65}$$

This can be further simplified using the recurrence relation,

$$K_{\nu+1}(x) - K_{\nu-1}(x) = \frac{2\nu}{x} K_\nu(x). \tag{A.66}$$

Thus,

$$
\begin{aligned}
K_4(x) - K_2(x) &= \frac{6}{x} K_3(x) \\
\Rightarrow K_4(x) &= \frac{6}{x} K_3(x) + K_2(x) \\
\Rightarrow K_4(x) - K_0(x) &= \frac{6}{x} K_3(x) + K_2(x) - K_0(x) \\
&= \frac{6}{x} K_3(x) + \frac{2}{x} K_1(x).
\end{aligned}
\tag{A.67}
$$

We may further use the relation,

$$
K_3(x) - K_1(x) = \frac{4}{x} K_2(x)
\tag{A.68}
$$

$$
\Rightarrow K3(x) = \frac{4}{x} K_2(x) + K_1(x).
\tag{A.69}
$$

Then,

$$
\begin{aligned}
K_4(x) - K_0(x) &= \frac{6}{x} \left(\frac{4}{x} K_2(x) + K_1(x) \right) + \frac{2}{x} K_1(x) \\
&= \frac{24}{x^2} K_2(x) + \frac{8}{x} K_1(x) \\
&= \frac{8}{x} \left(3 \frac{K_2(x)}{x} + K_1(x) \right).
\end{aligned}
\tag{A.70}
$$

With this, I_1 becomes,

$$
\begin{aligned}
I_1 &= \frac{T^4}{8} \left(\frac{m_g}{T} \right)^4 \sum_{l=1}^{\infty} \frac{8}{l \frac{m_g}{T}} \left[3 \frac{K_2 \left(l \frac{m_g}{T} \right)}{l \frac{m_g}{T}} + K_1 \left(l \frac{m_g}{T} \right) \right] \\
&= T^4 \sum_{l=1}^{\infty} \left(l \frac{mg}{T} \right)^4 \frac{1}{l^4} \frac{1}{l \frac{m_g}{T}} \left[3 \frac{K_2 \left(l \frac{m_g}{T} \right)}{l \frac{m_g}{T}} + K_1 \left(l \frac{m_g}{T} \right) \right] \\
&= T^4 \sum_{l=1}^{\infty} \frac{1}{l^4} \left[\left(l \frac{m_g}{T} \right)^3 K_1 \left(l \frac{m_g}{T} \right) + 3 \left(l \frac{m_g}{T} \right)^2 K_2 \left(l \frac{m_g}{T} \right) \right].
\end{aligned}
\tag{A.71}
$$

Thus the contribution to the total energy density from gluons

$$
\begin{aligned}
\varepsilon_g(T) &= \frac{g_g}{2\pi^2} I_1 \\
&= \frac{g_g T^4}{2\pi^2} \sum_{l=1}^{\infty} \frac{1}{l^4} \left[\left(l\frac{m_g}{T} \right)^3 K_1 \left(l\frac{m_g}{T} \right) + 3 \left(l\frac{m_g}{T} \right)^2 K_2 \left(l\frac{m_g}{T} \right) \right].
\end{aligned} \tag{A.72}
$$

Now,

$$
\begin{aligned}
I_q &= \int_0^{\infty} dk\, k^2 \frac{\omega_k}{e^{\omega_k/T} + 1} \\
&= \sum_{l=1}^{\infty} (-1)^{l-1} \int_0^{\infty} dk\, k^2 \omega_k e^{-l\frac{\omega_k}{T}}.
\end{aligned} \tag{A.73}
$$

Following the same steps as in the previous case we end up with,

$$
I_q = T^4 \sum_{l=1}^{\infty} \frac{(-1)^{l-1}}{l^4} \left[\left(l\frac{m_l}{T} \right)^3 K_1 \left(l\frac{m_l}{T} \right) + 3 \left(l\frac{m_l}{T} \right)^2 K_2 \left(l\frac{m_l}{T} \right) \right]. \tag{A.74}
$$

$$
\varepsilon_q(T) = \frac{12 n_q}{2\pi^2} I_2 \tag{A.75}
$$

$$
= \frac{12 n_q T^4}{2\pi^2} \sum_{l=1}^{\infty} \frac{(-1)^{l-1}}{l^4}
$$

$$
\left[\left(l\frac{m_q}{T} \right)^3 K_1 \left(l\frac{m_q}{T} \right) + 3 \left(l\frac{m_q}{T} \right)^2 K_2 \left(l\frac{m_q}{T} \right) \right]. \tag{A.76}
$$

Thus the total energy density can be obtained as,

$$
\varepsilon(T) = \varepsilon_g(T) + \varepsilon_u(T) + \varepsilon_d(T) + \varepsilon_s(T). \tag{A.77}
$$